Int J Thermophys (2010) 31:316–326
DOI 10.1007/s10765-010-0719-7

Densities, Viscosities, Sound Speeds, Refractive Indices, and Excess Properties of Binary Mixtures of Isoamyl Alcohol with Some Alkoxyethanols

Mahendra Nath Roy · Radhey Shyam Sah · Prasanna Pradhan

Received: 17 February 2009 / Accepted: 24 February 2010 / Published online: 16 March 2010

Abstract Densities and viscosities were measured for binary mixtures of isoamyl alcohol with 2-methoxyethanol, 2-ethoxyethanol, and 2-butoxyethanol over the entire range of composition at 303.15 K, 313.15 K, and 323.15 K and ultrasonic speeds and refractive indices at 303.15 K under atmospheric pressure. From the experimental values of density, viscosity, ultrasonic speed, and refractive index, the values of excess molar volume (V^{E}), viscosity deviations ($\Delta\eta$), deviations in isentropic compressibility (ΔK_S), and excess molar refraction (ΔR) have been calculated. The excess or deviation properties were found to be either negative or positive, depending on the molecular interactions and the nature of liquid mixtures.

Keywords Excess molar volume · Refractive index · Ultrasonic speed · Viscosity deviation

1 Introduction

Grouping of solvents into classes is often based on the nature of the intermolecular forces because the manner whereby solvent molecules are associated with each other brings about a marked effect on the resulting properties. The determination of density, viscosity, speed of sound, and refractive index is a valuable tool to develop new theoretical models and learn about the liquid state [1] because of the close

M. N. Roy (✉) · R. S. Sah · P. Pradhan
Department of Chemistry, North Bengal University, Darjeeling 734013, India
e-mail: mahendraroy2002@yahoo.co.in

R. S. Sah
e-mail: sahradhey@yahoo.com

P. Pradhan
e-mail: praspradhan_03@yahoo.com

connection between liquid structure and macroscopic properties. Ultrasonic properties and refractive index find extensive applications resulting from their ability of characterizing the physicochemical behavior of liquid systems. On the other hand, excess thermodynamic functions and deviations of non-thermodynamic properties of binary liquid mixtures are fundamental for understanding the interactions between molecules in these types of binary mixtures.

There has been a recent upsurge of interest [2,3] in the study of thermodynamic properties of binary liquid mixtures which has been used extensively to obtain information on intermolecular interactions and stereochemical effects in these solvents. The present work reports the density (ρ) and viscosity (η) for binary mixtures of isoamyl alcohol (I.A.A) with 2-methoxyethanol (2-M.E), 2-ethoxyethanol (2-E.E), and 2-butoxyethanol (2-B.E) over the entire range of composition at 303.15 K, 313.15 K, and 323.15 K. Also, the ultrasonic speed (u) and refractive index (n_D) have been reported for the binary mixtures at 303.15 K.

The amyl alcohols are used for the composition of perfumes and the synthesis of fruit essences. They are also used as solvents for surfaces and lacquer baths, inks for print, and dyes for wool as well as in the chemical production of photographic and pharmaceutical substances. Furthermore, they are an intermediate in the production of amyl acetate and other amyl esters. In some of these uses, a knowledge of their physical properties is very important. It is well known that alkoxyethanols have wide use as monomers in the production of polymers and emulsion formulations. They are also of considerable interest for studying the heteroproximity effects of the etheric oxygen on the –OH bond and, hence their influence on the associated nature of the species in these molecules. This work provides a test of various empirical equations to correlate viscosity, density, acoustic, and refractive index data of binary mixtures in terms of pure component properties.

2 Experimental

2.1 Chemicals

2-methoxyethanol, 2-ethoxyethanol, and 2-butoxyethanol (S.D. Fine Chemicals, AR, India) were purified as described in the literature [4]. Isoamyl alcohol was procured from Merck, India and was used as purchased. The pure chemicals were stored over activated 4 Å molecular sieves to reduce water content before use. The chemicals after purification were 99.8 % pure, and their purity was ascertained by GLC and also by comparing experimental values of density, viscosity, and refractive index with those reported in the literature when available, as presented in Table 1.

2.2 Measurements

Densities (ρ) were measured with an Ostwald–Sprengel type pycnometer having a bulb volume of about 25 cm^3 and an internal diameter of the capillary of about 0.1 cm. The measurements were carried out in a thermostat bath controlled to ±0.01 K. The viscosity (η) was measured by means of a suspended Ubbelohde type viscometer,

Table 1 Density (ρ), viscosity (η), sound speed (u), and refractive index (n_D) of the pure component liquids at different temperatures

T(K)	$\rho \times 10^{-3}$(kg·m^{-3})		η(mPa·s)		u(m·s^{-1})		n_D	
	This work	Literature	This work	Literature	This work	Literature	This work	Literature
Isoamyl alcohol								
303.15	0.8031	0.8032 [19]	3.2622	3.1111[19]	1197.4	1197.0 [19]	1.4035	–
313.15	0.7964	–	2.4409	–	–	–	–	–
323.15	0.7898	–	1.9396	–	–	–	–	–
2-Methoxyethanol								
303.15	0.9568	0.9558 [20]	1.5496	1.476 [20]	1324.3	1359.2 [21]	1.3983	–
313.15	0.9463	0.9462 [20]	1.2883	1.189 [20]	–	–	–	–
323.15	0.9378	–	1.0824	–	–	–	–	–
2-Ethoxyethanol								
303.15	0.9195	0.9212 [20]	1.6226	1.643 [20]	1301.5	1319.9 [21]	1.4065	–
313.15	0.9120	0.9123 [20]	1.3554	1.293 [20]	–	–	–	–
323.15	0.9038	–	1.1432	–	–	–	–	–
2-Butoxyethanol								
303.15	0.8920	0.8923 [20]	2.4864	2.408 [20]	1288.4	1322.0 [21]	1.4150	–
313.15	0.8842	0.8839 [20]	1.9788	1.869 [20]	–	–	–	–
323.15	0.8775	–	1.6525	–	–	–	–	–

calibrated at 298.15 K with triply distilled water and purified methanol using density and viscosity values from the literature. The flow times were accurate to ±0.1 s, and the uncertainty in the viscosity measurements was 2×10^{-4} mPa·s. The mixtures were prepared by mixing known volume of pure liquids in airtight-stopper bottles, and each solution thus prepared was distributed into three recipients to perform all the measurements in triplicate, with the aim of determining possible dispersion of the results obtained. Adequate precautions were taken to minimize evaporation losses during the actual measurements. The reproducibility in mole fractions was within ±0.0002. The mass measurements were carried out on a Mettler AG-285 electronic balance with a precision of ±0.01 mg. The uncertainty of density measurements was less than 0.0002 g·cm^{-3}.

Ultrasonic speeds of sound (u) were determined by a multifrequency ultrasonic interferometer (Mittal Enterprise, New Delhi, M-81) working at 1 MHz, calibrated with triply distilled and purified water, methanol, and benzene at 303.15 K. The uncertainty of the ultrasonic speed measurements was 0.8 m·s^{-1}. The details of the methods and techniques have been described in earlier articles [5–8]. The refractive index was measured with the help of an Abbe refractometer (USA), which works with the wavelength corresponding to the D line of sodium. The uncertainty of refractive index measurements was 0.0002 units. The refractometer was calibrated using twice distilled and deionized water, and calibration was checked after every few measurements. All experimental measurements were done under atmospheric pressure.

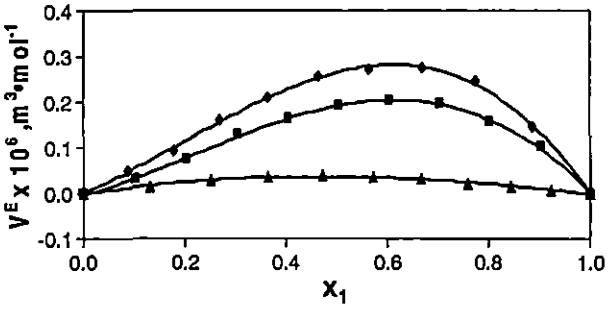

Fig. 1 Plots of excess molar volumes $V^E \times 10^6 (m^3 \cdot mol^{-1})$ against mole fraction (x_1) of isoamyl alcohol with 2-methoxyethanol (♦), 2-ethoxyethanol (■), and 2-butoxyethanol (▲) at 303.15 K

3 Results and Discussion

3.1 Excess Molar Volumes

The experimental densities (ρ), viscosities (η), excess molar volumes (V^E), and viscosity deviations ($\Delta\eta$) for the binary mixtures studied at 303.15 K, 313.15 K, and 323.15 K are reported in Table 2.

The excess molar volumes, V^E, for the mixtures were calculated using the following equation [9]:

$$V^E = \sum_{i=1}^{2} x_i M_i \, (1/\rho - 1/\rho_i) \tag{1}$$

where ρ is the density of the mixture and M_i, x_i, and ρ_i are the molar mass, mole fraction, and density of the ith component in the mixture, respectively.

Figure 1 illustrates that the excess molar volumes, V^E, for the binary systems of I.A.A with 2-M.E, 2-E.E, and 2-B.E. are positive over the entire range of composition at 303.15 K and follows the order 2-M.E > 2-E.E > 2-B.E. Similar trends were found for higher temperatures.

The sign of the excess volume (V^E) of a system depends on the relative magnitude of expansion/contraction on mixing of two liquids. If the factors causing expansion dominate the factors causing contraction, then V^E becomes positive. On the other hand, if the contractive factors dominate the expansive factors, then V^E becomes negative.

Mixing of I.A.A with alkoxyethanols induces a decrease in the molecular order in the latter, resulting in an expansion in volume and hence positive V^E values. The values of excess molar volumes V^E were found to decrease with an increase in the carbon chain length of alkoxyethanols. A similar result was found in the study of binary mixtures of chloroform with propan-1-ol and butan-1-ol [10]. The V^E values were found to increase with an increase in temperature over the complete composition range. A similar dependence of V^E values on temperature was reported elsewhere [11,12].

Table 2 Experimental values of density, ρ, viscosity, η, excess molar volume, V^E, and deviations in viscosity, $\Delta\eta$, for the binary mixtures under investigation at 303.15 K, 313.15 K, and 323.15 K

Mole fraction of I.A.A (x_1)	$\rho \times 10^{-3}$ ($kg \cdot m^{-3}$)	η(mPa · s)	$V^E \times 10^6$ ($m^3 \cdot mol^{-1}$)	$\Delta\eta$(mPa · s)
I.A.A (1)+2-M.E (2) 303.15 K				
0.0000	0.9568	1.5496	0.0000	0.0000
0.0875	0.9383	1.5784	0.0510	−0.1211
0.1775	0.9205	1.6106	0.0930	−0.2430
0.2701	0.9032	1.6521	0.1600	−0.3600
0.3653	0.8867	1.7492	0.2100	−0.4260
0.4633	0.8708	1.8200	0.2580	−0.5230
0.5643	0.8558	1.9339	0.2720	−0.5820
0.6683	0.8415	2.1190	0.2740	−0.5750
0.7754	0.8278	2.3539	0.2460	−0.5237
0.8860	0.8151	2.7148	0.1460	−0.3520
1.0000	0.8031	3.2622	0.0000	0.0000
313.15 K				
0.0000	0.9463	1.2883	0.0000	0.0000
0.0875	0.9282	1.3120	0.0530	−0.0772
0.1775	0.9108	1.3412	0.1070	−0.1517
0.2701	0.8939	1.3763	0.1790	−0.2232
0.3653	0.8776	1.4323	0.2560	−0.2771
0.4633	0.8622	1.4823	0.2940	−0.3400
0.5643	0.8476	1.5537	0.3100	−0.3850
0.6683	0.8336	1.6675	0.3060	−0.3910
0.7754	0.8205	1.8341	0.2550	−0.3480
0.8860	0.8081	2.0595	0.1520	−0.2500
1.0000	0.7964	2.4409	0.0000	0.0000
323.15 K				
0.0000	0.9378	1.0824	0.0000	0.0000
0.0875	0.9198	1.1114	0.0640	−0.0460
0.1775	0.9028	1.1526	0.1110	−0.0820
0.2701	0.8859	1.1689	0.1950	−0.1450
0.3653	0.8700	1.1921	0.2550	−0.2035
0.4633	0.8547	1.2236	0.3060	−0.2560
0.5643	0.8401	1.2801	0.3360	−0.2860
0.6683	0.8263	1.3552	0.3390	−0.3000
0.7754	0.8132	1.4811	0.2930	−0.2660
0.8860	0.8011	1.6708	0.1770	−0.1710
1.0000	0.7898	1.9396	0.0000	0.0000
I.A.A (1)+2-E.E (2) 303.15 K				
0.0000	0.9195	1.6226	0.0000	0.0000
0.1020	0.9061	1.6885	0.0313	−0.1013

Table 2 continued

Mole fraction of I.A.A (x_1)	$\rho \times 10^{-3}$ ($kg \cdot m^{-3}$)	η(mPa · s)	$V^E \times 10^6$ ($m^3 \cdot mol^{-1}$)	$\Delta\eta$(mPa · s)
0.2036	0.8929	1.7610	0.0750	−0.1953
0.3047	0.8801	1.8121	0.1288	−0.3101
0.4053	0.8677	1.8916	0.1644	−0.3956
0.5055	0.8558	1.9937	0.1920	−0.4578
0.6053	0.8443	2.1244	0.2020	−0.4906
0.7046	0.8333	2.3012	0.1973	−0.4767
0.8035	0.8228	2.4957	0.1560	−0.4443
0.9020	0.8126	2.8067	0.1040	−0.2947
1.0000	0.8031	3.2622	0.0000	0.0000
313.15 K				
0.0000	0.9120	1.3554	0.0000	0.0000
0.1020	0.8986	1.3851	0.0385	−0.0810
0.2036	0.8856	1.4245	0.0796	−0.1518
0.3047	0.8729	1.4688	0.1320	−0.2173
0.4053	0.8605	1.5295	0.1740	−0.2659
0.5055	0.8487	1.6041	0.1976	−0.3001
0.6053	0.8373	1.6804	0.2087	−0.3320
0.7046	0.8264	1.8119	0.2008	−0.3084
0.8035	0.8159	1.9451	0.1698	−0.2825
0.9020	0.8058	2.1431	0.1156	−0.1760
1.0000	0.7964	2.4409	0.0000	0.0000
323.15 K				
0.0000	0.9038	1.1432	0.0000	0.0000
0.1020	0.8905	1.1695	0.0400	−0.0550
0.2036	0.8777	1.1963	0.0830	−0.1090
0.3047	0.8651	1.2221	0.1370	−0.1637
0.4053	0.8530	1.2627	0.1790	−0.2033
0.5055	0.8413	1.3098	0.2020	−0.2360
0.6053	0.8300	1.3771	0.2180	−0.2482
0.7046	0.8192	1.4598	0.2090	−0.2445
0.8035	0.8088	1.5657	0.1850	−0.2174
0.9020	0.7990	1.7275	0.1230	−0.1340
1.0000	0.7898	1.9396	0.0000	0.0000
I.A.A (1) + 2-B.E (2) 303.15 K				
0.0000	0.8920	2.4864	0.0000	0.0000
0.1297	0.8822	2.4826	0.0142	−0.1043
0.2510	0.8725	2.4959	0.0282	−0.1852
0.3649	0.8631	2.5135	0.0370	−0.2560
0.4720	0.8539	2.5572	0.0400	−0.2953
0.5728	0.8450	2.5937	0.0364	−0.3370

Table 2 continued

Mole fraction of I.A.A (x_1)	$\rho \times 10^{-3}$ ($kg \cdot m^{-3}$)	η(mPa · s)	$V^E \times 10^6$ ($m^3 \cdot mol^{-1}$)	$\Delta\eta$(mPa · s)
0.6679	0.8386	2.6532	0.0313	−0.3514
0.7578	0.8277	2.7480	0.0231	−0.3262
0.8428	0.8193	2.8774	0.0158	−0.2629
0.9235	0.8111	3.0576	0.0080	−0.1452
1.0000	0.8031	3.2622	0.0000	0.0000
313.15 K				
0.0000	0.8842	1.9788	0.0000	0.0000
0.1297	0.8745	1.9694	0.0165	−0.0693
0.2510	0.8654	1.9674	0.0335	−0.1274
0.3649	0.8561	1.9873	0.0422	−0.1601
0.4720	0.8472	1.9969	0.0460	−0.2002
0.5728	0.8379	2.0284	0.0449	−0.2151
0.6679	0.8295	2.0671	0.0368	−0.2204
0.7578	0.8210	2.1207	0.0294	−0.2083
0.8428	0.8125	2.2001	0.0195	−0.1682
0.9235	0.8046	2.3034	0.0092	−0.1021
1.0000	0.7964	2.4409	0.0000	0.0000
323.15 K				
0.0000	0.8775	1.6525	0.0000	0.0000
0.1297	0.8677	1.6233	0.0190	−0.0664
0.2510	0.8582	1.6286	0.0356	−0.0960
0.3649	0.8488	1.6363	0.0495	−0.1209
0.4720	0.8398	1.6498	0.0540	−0.1382
0.5728	0.8310	1.6729	0.0514	−0.1440
0.6679	0.8223	1.7022	0.0473	−0.1420
0.7578	0.8139	1.7371	0.0383	−0.1329
0.8428	0.8057	1.7985	0.0280	−0.0960
0.9235	0.7976	1.8507	0.0190	−0.0669
1.0000	0.7898	1.9396	0.0000	0.0000

I.A.A Isoamyl alcohol, *2-M.E* 2-methoxyethanol, *2-E.E* 2-ethoxyethanol, *2-B.E* 2-butoxyethanol

3.2 Viscosity Deviations

The viscosity deviations ($\Delta\eta$) from a linear dependence on mole fraction were calculated [13] by

$$\Delta\eta = \eta - \sum_{i=1}^{2} x_i \eta_i \tag{2}$$

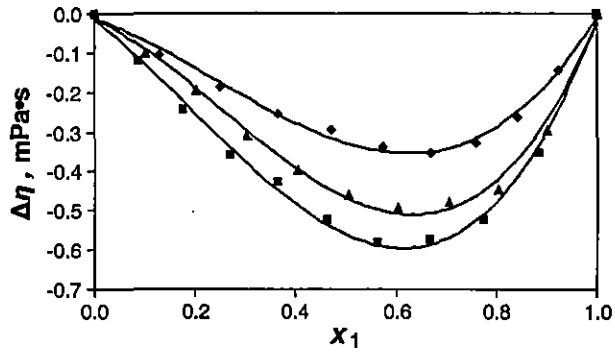

Fig. 2 Plots of viscosity deviations, $\Delta\eta$(mPa · s) against mole fraction (x_1) of isoamyl alcohol with 2-methoxyethanol (■), 2-ethoxyethanol (▲), and 2-butoxyethanol (◆) at 303.15 K

where η is the viscosity of the mixture and x_i and η_i are the mole fraction and viscosity of pure component i, respectively.

Deviations in viscosity ($\Delta\eta$) for the mixture of I.A.A with alkoxyethanols are negative as depicted in Fig. 2, and the magnitude of the negative deviation increases with the increasing chain length of alkoxyalkanols. The trend in negative deviation of $\Delta\eta$ is 2-M.E > 2-E.E > 2-B.E at 303.15 K and also at higher temperatures. The $\Delta\eta$ values show a systematic increase with increase in temperature for the binary mixtures. Similar results have been reported earlier [11]. Also, the deviations in $\Delta\eta$ values are found to be opposite to the sign of excess molar volumes V^{E} for all three binary mixtures, which is in agreement with the view proposed by Brocos et al. [14, 15]. A correlation between the sign of $\Delta\eta$ and V^{E} (Table 2) has been observed for a number of binary solvent systems [16, 17], i.e., $\Delta\eta$ is positive when V^{E} is negative and vice-versa.

3.3 Deviations in Isentropic Compressibility

The isentropic compressibility, K_S, and deviation in isentropic compressibility, ΔK_S, were calculated using the following relations:

$$K_S = (u^2\rho)^{-1} \tag{3}$$

$$\Delta K_S = K_S - \sum_{i=1}^{2} x_i K_{Si} \tag{4}$$

where u and K_S are the speed of sound and isentropic compressibility of the mixture, respectively, and K_{Si} is the isentropic compressibility of the ith component in the mixture. The experimental speed of sound, isentropic compressibility, and deviation in isentropic compressibility are listed in Table 3 and are graphically represented in Fig. 3 as a function of mole fraction of I.A.A. From Fig. 3, it is evident that the ΔK_S values are positive and the magnitude of the positive values decreases with increasing chain length of the alcohols. The order of ΔK_S values is: 2-M.E > 2-E.E > 2-B.E.

Table 3 Experimental values of ultrasonic speed, u, isentropic compressibility, K_S, deviation in isentropic compressibility, ΔK_S, refractive index, n_D, and excess molar refraction, ΔR, for the binary mixtures at 303.15 K

Mole fraction of I.A.A (x_1)	u ($m \cdot s^{-1}$)	$K_S \times 10^{12}$ (Pa^{-1})	$\Delta K_S \times 10^{12}$ (Pa^{-1})	n_D	$\Delta R \times 10^{-6}$ ($m^3 \cdot mol^{-1}$)
I.A.A (1)+2-M.E (2) 303.15 K					
0.0000	1324.3	595.9	0.0	1.3983	0.0000
0.0875	1312.1	619.1	21.1	1.3988	0.0076
0.1775	1299.2	643.6	39.2	1.3993	0.0137
0.2701	1287.4	668.0	52.6	1.3999	0.0314
0.3653	1274.8	694.0	62.2	1.4004	0.0412
0.4633	1261.2	721.9	67.6	1.4009	0.0513
0.5643	1248.8	749.2	66.8	1.4014	0.0540
0.6683	1235.7	778.3	60.5	1.4020	0.0600
0.7754	1223.3	807.3	47.5	1.4025	0.0545
0.8860	1210.5	837.2	27.5	1.4030	0.0322
1.0000	1197.4	868.5	0.0	1.4035	0.0000
I.A.A (1)+2-E.E (2) 303.15 K					
0.0000	1301.5	1301.5	0.0	1.4065	0.0000
0.1020	1292.4	1292.4	16.8	1.4062	0.0175
0.2036	1282.4	1282.4	31.0	1.4059	0.0290
0.3047	1272.7	1272.7	41.3	1.4055	0.0392
0.4053	1262.9	1262.9	47.9	1.4052	0.0432
0.5055	1251.2	1251.2	51.6	1.4049	0.0396
0.6053	1240.6	1240.6	50.3	1.4046	0.0320
0.7046	1229.3	1229.3	44.9	1.4043	0.0223
0.8035	1219.2	1219.2	34.5	1.4040	0.0148
0.9020	1208.7	1208.7	19.6	1.4037	0.0065
1.0000	1197.4	1197.4	0.0	1.4035	0.0000
I.A.A (1)+2-B.E (2) 303.15 K					
0.0000	1288.4	675.3	0.0	1.4150	0.0000
0.1297	1279.8	692.1	14.6	1.4138	0.0136
0.2510	1270.3	710.2	26.2	1.4127	0.0194
0.3649	1261.8	727.7	33.3	1.4115	0.0223
0.4720	1251.8	747.3	38.0	1.4104	0.0221
0.5728	1242.3	766.8	39.1	1.4093	0.0208
0.6679	1233.5	785.9	36.7	1.4080	0.0176
0.7578	1224.2	806.1	31.7	1.4069	0.0140
0.8428	1215.3	826.4	23.7	1.4058	0.0116
0.9235	1206.4	847.1	13.1	1.4047	0.0047
1.0000	1197.4	868.4	0.0	1.4035	0.0000

I.A.A Isoamyl alcohol, *2-M.E* 2-methoxyethanol, *2-E.E* 2-ethoxyethanol, *2-B.E* 2-butoxyethanol

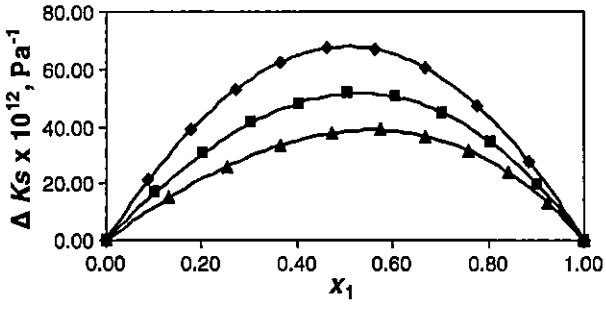

Fig. 3 Plots of deviation in isentropic compressibility $\Delta K_S \times 10^{12}(\mathrm{Pa}^{-1})$ against mole fraction (x_1) of isoamyl alcohol with 2-methoxyethanol (♦), 2-ethoxyethanol (■), and 2-butoxyethanol (▲) at 303.15 K

3.4 Excess Molar Refraction

The molar refraction, $[R]$, can be evaluated from the Lorentz–Lorenz relation [18] and gives more information than n_D about mixture phenomena because it takes into account the electronic perturbation of a molecular orbital during the liquid mixture process and $[R]$ is also directly related to the dispersion forces,

$$[R] = \left(n_D^2 - 1/n_D^2 + 2\right)(M/\rho) \tag{5}$$

where $[R]$, n_D^2, and M are, respectively, the molar refraction, the refractive index, and the molar mass of the mixture. Deviations for the molar refraction were calculated from the following relation:

$$M = x_1 M_1 + (1 - x_1) M_2 \tag{6}$$

$$\Delta R = [R] - (x_1[R]_1 + x_2[R]_2) \tag{7}$$

The value of ΔR is positive (Table 3) for all systems indicating that the dispersion forces are higher in the mixture than in the pure liquids. The deviations in refractive

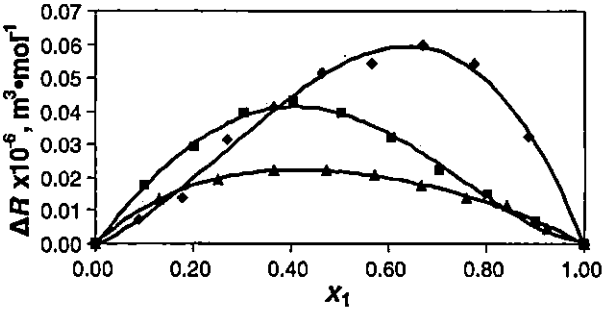

Fig. 4 Plots of molar refraction $\Delta R \times 10^{-6}(\mathrm{m}^3 \cdot \mathrm{mol}^{-1})$ against mole fraction (x_1) of isoamyl alcohol with 2-methoxyethanol (♦), 2-ethoxyethanol (■), and 2-butoxyethanol (▲) at 303.15 K

indices are shown in Fig. 4. The ΔR values for the binary mixtures under study follows the order 2-M.E > 2-E.E > 2-B.E with a maximum at around $x_1 \sim 0.3$ to 0.4.

4 Conclusion

After a thorough study of the behavior of alkoxyethanols and isoamyl alcohol, we get a clear idea about the molecular interactions between the components and it was found that the interactions between the solvent molecules increase with increasing chain length of alkoxyethanols.

Acknowledgment The authors are grateful to the Departmental Special Assistance Scheme under the University Grants Commission, New Delhi (No. 540/6/DRS/2002, SAP-1) for financial support.

References

1. C.R. Reid, B.E. Poling, *The Properties of Gases and Liquids* (McGraw Hill, New York, 1998), Chap. 1
2. E. Perez, M. Cardoso, A.M. Mainar, J.I. Pardo, J.S. Urieta, J. Chem. Eng. Data **48**, 1306 (2003)
3. J.N. Nayak, T.M. Aminabhavi, M.I. Aralaguppi, J. Chem. Eng. Data **48**, 1152 (2003)
4. N.V. Sastry, S.R. Patel, Int. J. Thermophys. **21**, 1153 (2000)
5. M.N. Roy, A. Choudhury, A. Sinha, J. Teach. Res. Chem **11**, 12 (2004)
6. D.K. Hazra, M.N. Roy, B. Das, Indian J. Chem. Technol. **1**, 93 (1994)
7. M.N. Roy, A. Jha, R. Dey, J. Chem. Eng. Data **46**, 1327 (2001)
8. M.N. Roy, A. Sinha, B. Sinha, J. Sol. Chem. **34**, 1319 (2005)
9. P.S. Nikam, L.N. Shirsat, M. Hasan, J. Indian Chem. Soc. **77**, 244 (2000)
10. B.K. Ujjan, P.H Apoorva, B.S. Arun, H. Mehdi, J. Chem. Eng. Data **51**, 60 (2006)
11. T.N. Aminabhabi, B. Gopalkrisna, J. Chem. Eng. Data **39**, 529 (1994)
12. M. Singh, J. Ind. Chem. Soc. **79**, 659 (2002)
13. S. Glasstone, K.J. Laidler, H. Eyring, *The Theory of Rate Processes: The Kinetics of Chemical Reactions, Viscosity, Diffusion and Electrochemical Phenomena* (McGraw-Hill, New York, 1941)
14. P. Brocos, A. Pineiro, R. Bravo, A. Amigo, Phys. Chem. Chem. Phys. **5**, 550 (2003)
15. A. Pineiro, P. Brocos, A. Amigo, M. Pintos, R. Bravo, Phys. Chem. Liq. **38**, 251 (2000)
16. D.S. Gill, T.S. Cheema, Z. Phys. Chem. (N.F.) **134**, 205 (1983)
17. Y. Marcus, *Ion Solvation* (Wiley, New York, 1985)
18. V. Minkin, O. Osipov, Y. Zhdanov (eds.), *Dipole Moments in Organic Chemistry* (Plenum Press, New York, London, 1970)
19. M.N. Roy, A. Sinha, Fluid Phase Equilib. **243**, 133 (2006)
20. D. Venkatesulu, P. Venkatesu, M.V.P. Rao, J. Chem. Eng. Data **42**, 365 (1997)
21. I. Mozo, I.G. de la Fuente, J.A. Gonzalez, J.C. Cobos, N. Riesco, J. Chem. Eng. Data **53**, 1404 (2008)

Study of the Solution Properties of Ternary Mixtures of 1,3-Dioxolane (1), Diethyl Ether (2), and *n*-Amyl Alcohol (3) and the Corresponding Binary Mixtures by Density, Viscosity, Refractivity, and Ultrasonic Speed Measurements at 298.15 K†

Radhey Shyam Sah, Biswajit Sinha, and Mahendra Nath Roy*

Department of Chemistry, University of North Bengal, Darjeeling 734013, West Bengal, India

The excess molar volume (V^E), viscosity deviation ($\Delta\eta$), deviation in isentropic compressibility (ΔK_S), and excess molar refractivity (ΔR) have been investigated using experimentally measured densities, viscosities, speeds of sound, and refractive indices for the three binary mixtures 1,3-dioxolane (1) + diethyl ether (2), diethyl ether (1) + *n*-amyl alcohol (2), and 1,3-dioxolane (1) + *n*-amyl alcohol (2) and the corresponding ternary mixture 1,3-dioxolane (1) + diethyl ether (2) + *n*-amyl alcohol (3) at 298.15 K. The calculated quantities were further fitted to the Redlich–Kister equation to estimate the binary fitting parameters and standard deviations from the regression lines. The excess or deviation properties were found to be either negative or positive depending on the molecular interactions and the nature of the liquid mixtures.

Introduction

A knowledge of densities, excess volumes, and viscosities of fluids and fluid mixtures is essential for understanding the molecular interactions between unlike molecules and developing new theoretical models as well as for engineering applications in the process industry. Ultrasonic methods have found extensive applications because of their ability to characterize the physicochemical behavior of liquid systems from absorption and velocity data. It is also possible to investigate molecular packing, molecular motion, and various types and extents of intermolecular interactions influenced by the size, shape, and chemical nature of the component molecules and the microscopic structures of the liquids.

Amyl alcohols are used fundamentally for the composition of perfumes and the synthesis of fruit essences. They are also used as solvents for surfaces and lacquer baths, inks for print, and dyes for wool as well as in the chemical production of photographic and pharmaceutical substances. Furthermore, they are an intermediate in the production of amyl acetate and other amyl esters. 1,3-Dioxolane is a versatile solvent that is used in the separation of saturated and unsaturated hydrocarbons and in pharmaceutical synthesis and also serves as a solvent for many polymers.[1,2]

Ethers such as diethyl ether are regarded as ideal potential fuel alternatives or additives, which have good combustion characteristics. The investigation of the thermophysical properties is very important for the increased applications of oxygenated fuels or fuel additives. Considering all of these aspects, we undertook investigations of the thermodynamic and transport properties of binary and ternary mixtures involving 1,3-dioxolane (1,3-DO), diethyl ether (DEE), and *n*-amyl alcohol (AL).

In this paper, we report excess molar volumes (V^E), viscosity deviations ($\Delta\eta$), deviations in isentropic compressibility (ΔK_S), and excess molar refractivities (ΔR) for the three binary mixtures 1,3-DO (1) + DEE (2), 1,3-DO (1) + AL (2), and DEE (1) + AL (2) and the corresponding ternary mixture 1,3-DO (1) + DEE (2) + AL (3) at 298.15 K over the entire range of composition. The excess or deviation properties of the binary mixtures were fitted to the Redlich–Kister polynomial equation to obtain their coefficients and have been interpreted in terms of molecular interactions and structural effects.

Experimental Section

Materials. 1,3-Dioxolane (CAS no. 646-06-0), *n*-amyl alcohol (CAS no. 71-41-0), and diethyl ether (CAS no. 60-29-7) with minimum mass fraction purities of 0.99 used in this study were purchased from S.D.Fine-Chem Ltd. (Mumbai, India). The pure chemicals were stored over activated 4 Å molecular sieves to reduce their water content before use. The purity of each substance was evaluated by comparing experimental values of density, viscosity, speed of sound, and refractive index with those reported in the literature whenever available, as presented in Table 1.

Apparatus and Procedures. Densities (ρ) were measured with an Ostwald–Sprengel-type pycnometer having a bulb volume of about 25 cm^3 and a capillary internal diameter of about 0.1 cm. The measurements were done in a thermostat bath controlled to ± 0.01 K. Viscosity (η) was measured by means of a suspended Ubbelohde-type viscometer calibrated at 298.15 K with triply distilled water and purified methanol using density and viscosity values from the literature. The flow times were accurate to ± 0.1 s, and the uncertainty in the viscosity measurements was ± $2 \cdot 10^{-4}$ mPa·s. The mixtures were prepared by mixing known volumes of the pure liquids in airtight stopper bottles, and each solution thus prepared was distributed into three receptacles to perform all of the measurements in triplicate, with the aim of determining possible dispersion of the obtained results. Adequate precautions were taken to minimize evaporation losses during the actual measurements. The reproducibility of the mole fraction was within ± 0.0002. The mass measurements were done on a Mettler AG-285 electronic balance with a precision of ± 0.01 mg. The precision of the density measurements was ± $3 \cdot 10^{-4}$ g·cm^{-3}.

Ultrasonic speeds of sound (u) were determined using a multifrequency ultrasonic interferometer (M-81, Mittal Enterprises, New Delhi, India) working at 1 MHz that had been calibrated with triply distilled and purified water, methanol, and benzene at 303.15 K. The precision of the ultrasonic speed measurements was ± 0.2 m·s^{-1}. The details of the methods and techniques have been described in earlier papers.[3–5]

† Part of the "Sir John S. Rowlinson Festschrift".

* Corresponding author. Tel.: +91 353 2776381. Fax: +91 353 2699001. E-mail: mahendraroy2002@yahoo.co.in.

10.1021/je100594u
Published on Web 08/26/2010

Table 1. Densities (ρ), Viscosities (η), Speeds of Sound (u), and Refractive Indices (n_D) of the Pure Liquids at T = 298.15 K

	$10^{-3}\cdot\rho$/kg·m^{-3}		η/mPa·s		u/m·s^{-1}		n_D	
liquid	exptl	lit	exptl	lit	exptl	lit	exptl	lit
1,3-DO	1.0587	1.0586[14]	0.589	0.5886[14]	1339.4	1338.8[15]	1.3985	1.398[16]
AL	0.8112	0.8110[17]	3.504	3.510[18]	1271.6	1274.1[19]	1.4100	1.409[20]
DEE	0.7083	0.7083[21]	0.247	–	982.3	983[21]	1.3515	–

Table 2. Densities (ρ), Viscosities (η), Excess Molar Volumes (V^E), and Viscosity Deviations ($\Delta\eta$) for Binary Mixtures of 1,3-Dioxolane, Diethyl Ether, and n-Amyl Alcohol at T = 298.15 K

	$10^{-3}\cdot\rho$	η	$10^6\cdot V^E$	$\Delta\eta$
x_1	kg·m^{-3}	mPa·s	m^3·mol^{-1}	mPa·s
	1,3-Dioxolane (1) + Diethyl Ether (2)			
0.0000	0.7083	0.247	0.000	0.000
0.1000	0.7364	0.266	−0.533	−0.016
0.2000	0.7656	0.284	−0.905	−0.031
0.3001	0.7963	0.306	−1.176	−0.044
0.4001	0.8290	0.331	−1.381	−0.053
0.5001	0.8634	0.360	−1.480	−0.058
0.6001	0.8997	0.394	−1.480	−0.058
0.7001	0.9382	0.435	−1.400	−0.052
0.8000	0.9770	0.478	−1.072	−0.043
0.9000	1.0184	0.531	−0.694	−0.025
1.0000	1.0587	0.589	0.000	0.002
	1,3-Dioxolane (1) + n-Amyl Alcohol (2)			
0.0000	0.8112	3.504	0.000	0.000
0.1168	0.8329	2.505	−0.287	−0.659
0.2293	0.8545	1.885	−0.414	−0.951
0.3377	0.8766	1.440	−0.460	−1.080
0.4424	0.8992	1.063	−0.440	−1.152
0.5434	0.9225	0.906	−0.377	−1.014
0.6409	0.9468	0.756	−0.290	−0.880
0.7352	0.9725	0.647	−0.213	−0.714
0.8264	0.9993	0.570	−0.117	−0.525
0.9146	1.0282	0.541	−0.058	−0.297
1.0000	1.0587	0.589	0.000	0.000
	Diethyl Ether (1) + n-Amyl Alcohol (2)			
0.0000	0.8112	3.504	0.000	0.000
0.1167	0.8052	2.651	−0.750	−0.384
0.2292	0.7975	1.966	−1.250	−0.714
0.3377	0.7889	1.491	−1.575	−0.847
0.4423	0.7797	1.123	−1.788	−0.884
0.5433	0.7704	0.829	−1.950	−0.859
0.6409	0.7595	0.620	−1.860	−0.761
0.7352	0.7479	0.481	−1.638	−0.602
0.8263	0.7361	0.382	−1.345	−0.413
0.9146	0.7230	0.314	−0.820	−0.203
1.0000	0.7083	0.247	0.000	0.000

Refractive indices (n_D) were measured with the help of an Abbe refractometer. The accuracy of the refractive index measurements was ± 0.0002 units. The refractometer was calibrated twice using distilled and deionized water, and the calibration was checked after every few measurements.

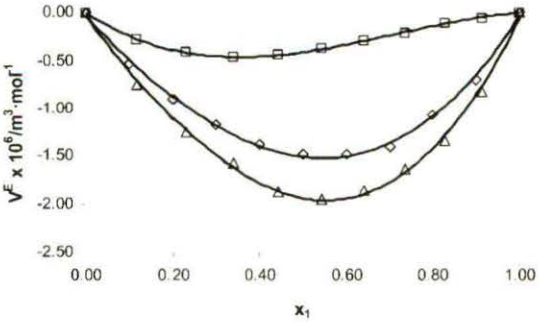

Figure 1. Excess molar volumes $V^E\cdot10^6$/m^3·mol^{-1} as functions of mole fraction (x_1) for the three binary subsystems at T = 298.15 K: □, 1,3-dioxolane (1) + n-amyl alcohol (2); ◇, 1,3-dioxolane (1) + diethyl ether (2); △, diethyl ether (1) + n-amyl alcohol (2).

Results and Discussion

We calculated excess molar volumes (V^E), viscosity deviations ($\Delta\eta$), deviations in isentropic compressibility (ΔK_S), and excess molar refractivities (ΔR) at 298.15 K for binary mixtures of diethyl ether, dichloromethane, and n-amyl alcohol over the whole composition range. The variations of the excess properties over the entire range of composition for the binary mixtures are depicted in Figures 1−4.

Excess Molar Volume. Density (ρ) values were used to calculate the excess molar volumes (V^E) for binary (n = 2) and ternary (n = 3) mixtures using the following equation:[6]

$$V^E = \sum_{i=1}^{n} x_i M_i \left(\frac{1}{\rho} - \frac{1}{\rho_i}\right) \quad (1)$$

where ρ is the density of the mixture and M_i, x_i, and ρ_i are the molar mass, mole fraction, and density, respectively, of the ith component in the mixture.

V^E is the result of contributions from several opposing effects. These may be divided arbitrarily into three types, namely, physical, chemical, and structural. Physical contributions, which are nonspecific interactions between the real species present in the mixture, make a positive contribution to V^E. Chemical or specific intermolecular interactions result in a volume decrease, resulting in a negative contribution to V^E. Structural contributions are mostly negative and arise from several effects, especially from interstitial accommodation and changes in free volume.[7]

The values of V^E were found to be negative for all of the binary mixtures, as reported in Table 2 and depicted graphically in Figure 1; the order of the negative deviations is schematically depicted below:

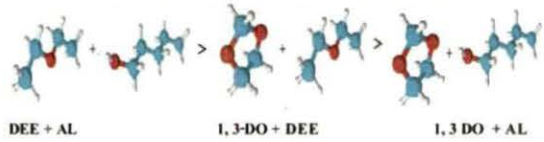

These phenomena result from differences in the energies of interaction between the molecules and packing effects. Disruption of the ordered structure of the pure component during

Table 3. Densities (ρ), Viscosities (η), Excess Molar Volumes (V^E), and Viscosity Deviations ($\Delta\eta$) for Ternary Mixtures of 1,3-Dioxolane (1) + Diethyl Ether (2) + n-Amyl Alcohol (3) at T = 298.15 K

		$10^{-3}\cdot\rho$	η	$10^6\cdot V^E$	$\Delta\eta$
x_1	x_2	kg·m^{-3}	mPa·s	m^3·mol^{-1}	mPa·s
0.5001	0.4999	0.8634	0.360	−1.480	−0.058
0.4574	0.4572	0.8602	0.431	−1.595	−0.121
0.4132	0.4131	0.8567	0.480	−1.668	−0.222
0.3676	0.3675	0.8525	0.552	−1.680	−0.322
0.3205	0.3204	0.8477	0.651	−1.608	−0.421
0.2717	0.2716	0.8424	0.759	−1.476	−0.543
0.2212	0.2211	0.8367	0.966	−1.293	−0.607
0.1689	0.1688	0.8307	1.243	−1.046	−0.654
0.1146	0.1146	0.8246	1.682	−0.770	−0.609
0.0584	0.0584	0.8181	2.304	−0.424	−0.476
0.0000	0.0000	0.8112	3.404	0.000	0.000

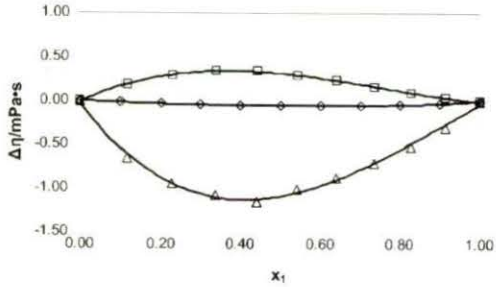

Figure 2. Viscosity deviations $\Delta\eta$/m·Pa s as functions of mole fraction (x_1) for the three binary subsystems at $T = 298.15$ K: □, 1,3-dioxolane (1) + *n*-amyl alcohol (2); ◇, 1,3-dioxolane (1) + diethyl ether (2); △, diethyl ether (1) + *n*-amyl alcohol (2).

Table 4. Ultrasonic Speeds (u), Isentropic Compressibilities (K_S), Deviations in Isentropic Compressibility (ΔK_S), Refractive Indices (n_D), and Excess Molar Refractivities (ΔR) for Binary Mixtures of 1,3-Dioxolane, Diethyl Ether, and *n*-Amyl Alcohol at $T = 298.15$ K

x_1	u / m·s^{-1}	$10^{12}\cdot K_S$ / Pa^{-1}	$10^{12}\cdot\Delta K_S$ / Pa^{-1}	n_D	$10^{-6}\cdot\Delta R$ / m^3·mol^{-1}
		1,3-Dioxolane (1) + Diethyl Ether (2)			
0.0000	982.3	1463.2	0.00	1.3515	0.0000
0.1000	1003.9	1347.5	−22.0	1.3568	−0.0390
0.2000	1033.4	1223.1	−52.7	1.3604	−0.0781
0.3001	1067.4	1102.1	−80.0	1.3649	−0.1054
0.4001	1108.5	981.7	−106.7	1.3696	−0.1268
0.5001	1152.8	871.6	−123.2	1.3743	−0.1460
0.6001	1191.4	783.1	−118.0	1.3791	−0.1520
0.7001	1230.9	703.5	−104.0	1.3842	−0.1320
0.8000	1265.3	639.3	−74.5	1.3893	−0.1000
0.9000	1302.4	578.9	−41.3	1.3956	−0.0530
1.0000	1339.4	526.5	0.0	1.3985	0.0000
		1,3-Dioxolane (1) + *n*-Amyl Alcohol (2)			
0.0000	1271.6	762.4	0.0	1.4100	0.0000
0.1168	1278.8	734.2	−0.7	1.4085	−0.1038
0.2293	1287.5	705.9	−2.4	1.4072	−0.1510
0.3377	1296.8	678.3	−4.4	1.4060	−0.1715
0.4424	1305.0	653.0	−5.0	1.4050	−0.1616
0.5434	1313.4	628.4	−5.8	1.4040	−0.1365
0.6409	1321.5	604.8	−6.4	1.4030	−0.1054
0.7352	1327.1	583.9	−5.1	1.4022	−0.0730
0.8264	1332.7	563.4	−4.1	1.4010	−0.0415
0.9146	1337.0	544.1	−2.5	1.4000	−0.0121
1.0000	1339.5	526.5	−0.0	1.3985	0.0000
		Diethyl Ether (1) + *n*-Amyl Alcohol (2)			
0.0000	1271.6	762.4	0.0	1.4100	0.0000
0.1167	1241.8	803.5	−40.7	1.4043	−0.1830
0.2292	1216.7	846.3	−76.7	1.3977	−0.2680
0.3377	1193.9	889.3	−109.7	1.3922	−0.2740
0.4423	1172.2	933.3	−139.0	1.3874	−0.2480
0.5433	1141.6	996.6	−146.5	1.3825	−0.2054
0.6409	1110.7	1068.2	−143.3	1.3774	−0.1430
0.7352	1077.3	1152.1	−125.5	1.3724	−0.0720
0.8263	1046.3	1240.8	−100.7	1.3664	−0.0350
0.9146	1011.2	1350.8	−52.5	1.3601	−0.0070
1.0000	982.3	1463.2	0.0	1.3515	0.0000

formation of the mixture leads to a positive effect on excess volume, while formation of order in the mixture leads to a negative contribution. The negative V^E values indicate the specific interactions, such as intermolecular hydrogen bonding and interstitial accommodation of the mixing components because of the difference in molar volumes.

The ρ and V^E values for the ternary mixture 1,3-DO (1) + DEE (2) + AL (3) are reported in Table 3. The V^E values are negative in the low mole fraction region for AL, suggesting a specific intermolecular interaction between the two components 1,3-DO (1) and DEE (2), but as the mole

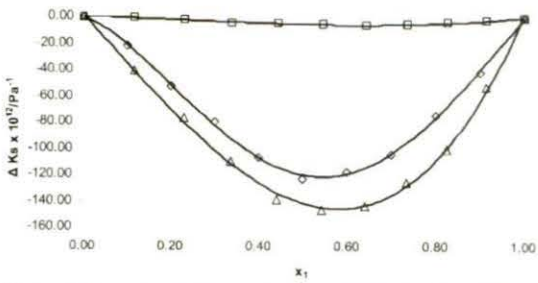

Figure 3. Deviations in isentropic compressibility $\Delta K_s \cdot 10^{12}$/Pa^{-1} as functions of mole fraction (x_1) for the three binary subsystems at $T = 298.15$ K: □, 1,3-dioxolane (1) + *n*-amyl alcohol (2); ◇, 1,3-dioxolane (1) + diethyl ether (2); △, diethyl ether (1) + *n*-amyl alcohol (2).

Table 5. Ultrasonic Speeds (u), Isentropic Compressibilities (K_S), Deviations in Isentropic Compressibility (ΔK_S), Refractive Indices (n_D), and Excess Molar Refractivities (ΔR) for Ternary Mixtures of 1,3-Dioxolane (1) + Diethyl Ether (2) + *n*-Amyl Alcohol (3) at $T = 298.15$ K

x_1	x_2	u / m·s^{-1}	$10^{12}\cdot K_S$ / Pa^{-1}	$10^{12}\cdot\Delta K_S$ / Pa^{-1}	n_D	$10^{-6}\cdot\Delta R$ / m^3·mol^{-1}
0.5001	0.4999	1149.2	877.0	−83.7	1.3750	−0.1081
0.4574	0.4572	1165.9	858.4	−88.7	1.3775	0.0710
0.4132	0.4131	1183.4	843.3	−92.7	1.3805	0.1540
0.3676	0.3675	1196.6	828.9	−89.0	1.3850	0.2608
0.3205	0.3204	1207.6	815.9	−80.5	1.3875	0.3340
0.2717	0.2716	1213.9	805.6	−64.5	1.3925	0.3829
0.2212	0.2211	1224.6	796.9	−53.2	1.3945	0.3600
0.1689	0.1688	1235.8	788.3	−41.1	1.3980	0.3049
0.1146	0.1146	1246.7	780.3	−27.6	1.4005	0.1720
0.0584	0.0584	1258.2	772.2	−13.4	1.4035	0.0140
0.0000	0.0000	1271.6	762.4	0.00	1.4100	0.0000

fraction of AL in the ternary mixture increases, the magnitude of V^E decreases, suggesting that dispersion forces now begin to operate. Thus, it can be said that the addition of AL to a binary mixture of 1,3-DO (1) and DEE (2) causes a decrease in the intermolecular interactions between the mixture components.

Viscosity Deviation. The measured η values for binary systems are listed in Table 2 and depicted graphically in Figure 2. The viscosity deviations ($\Delta\eta$) from a linear dependence for binary ($n = 2$) and ternary ($n = 3$) mixtures can be calculated as[13]

$$\Delta\eta = \eta - \sum_{i=1}^{n} x_i\eta_i \qquad (2)$$

where η is the viscosity of the mixture and x_i and η_i are the mole fraction and viscosity, respectively, of pure component i.

The values of $\Delta\eta$ over entire range of mole fraction for the binary mixtures follow the trend which is schematically shown below:

The trend in the deviations of the $\Delta\eta$ values was found to be the opposite of that in the V^E values for all three binary mixtures, in agreement with the view proposed by Brocos et al.[8] The values of $\Delta\eta$ for the ternary mixture are listed in Table 3. For

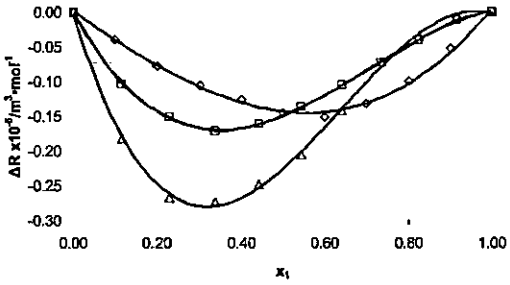

Figure 4. Excess molar refractivities $\Delta R \cdot 10^{-6}/m^3 \cdot mol^{-1}$ as functions of mole fraction (x_1) for the for the three binary subsystems at $T = 298.15$ K: □, 1,3-dioxolane (1) + *n*-amyl alcohol (2); ◇, 1,3-dioxolane (1) + diethyl ether (2); △, diethyl ether (1) and *n*-amyl alcohol (2).

Table 6. Redlich–Kister Coefficients (a_n) and Standard Deviations (σ) for the Binary Mixtures at $T = 298.15$ K

excess property	a_0	a_1	a_2	a_3	σ
1,3-Dioxolane (1) + Diethyl Ether (2)					
$10^6 \cdot V^E/m^3 \cdot mol^{-1}$	−5.915	−1.079	−1.113		0.021
$\Delta\eta$/mPa·s	−0.230	−0.056			0.001
$10^{12} \cdot \Delta K_S/Pa^{-1}$	−480.02	−127.24	222.66		1.81
$10^{-6} \cdot \Delta R/m^3 \cdot mol^{-1}$	−0.5842	−0.2040	0.0988	0.1994	0.0024
1,3-Dioxolane (1) + *n*-Amyl Alcohol (2)					
$10^6 \cdot V^E/m^3 \cdot mol^{-1}$	−1.623	1.286	−0.196		0.005
$\Delta\eta$/mPa·s	−3.717	2.154	−0.732	0.356	0.013
$10^{12} \cdot \Delta K_S/Pa^{-1}$	−22.97	−13.39	6.97		0.27
$10^{-6} \cdot \Delta R/m^3 \cdot mol^{-1}$	−0.5995	0.4953			0.0019
Diethyl Ether (1) + *n*-Amyl Alcohol (2)					
$10^6 \cdot V^E/m^3 \cdot mol^{-1}$	−7.480	−1.698	−1.748		0.029
$\Delta\eta$/mPa·s	−3.548	0.820	0.352		0.014
$10^{12} \cdot \Delta K_S/Pa^{-1}$	−574.02	−204.92	69.38		2.30
$10^{-6} \cdot \Delta R/m^3 \cdot mol^{-1}$	−0.8943	1.0672	−0.0883		0.0048

the ternary mixture, the viscosity deviations are negative over the entire range of composition. These can be interpreted qualitatively by considering the effect of the intermolecular interactions and the shapes of the components.

Deviation in Isentropic Compressibility. Isentropic compressibility (K_S) and deviations in isentropic compressibility (ΔK_S) for binary ($n = 2$) and ternary ($n = 3$) mixtures were calculated using the following relations:

$$K_S = (u^2\rho)^{-1} \tag{4}$$

$$\Delta K_S = K_S - \sum_{i=1}^{n} x_i K_{S,i} \tag{5}$$

where u and K_S are the speed of sound and isentropic compressibility, respectively, for the mixture and x_i and $K_{S,i}$ are the mole fraction and isentropic compressibility, respectively, for the ith component in the mixture.

It is evident from Table 4 and Figure 3 that the ΔK_S values for the binary mixtures are negative over the entire composition range and that order of negative deviation is as follows: DEE (1) + AL (2) > 1,3-DO (1) + DEE (2) > 1,3-DO (1) + AL (2). These results can be explained in terms of molecular interactions[9,10] between unlike molecules. It appears from the sign and magnitude of ΔK_S that specific interactions between the mixture components exist. These results are in excellent agreement with those for V^E discussed earlier.

The values of ΔK_S for the ternary mixture (Table 5) are negative over the entire composition range, which suggests that specific interactions exist between the mixture components.[11]

Excess Molar Refractivity. The molar refractivity [R] gives more information than n_D about the mixture phenomenon because it takes into account electronic perturbations of the molecular orbitals during the liquid mixture process; in addition, [R] is directly related to the dispersion forces, It can be evaluated from the Lorentz–Lorenz relation:[12]

$$[R] = \left(\frac{n_D^2 - 1}{n_D^2 + 2}\right)\left(\frac{M}{\rho}\right) \tag{6}$$

where [R], n_D, and M are the molar refractivity, refractive index, and molar mass of the mixture, respectively. The excess molar refractivity was calculated from the following relation:

$$\Delta R = [R] - (x_1[R]_1 + x_2[R]_2) \tag{7}$$

The values of n_D and ΔR for the binary mixtures are presented in Table 4, and the ΔR values are depicted graphically in Figure 4. The data for ternary mixtures are reported in Table 5.

The excess properties (V^E, $\Delta\eta$, ΔK_S, ΔR) for the binary mixtures were fitted to the Redlich–Kister polynomial equation,[13]

$$Y^E = x_1x_2\sum_{n=0}^{K} a_n(x_1 - x_2)^n \tag{8}$$

where Y^E denotes an excess property. The coefficients a_n were obtained by fitting eq 8 to the experimental results using a least-squares regression method. In each case, the optimal number of coefficients, K, was ascertained from an approximation of the variation in the standard deviation. The fitted values of the coefficients along with the standard deviations are summarized for all of the mixtures in Table 6. The standard deviation was calculated using the equation

$$\sigma = \left[\frac{\sum (Y^E_{expl} - Y^E_{calcd})^2}{(N - m)}\right]^{1/2} \tag{9}$$

where N is the number of data points and m is the number of coefficients.

Literature Cited

(1) Janz, G. G.; Tomkins, R. P. T. *Nonaqueous Electrolytes Handbook*; Academic Press: New York, 1973; Vol. 2.
(2) Jasinski, R. *High Energy Batteries*; Plenum Press: New York, 1967.
(3) Hazra, D. K.; Roy, M. N.; Das, B. Densities and viscosities of the binary aqueous mixture of tetrahydrofuran and 1,2-dimethoxyethane at 298, 308, and 318 K. *Indian J. Chem. Technol.* **1994**, *1*, 93–97.
(4) Roy, M. N.; Jha, A.; Dey, R. Study of Ion-Solvent Interactions of Some Alkali Metal Chlorides in Tetrahydrofuran + Water Mixture at Different Temperatures. *J. Chem. Eng. Data* **2001**, *46*, 1327–1329.
(5) Roy, M. N.; Sinha, A.; Sinha, B. Excess Molar Volumes, Viscosity Deviations, and Isentropic Compressibility of Binary Mixtures Containing 1,3-Dioxolane and Monoalcohols at 303.15 K. *J. Solution Chem.* **2005**, *34*, 1311–1325.
(6) Nikam, P. S.; Sawant, A. B. Limiting apparent molar volumes and their temperature derivatives for ammonium, potassium and aluminium sulphates in aqueous DMF. *J. Indian Chem. Soc.* **2000**, *77*, 197–200.
(7) Kharat, S. J.; Nikam, P. S. Density and viscosity studies of binary mixtures of aniline + benzene and ternary mixtures of (aniline + benzene + *N,N*-dimethylformamide) at 298.15, 303.15, 308.15, and 313.15 K. *J. Mol. Liq.* **2007**, *131–132*, 81–86.

(8) Brocos, P.; Pineiro, A.; Bravo, R.; Amigo, A. Refractive indices, molar volumes and molar refractions of binary liquid mixtures: Concepts and correlations. *Phys. Chem. Chem. Phys.* **2003**, *5*, 550–557.

(9) Povey, M. J. W.; Hindle, S. A.; Kennedy, J. D.; Stec, Z.; Taylor, R. G. The molecular basis for sound velocity in *n*-alkanes, 1-alcohols and dimethylsiloxanes. *Phys. Chem. Chem. Phys.* **2003**, *5*, 73–78.

(10) Lafuente, C.; Giner, B.; Villares, A.; Gascon, I.; Cea, P. Speeds of Sound and Isentropic Compressibilities of Binary Mixtures Containing Cyclic Ethers and Haloalkanes at 298.15 and 313.15 K. *Int. J. Thermophys.* **2004**, *25*, 1735–1746.

(11) Aminbhavi, T. M.; Phyade, H. T. S.; Aralaguppi, M. I.; Khinnavar, R. S. Densities, Viscosities, and Speeds of Sound for Diethylene Glycol Dimethyl Ether + Methyl Acetate. *J. Chem. Eng. Data* **1993**, *38*, 540–541.

(12) *Dipole Moments in Organic Chemistry*; Minkin, V., Osipov, O., Zhdanov, Y., Eds.; Plenum Press: New York, 1970.

(13) Gill, D. S.; Kaur, T.; Kaur, H. Ultrasonic velocity, permittivity, density, viscosity and proton nuclear magnetic resonance measurements of binary mixtures of benzonitrile with organic solvents. *J. Chem. Soc., Faraday Trans.* **1993**, *89*, 1737–1740.

(14) Gascon, I.; Mainar, A. M.; Royo, F. M.; Urieta, J. S. Experimental viscosities and viscosity predictions of the ternary mixture (cyclohexane + 1,3-dioxolane + 2-butanol) at 298.15 and 313.15 K. *J. Chem. Eng. Data* **2000**, *45*, 751–755.

(15) Giner, B.; Villares, A.; Gascon, P.; Cea, P.; Lafuente, C. Speeds of sound and isentropic compressibilities of binary mixtures containing cyclic ethers and haloalkanes at 298.15 and 313.15 K. *Int. J. Thermophys.* **2004**, *25*, 1735–1746.

(16) Ottani, S.; Vitalini, D.; Comelli, F.; Castellari, C. Densities, Viscosities, and Refractive Indices of Poly(ethyleneglycol) 200 and 400 + Cyclic Ethers at 303.15 K. *J. Chem. Eng. Data* **2002**, *47*, 1197–1204.

(17) Orge, B.; Iglesias, M.; Marino, G.; Casas, L. M.; Tojo, J. Excess molar volumes of ternary mixtures containing benzene, cyclohexane, 1-pentanol and anisole at 298.15 K. *Phys. Chem. Liq.* **2005**, *43*, 551–557.

(18) Sastry, N. V.; Valand, M. K. Viscosities and Densities for Heptane + 1-Pentanol, + 1-Hexanol, + 1-Heptanol, + 1-Octanol, + 1-Decanol, and + 1-Dodecanol at 298.15 K and 308.15 K. *J. Chem. Eng. Data* **1996**, *41*, 1426–1428.

(19) Mehra, R. Application of refractive index mixing rules in binary systems of hexadecane and heptadecane with *n*-alkanols at different temperatures. *Proc. Indian Acad. Sci. (Chem. Sci.)*. **2003**, *115*, 147–154.

(20) Ribeiro, A. F.; Langa, E.; Mainar, A. M.; Pardo, J. I.; Urieta, J. S. Excess Molar Enthalpy, Density, and Speed of Sound for the Mixtures *β*-Pinene + 1- or 2-Pentanol at (283.15, 298.15, and 313.15) K. *J. Chem. Eng. Data* **2006**, *51*, 1846–1851.

(21) Savaroglu, G.; Aral, E. Excess isocentropic compressibility and speed of sound of the ternary mixture 2-propanol + diethyl ether + *n*-hexane and the constituent binary mixtures at 298.15 K. *Pramana* **2006**, *66*, 435–446.

Received for review May 30, 2010. Accepted August 13, 2010. The authors are grateful to the Departmental Special Assistance Scheme under the University Grants Commission, New Delhi (540/6/DRS/2007, SAP-2) for financial support.

JE100594U

G Model
FLUID 8873 1–6
ARTICLE IN PRESS

Fluid Phase Equilibria xxx (2011) xxx–xxx

Contents lists available at ScienceDirect

Fluid Phase Equilibria

journal homepage: www.elsevier.com/locate/fluid

Ion association and solvation behavior of some alkali metal acetates in aqueous 2-butanol solutions at $T = 298.15$, 303.15 and 308.15 K

Radhey Shyam Sah, Biswajit Sinha, Mahendra Nath Roy*

Department of Chemistry, University of North Bengal, Darjeeling 734013, India

ARTICLE INFO

Article history:
Received 7 April 2011
Received in revised form 17 May 2011
Accepted 25 May 2011
Available online xxx

Keywords:
Alkali metal acetates
Aqueous 2-butanol solution
Limiting molar conductances
Walden products
Preferential solvation

ABSTRACT

Molar conductance of lithium acetate, sodium acetate and potassium acetate were studied in aqueous 2-butanol solutions with an alcohol mass fraction (w_2) of 0.70, 0.80 and 0.90 at 298.15, 303.15 and 308.15 K. The conductance data were analyzed with the Fuoss conductance–concentration equation to evaluate the limiting molar conductances (Λ_0), association constants ($K_{A,c}$) and cosphere diameter (R) for ion-pair formation. Gibbs energy (ΔG^0), enthalpy (ΔH^0) and entropy (ΔS^0) for ion-association reaction were derived from the temperature dependence of $K_{A,c}$. Activation energy for ionic movement ($\Delta H^{\#}$) was derived from the temperature dependence of Λ_0. Based on the composition dependence of Walden products ($\Lambda_0\eta_0$) and different thermodynamic properties (ΔG^0, ΔH^0, ΔS^0 and $\Delta H^{\#}$), the influence of the solvent composition on ion-association and solvation behavior of ions were discussed in terms of ion–solvent, ion–ion interactions and the structural changes in the mixed solvent media.

1. Introduction

The solvation behavior of ions in solutions can be well understood in terms of ion–solvent, ion–ion and solvent–solvent interactions. Ion solvation is one of the most important factors determining the rate and mechanism of various physico-chemical processes occurring in solutions with ionic species as intermediates. Also conductance study of electrolytes over a range of temperature in pure and mixed solvent media provides valuable information about their thermodynamic behavior. Usually a mixture is repeatedly tested by electrolytes with a common ion (anion or cation) to confirm the trend of changes and to reveal the influences of the co-ion on the quantities derived. In such a direction, aqueous binary mixtures of organic solvents with a varying range of composition are most frequently investigated solvent media [1–5]. Also a number of conductometric [6] and related studies of different electrolytes in non-aqueous solvents, specially mixed organic solvents, have been made for their optimal use in high energy batteries [7] and for understanding organic reaction mechanisms [8]. Ionic association of electrolytes in solution depends upon the mode of solvation of its ions [9–17], which in its turn depends on the nature of the solvent or solvent mixtures. Such solvent properties as viscosity and the relative permittivity were taken into consideration as these properties help in determining the extent of ion association and the solvent–solvent interactions.

2-Butanol is a colorless flammable secondary alcohol with limited mutual solubility in water but completely miscible with polar organic solvent such as ethers and other alcohols. It is primarily used as a precursor to the industrial solvent, methyl ethyl ketone. Aqueous 2-butanol mixture is a poorly studied media due to limited mutual solubility of the constituent liquids and conductance study of alkali metal acetates in aqueous 2-butanol mixture is still rare, though the conductance studies on alkali metal halides in aqueous 2-butanol mixtures have been described frequently in the literature [13–17]. Therefore, in the present work an attempt has been undertaken to discuss the molar conductances (Λ) and association constants ($K_{A,c}$) of three alkali metal acetates viz., lithium acetate (LiAc), sodium acetate (NaAc) and potassium acetate (KAc) in aqueous 2-butanol mixtures at 298.15, 303.15 and 308.15 K. The alkali metal acetates were selected, because unlike halides acetate anion is unsymmetrical in structure with both a hydrophilic and hydrophobic end and it may suffer extensive solvation via hydrogen bond interactions [18] in aqueous alcoholic media. Experimental results were treated by Fuoss conductance–concentration equation [19,20] to obtain limiting molar conductance (Λ_0) and association constant ($K_{A,c}$) which served further to calculate the Walden product ($\Lambda_0\eta_0$) and other thermodynamic quantities of

* Corresponding author. Tel.: +91 353 2776381; fax: +91 353 2699001.
E-mail addresses: mahendraroy2002@yahoo.co.in, rinky_027@rediffmail.com (M.N. Roy).

0378-3812/$ – see front matter © 2011 Published by Elsevier B.V.
doi:10.1016/j.fluid.2011.05.017

Table 1
Density (ρ_0), viscosity (η_0), relative permittivity (ε_r) and conductivity (λ_0) of aqueous 2-butanol solutions.

Mass fraction of 2-butanol (w_2)	$\rho_0 \times 10^{-3}$ (kg m^{-3})		η_0 (mPa s)		$\lambda_0 \times 10^{4}$ (S cm^{-1})	ε_r
	This work	Lit[b]	This work	Lit[b]		
	298.15 K					
0.70	0.8638	0.8635	3.342	3.343	14.4 [16]	25.0 [16]
0.80	0.8436	0.8426	3.098	3.099	4.1 [16]	20.0 [16]
0.90	0.8228	0.8216	2.812	2.811	2.3 [16]	16.6 [16]
	303.15 K					
0.70	0.8596	0.8590	2.795	2.796	16.7 [16]	24.3 [16]
0.80	0.8392	0.8382	2.608	2.607	4.5 [16]	19.4 [16]
0.90	0.8188	0.8174	2.375	2.373	2.6 [16]	16.0 [16]
	308.15 K					
0.70	0.8551	0.8545	2.377	2.376	19.3 [16]	23.5 [16]
0.80	0.8348	0.8337	2.216	2.214	5.2 [16]	18.8 [16]
0.90	0.8135	0.8131	2.029	2.027	2.9 [16]	15.4 [16]

the ion-association reaction (ΔG^0, ΔH^0 and ΔS^0). The calculation was further extended to derive the activation energy of the ionic transport ($\Delta H^{\#}$) and described accordingly.

2. Experimental

The alkali metal acetates selected for the present work, i.e., lithium acetate (LiAc), sodium acetate (NaAc) and potassium acetate (KAc) each of A.R. grade (purity >99.5%) were procured from Merck, India and purified as described in the literature [21]. 2-Butanol (A.R. grade, Merck, India, purity >99.5%) was shaken well with anhydrous K_2CO_3 and left over night, next it was distilled at 372 K [21]. The purity of the chemicals, checked by gas–liquid chromatography, were better than 99.8%.

Doubly distilled de-ionized water with a specific conductance $<1 \times 10^{-6}$ S cm^{-1} at 298.15 K was used for preparing the mixed solvents by mass. For the preparation of the solvent mixture required weighted amount of water was transferred to a volumetric flask of 500 ml and the flask was filled up to the mark with 2-butanol at 298.15 K. The relative error in solvent composition was about 1%. Concentrated stock solutions of each electrolyte in the mixed solvents were prepared by mass. For conductance runs the working solutions were obtained by mass dilution of the stock solutions and densities of the solutions were measured with a vibrating-tube density meter (Anton Paar, DMA 4500M), maintained at ±0.01 K of the desired temperatures and calibrated at the experimental temperatures with doubly distilled water and dry air. The uncertainty in density was estimated to be ±0.0001 g cm^{-3}. The density coefficient D (kg^2 dm^{-3} mol^{-1}) was obtained assuming a linear change of solvent density [22] on its molality m following the relation $\rho = \rho_0 + Dm$, where ρ, ρ_0 are the densities of the solutions and solvent mixtures, respectively. The density coefficient was assumed to be temperature invariant but dependent on the nature of the electrolyte and its values were (0.0642, 0.1325, 0.0875) in the solvent mixture with an alcohol mass fraction $w_2 = 0.70$, (0.3429, 0.1789, 0.3621) in the solvent mixture with $w_2 = 0.80$ and (0.3356, 0.3576, 0.6496) in the solvent mixture with $w_2 = 0.90$, respectively for LiAc, NaAc and KAc. These values were used to convert the test solution molality (m) into molarity (c) by means of the relation:

$$c = \frac{1000\ m\rho}{1000 + mM} \quad (1)$$

where M is the molecular weight of alkali metal acetates.

In order to neglect the influence of triple ions or higher ionic aggregations on conductivity, the highest molarity of the working solutions were kept around $c_{max} = 3.2 \times 10^{-7} \varepsilon_r^3$ at 298.15 K [15]. The uncertainty of molarity of different salt solutions is evaluated to ±0.0001 mol dm^{-3}. Actually several independent solutions were prepared and the runs were performed to ensure reproducibility of the results. Appropriate corrections were also made for the specific conductance of the solvents at all temperatures. The viscosity was measured by means of a suspended Ubbelohde type viscometer, calibrated at 298.15 ± 0.01 K with doubly distilled water and purified methanol using density and viscosity values from the literature [2,23,24] and the efflux times of flow were recorded with a digital stopwatch correct to ±0.01 s. The uncertainty of the viscosity measurements was ±0.003 mPa s. The details of the methods and measurement techniques had been described elsewhere [25,26].

The conductance measurements were carried out in a Systronic 308 conductivity bridge (accuracy ±0.01%) using a dip-type immersion conductivity cell, CD-10. The cell was calibrated by the method of Lind et al. [27] using aqueous potassium chloride solutions. Measurements were made in a water bath maintained within ±0.01 K of desired temperature. During the conductance runs cell constant was within the range 1.10–1.12 cm^{-1}. The conductance data were reported at a frequency of 1 kHz and the accuracy was ±0.3%. During all the three measurements uncertainty of temperatures was ±0.01 K.

3. Discussion

The solvent properties of aqueous 2-butanol solutions are reported in Table 1, where ε_r is relative permittivity, ρ_0 the density, η_0 the viscosity and λ_0 conductance of the solvent mixtures, respectively. Molar conductivities of the studied alkali metal acetates at different molalities are given in Table 2 and depicted in Fig. 1. The conductance data were analyzed in terms of limiting molar conductance Λ_0 and ion-association constant $K_{A,c}$ of the electrolytes using Fuoss conductance–concentration equation [19,20], resolved by an iterative procedure programmed in a computer as suggested by Fuoss [19]. For such an analysis initial Λ_0 values for the iterative procedure were obtained from Shedlovsky extrapolation [28] of the experimental data using least square treatment. Shedlovsky method involves a linear extrapolation of conductance data given by the relation,

$$\frac{1}{\Lambda S(z)} = \frac{1}{\Lambda_0} + \frac{K_{A,c}}{\Lambda_0^2} c\Lambda f_{\pm}^2 S(z) \quad (2)$$

where Λ_0 is limiting molar conductivity and other symbols have their usual meaning described earlier [1,29].

So with a given set of conductivity values (c_i, Λ_i, $i = 1, 2, \ldots, n$), three adjustable parameters, i.e., Λ_0, $K_{A,c}$ and the distance parameter R were derived from the Fuoss conductance equation. Here R is the association distance or co-sphere diameter, i.e. the maximum center-to-center distance between the ions in the solvent separated ion-pairs (SIP). Since there is no precise method [30] for determining the R-value and for the electrolytes studied no significant minima were obtained in the σ_Λ versus R-curve and thus in order to treat the data in our system, R-values were preset at the

Please cite this article in press as: R.S. Sah, et al., Ion association and solvation behavior of some alkali metal acetates in aqueous 2-butanol solutions at $T = 298.15$, 303.15 and 308.15 K, Fluid Phase Equilib. (2011), doi:10.1016/j.fluid.2011.05.017

Table 2
Molar conductivities (Λ) of the alkali metal acetates at various molalities (m) in aqueous 2-butanol solutions with different 2-butanol mass fraction (w_2) at different temperatures.

$m \times 10^4$ (mol kg^{-1})	Λ (S cm^2 mol^{-1})		
	298.15 K	303.15 K	308.15 K
LiAc (w_2 = 0.70)			
6.9	16.63	20.67	24.29
11.6	15.60	19.39	23.32
17.4	14.87	18.50	22.64
23.2	13.90	18.20	22.06
29.0	13.42	17.40	21.38
40.5	12.29	16.09	20.51
46.3	11.75	15.60	20.00
52.1	11.33	15.50	19.54
57.9	10.95	15.00	19.05
63.7	10.45	14.60	18.57
NaAc (w_2 = 0.70)			
6.9	15.83	19.6	22.60
11.6	14.88	18.60	21.80
17.4	14.00	17.70	21.00
23.2	13.27	17.00	20.40
29.0	12.70	16.40	19.80
40.5	11.60	15.39	18.80
46.3	11.09	14.95	18.20
52.1	10.61	14.30	17.70
57.9	10.13	14.20	17.20
63.7	9.64	13.50	16.70
KAc (w_2 = 0.70)			
6.9	14.57	18.22	21.10
11.6	13.60	17.33	20.23
17.4	12.80	16.36	19.50
23.2	12.06	15.82	18.80
29.0	11.43	14.93	18.29
40.5	10.46	13.96	17.20
46.3	9.93	13.42	16.70
52.1	9.50	12.98	16.20
57.9	9.07	12.53	15.80
63.7	8.71	12.36	15.50
LiAc (w_2 = 0.80)			
3.6	15.91	20.20	22.70
5.9	15.43	19.30	22.00
8.3	14.63	18.80	21.40
11.9	14.00	18.10	20.70
14.2	13.50	17.50	20.20
17.8	13.02	16.90	19.50
20.2	12.70	16.50	19.00
23.7	12.00	16.00	18.40
26.1	11.65	15.60	17.38
29.6	11.25	15.00	17.20
NaAc (w_2 = 0.80)			
3.6	15.11	18.90	21.80
5.9	14.64	18.13	20.80
8.3	14.00	17.60	20.10
11.9	13.36	17.00	19.32
14.2	12.86	16.40	18.90
17.8	12.29	15.81	18.00
20.2	11.89	15.45	17.60
23.7	11.33	14.80	16.96
26.1	11.01	14.38	16.52
29.6	10.57	13.74	16.03
KAc (w_2 = 0.80)			
3.6	14.71	17.50	19.50
5.9	14.07	16.61	18.60
8.3	13.36	15.89	18.00
11.9	12.71	15.09	17.30
14.2	12.40	14.55	16.60
17.8	11.79	14.00	16.00
20.2	11.43	13.60	15.54
23.7	11.00	12.95	14.73
26.1	10.64	12.70	14.29
29.6	10.00	12.40	13.80
LiAc (w_2 = 0.90)			
1.2	14.40	19.00	21.50
3.6	13.29	17.54	20.16
6.1	12.36	16.60	19.09
7.3	12.07	16.42	18.80
8.5	11.71	16.02	18.20
10.9	11.20	15.11	17.40
12.2	10.85	14.89	17.20
13.4	10.64	14.65	16.90
14.6	10.36	14.25	16.40
17.0	10.00	13.93	15.60
NaAc (w_2 = 0.90)			
1.2	12.69	17.36	19.60
3.6	11.60	16.20	18.00
6.1	10.88	15.07	17.00
7.3	10.56	14.64	16.62
8.5	10.25	14.14	16.13
10.9	9.69	13.69	15.50
12.2	9.38	13.40	15.10
13.4	9.13	12.88	14.69
14.6	8.94	12.64	14.50
17.0	8.50	12.00	13.88
KAc (w_2 = 0.90)			
1.2	11.69	16.60	17.32
3.6	10.56	15.21	16.07
6.1	9.88	14.20	15.14
7.3	9.50	13.88	14.79
8.5	9.20	13.56	14.36
10.9	8.75	12.94	13.66
12.2	8.56	12.60	13.30
13.4	8.31	12.29	13.00
14.6	8.00	11.93	12.64
17.0	7.56	11.40	12.14

center-to-center distance of solvent separated ion-pairs [1,19,20], i.e., $R = a + d$; where $a = r_c^+ + r_c^-$ and d is the average distance corresponding to the side of a cell occupied by a solvent molecule. The definitions of d and related terms have been described in the literature [1,19,20]. The values of the crystallographic radii for the alkali

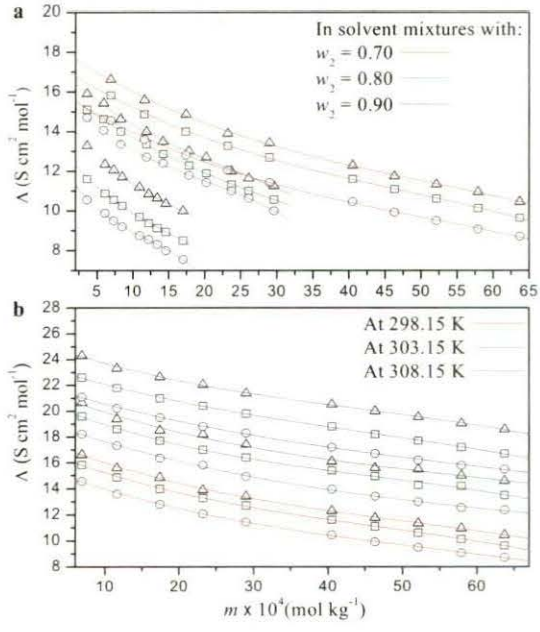

Fig. 1. Plots of molar conductances (Λ) of alkali metal acetates versus molality (m) in aqueous 2-butanol solutions: (a) with different mass fraction of 2-butanol (w_2) at 298.15 K and (b) at different temperatures with w_2 = 0.70 at different temperatures. Symbols: (△) LiAc; (□) NaAc; (○) KAc. Symbols represent experimental values and solid lines represent calculated ones.

Please cite this article in press as: R.S. Sah, et al., Ion association and solvation behavior of some alkali metal acetates in aqueous 2-butanol solutions at T = 298.15, 303.15 and 308.15 K, Fluid Phase Equilib. (2011), doi:10.1016/j.fluid.2011.05.017

metal cations were obtained form literature [31] and that of acetate anion was calculated to be 2.28 Å according to a scheme suggested by Marcus [32].

The Fuoss conductance–concentration equation [19,20] may be represented by a set of relations as follows:

$$\Lambda = p[\Lambda_0(1 + R_X) + E_L] \tag{3}$$

$$p = 1 - \alpha(1 - \gamma) \tag{4}$$

$$\gamma = 1 - K_{A,c} c\gamma^2 f_\pm^2 \tag{5}$$

$$-\ln f = \frac{\beta\kappa}{2(1 + K_R)} \tag{6}$$

$$\beta = \frac{e^2}{\varepsilon_r K_B T} \tag{7}$$

$$K_{A,c} = \frac{K_R}{1 - \alpha} = K_R(1 + K_S) \tag{8}$$

where R_X is the relaxation field effect, E_L is the electrophoretic counter current, κ^{-1} is the radius of the ionic atmosphere, ε_r is the relative permittivity of the solvent, γ is the fraction of solute present as unpaired ion and other symbols have usual significance as described earlier [1,19,20].

We input for our program the number of data, n; followed by relative permittivity of the solvent mixture, ε_r; initial Λ_0 values, T, ρ, molecular weight of the solvents along with c_i, Λ_i, values with $i = 1, 2, \ldots, n$ and an instruction to cover pre-selected range of R-values increased by a step 0.1 Å for the iterative process. Actual calculations involved determination of Λ_0 and $K_{A,c}$ values with minimum standard deviation (σ_Λ) defined as,

$$\sigma_\Lambda^2 = \sum_{i=1}^{n} \frac{[\Lambda_i(\text{calc}) - \Lambda_i(\text{obs})]^2}{n - p} \tag{9}$$

Thus, conductance data were analyzed by fixing the distance of closest approach R with two parameters fit ($p = 2$). Table 3 shows that for all the electrolytes studied, the limiting molar conductances (Λ_0) increase as the temperature increases but decrease as the mass fraction of 2-butanol in the solvent mixtures increase. This trend in limiting molar conductance (Λ_0) can be well described by the viscosity behavior of the solvent media. A perusal of Tables 1 and 2 show that the conductance of the alkali metal acetates decreases along with a parallel decrease in viscosity and density of the solvent mixtures (due to addition of more alcohol) at particular experimental temperature, suggesting that the effective ionic size of the cations necessarily increases [33], i.e., preferential solvation of the alkali metal acetates occurs in aqueous 2-butanol mixtures. But the limiting molar conductances (Λ_0) follow the order: LiAc > NaAc > KAc suggesting that solvation increases the ionic sizes of cations in such a way that the sizes of the solvated cations follows the crystallographic radii order for the alkali metal ions in aqueous 2-butanol solutions. The values of $K_{A,c}$ follows the order: LiAc < NaAc < KAc for all the solvent composition and experimental temperature, i.e., with increasing alcohol content the association equilibrium shifts to the right of the above order as a result of decrease in mixture permittivity.

Walden products ($\Lambda_0\eta_0$) for the alkali metal acetates are given in Table 4. The variation of Walden products ($\Lambda_0\eta_0$) with solvent composition and temperature may be attributed to changes in ion–solvation and ion–solvent interactions. Walden product ($\Lambda_0\eta_0$) either varies slightly with temperature or is almost independent of temperature for the electrolytes studied within the experimental errors but decreases with increasing mass fraction of the alcohol. This is most probably due to pre-solvation of ions (by alcohol molecules) that lead to an increase of the hydrodynamic radii of ions and decrease of their mobility. The values of

Table 3
Limiting molar conductivities (Λ_0), ion-association constants ($K_{A,c}$ and $K_{A,m}$), distance parameter (R) and standard deviations (σ_Λ) of experimental Λ from the Fuoss conductance–concentration equation in aqueous 2-butanol solutions.

Temp (K)	Λ_0(S cm^2 mol^{-1})	$K_{A,c}$(dm^3 mol^{-1})	R(Å)	σ_Λ(S cm^2 mol^{-1})
LiAc (w_2 = 0.70)				
298.15	20.43 ± 0.12	441.23 ± 0.24	6.32	0.23
303.15	23.54 ± 0.11	246.13 ± 0.22	6.33	0.20
308.15	26.87 ± 0.10	147.98 ± 0.20	6.34	0.18
NaAc (w_2 = 0.70)				
298.15	19.82 ± 0.13	494.73 ± 0.26	6.67	0.28
303.15	22.66 ± 0.14	271.57 ± 0.24	6.68	0.18
308.15	25.53 ± 0.15	187.77 ± 0.21	6.69	0.25
KAc (w_2 = 0.70)				
298.15	18.58 ± 0.20	566.12 ± 0.31	7.05	0.24
303.15	21.62 ± 0.10	335.72 ± 0.21	7.06	0.18
308.15	23.93 ± 0.14	207.19 ± 0.21	7.07	0.17
LiAc (w_2 = 0.80)				
298.15	18.66 ± 0.15	549.81 ± 0.27	6.57	0.21
303.15	22.82 ± 0.12	388.51 ± 0.26	6.58	0.18
308.15	25.76 ± 0.11	360.96 ± 0.22	6.59	0.37
NaAc(w_2 = 0.80)				
298.15	17.89 ± 0.11	588.63 ± 0.20	6.92	0.23
303.15	21.63 ± 0.12	433.00 ± 0.23	6.93	0.26
308.15	24.81 ± 0.10	430.67 ± 0.22	6.94	0.21
KAc (w_2 = 0.80)				
298.15	17.36 ± 0.14	619.29 ± 0.24	7.29	0.20
303.15	20.39 ± 0.11	581.85 ± 0.23	7.30	0.11
308.15	22.76 ± 0.18	542.13 ± 0.28	7.31	0.28
LiAc (w_2 = 0.90)				
298.15	15.96 ± 0.11	856.24 ± 0.20	6.88	0.13
303.15	20.68 ± 0.18	644.12 ± 0.29	6.89	0.16
308.15	23.55 ± 0.17	622.63 ± 0.25	6.90	0.27
NaAc (w_2 = 0.90)				
298.15	14.23 ± 0.09	988.22 ± 0.02	7.23	0.17
303.15	19.32 ± 0.10	841.43 ± 0.14	7.24	0.23
308.15	21.54 ± 0.12	761.38 ± 0.09	7.25	0.17
KAc (w_2 = 0.90)				
298.15	13.81 ± 0.18	1117.20 ± 0.26	7.60	0.16
303.15	18.38 ± 0.20	865.99 ± 0.29	7.61	0.18
308.15	19.24 ± 0.18	813.07 ± 0.30	7.62	0.23

Walden products ($\Lambda_0\eta_0$) follow the order: LiAc > NaAc > KAc for a particular solvent mixture at an experimental temperature. This difference in association behavior can be attributed to the differences in the acetate ion–cation interactions and may not be due to specific solvent effects alone. However, the order in Walden products indicates a hydrodynamic radius enlargement for the cations (from Li^+ to Na^+). Though smaller ions are expected to be strongly solvated, the position of the curves in Fig. 2 ($\Lambda_0\eta_0$ versus w_2) suggests a relationship $Li^+ < Na^+ < K^+$ for this radius. We have earlier found just the opposite result for the studied alkali metal acetates in aqueous glycerol solutions [34] suggesting that smaller ions are strongly solvated, though such differences gradually diminished at higher concentrations of glycerol. But in the present work

Table 4
Walden products ($\Lambda_0\eta_0$) of the electrolytes studied in aqueous 2-butanol solutions.

Mass fraction of 2-butanol (w_2)	$\Lambda_0\eta_0$ (S cm^2 mol^{-1} mPa s)		
	298.15 K	303.15 K	308.15 K
LiAc			
0.70	68.28	65.79	63.87
0.80	57.81	59.51	57.08
0.90	44.88	49.11	47.78
NaAc			
0.70	66.24	63.35	60.68
0.80	55.42	56.41	54.98
0.90	40.01	45.88	43.70
KAc			
0.70	62.09	60.43	56.88
0.80	53.78	53.18	50.44
0.90	37.06	43.65	39.04

Please cite this article in press as: R.S. Sah, et al., Ion association and solvation behavior of some alkali metal acetates in aqueous 2-butanol solutions at T = 298.15, 303.15 and 308.15 K, Fluid Phase Equilib. (2011), doi:10.1016/j.fluid.2011.05.017

Table 5
Activation enthalpy of ionic transport ($\Delta H^{\#}$) and thermodynamic parameters of the ion-association reaction (ΔH^0, ΔG^0 and ΔS^0) for the electrolytes under study in aqueous 2-butanol solutions at 298.15 K.

Mass fraction of 2-butanol (w_2)	$\Delta H^{\#}$ (kJ mol^{-1})	ΔH^0 (kJ mol^{-1})	ΔG^0 (kJ mol^{-1})	ΔS^0 (J K^{-1} mol^{-1})
LiAc				
0.70	20.4	−84.2	−14.7	−232.9
0.80	24.1	−33.1	−15.2	−59.9
0.90	29.2	−25.3	−16.2	−30.5
NaAc				
0.70	18.8	−74.8	−15.0	−200.7
0.80	24.4	−24.8	−15.4	−31.7
0.90	31.2	−20.8	−16.6	−14.1
KAc				
0.70	18.8	−77.5	−15.3	−208.4
0.80	20.2	−10.9	−15.5	15.3
0.90	28.5	−25.2	−16.9	−27.9

the reversed trend in hydrodynamic radii is very interesting. No doubt aqueous 2-butanol solutions are comparatively less characterized by intermolecular hydrogen bond interaction, so more extensive ion–solvent interaction is thus expected. But the degree of ion–solvent interaction or preferential interaction (solvation) is such that the effective size of the solvated cations follows the order $Li^+ < Na^+ < K^+$. This indicates that the alkali metal cations prefer water molecules to 2-butanol molecules in their solvation or coordination sphere. Such a reversed order for solvated cations has also been reported earlier in literature [35,36] and Kay [37] has suggested that the difference is attributable to the differences in the acetate ion–cation interactions rather than solvent effects.

The distance parameter R, shown in Table 3, is the least distance that two free ions can approach before they merge into ion pair. R values were found to increase with increase in both the temperature and mass fraction of alcohol (w_2) in the solvent mixture. These effects can be attributed to the thermal activation of the solvent sheath due to the activation of the solvent molecules at enhanced temperature and more molecular volume of 2-butanol molecules than water.

In order to minimize the contribution of the thermal expansion of the solvent to the reaction enthalpy, $K_{A,c}$ was converted to molality scale using the equation [15]:

$$K_{A,m} = K_{A,c}\rho_0 \quad (10)$$

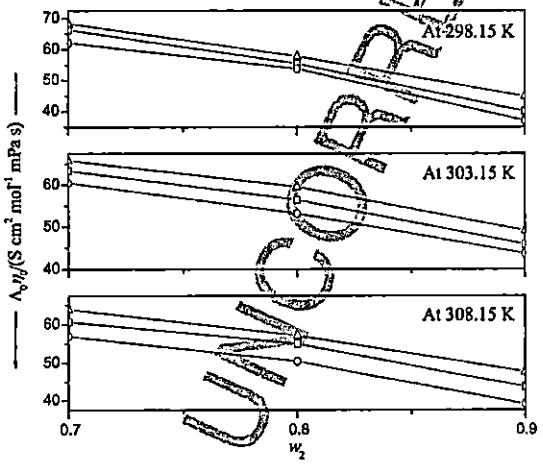

Fig. 2. Plots of Walden products ($\Lambda_0\eta_0$) versus mass fraction (w_2) of 2-butanol in aqueous 2-butanol solutions for alkali metal acetates at different temperature. Symbol: (Δ) LiAc; (□) NaAc; (○) KAc.

The enthalpy of the ion-association (ΔH^0) and the activation enthalpy of charge transfer ($\Delta H^{\#}$), assuming both the parameters as temperature independent, were evaluated by the least squares analysis of the relations:

$$\ln K_{A,m} = \frac{\Delta H^0}{R_g T} + I \quad (11)$$

$$\ln \Lambda_0 + \frac{2}{3}\ln \rho_0 = -\frac{\Delta H^{\#}}{R_g T} + I' \quad (12)$$

The second term on the left hand side of Eq. (12) originated [38] from $(1/3)\,(\partial \ln V/\partial T)_P$, V stands for the volume of the cube containing a unit mass of solvent and R_g is the universal gas constant. The standard deviations (σ) of linear fit for Eqs. (11) and (12) were within 0.000–0.002. Gibbs energy (ΔG^0) of the ion-association reaction was calculated by the relation [39]:

$$\Delta G^0 = -R_g T \ln K_{A,m} \quad (13)$$

and the standard enthalpy of ion-pair formation was calculated by the relation [39]:

$$\Delta S^0 = \frac{\Delta H^0 - \Delta G^0}{T} \quad (14)$$

Values of these thermodynamic properties at 298.15 K are presented in Table 5. The negative values of ΔH^0 and ΔG^0 can be explained by participation of specific covalent interaction in the ion-association process. But the binding entropy (ΔS^0) between the ions was found to be negative to unfavor the ion-association

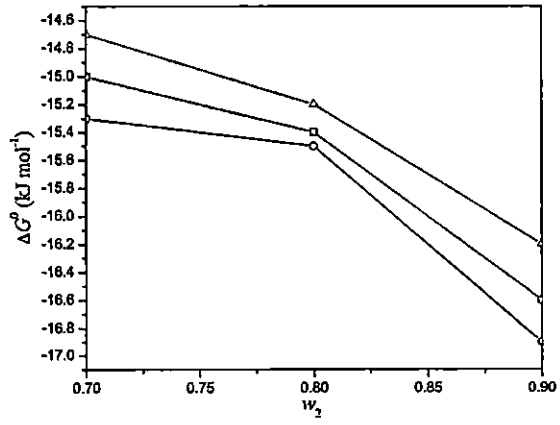

Fig. 3. Plots of Walden products (ΔG^0) versus mass fraction (w_2) of 2-butanol in aqueous 2-butanol solutions for alkali metal acetates at 298.15 K. Symbol: (Δ) LiAc; (□) NaAc; (○) KAc.

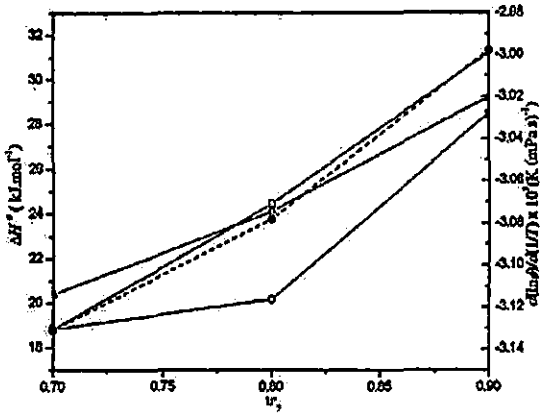

Fig. 4. Activation enthalpy of the charge transport ($\Delta H^{\#}$, solid lines) and the temperature gradient of fluidity (●, dashed line) for the aqueous 2-butanol mass fraction (w_2) at 298.15 K. Symbols: (Δ) Li^+; (□) Na^+; (○) K^+.

process and thus favoring ion solvation process. The uniformly descending nature of the curves (ΔG^0) in Fig. 3 indicates a greater degree of association at comparatively lower solvent permittivity. However, comparatively higher values of $K_{A,c}$ than the limiting molar conductances (Λ_0) indicate that the studied electrolytes are sufficiently associated in aqueous 2-butanol mixtures and this fact is in line with the low to moderate relative permittivity of the solvent media. The activation enthalpy of ionic movement or charge transfer ($\Delta H^{\#}$) as depicted in Fig. 4 exhibits close similarity to the dependence of the fluidity (reciprocal viscosity) temperature gradient ($d(\ln\phi)/d(1/T)$) on the solvent composition presented by a dashed line. According to Brummer and Hills [38,39] the activation enthalpy of charge transfer ($\Delta H^{\#}$) at constant pressure is a temperature dependent complex quantity,

$$\Delta H^{\neq} = \Delta U^{\neq} + (\pi + P)\Delta V^{\neq} \quad (15)$$

where $\Delta H^{\neq}$ is the volume of activation for unit displacement of a mole of ions, $\Delta U^{\neq}$ is the internal energy change for the same displacement at constant volume, π is the internal pressure of the solvent, $(\partial U/\partial V)_T$. $\Delta V^{\neq}$ increases and corresponding $\Delta U^{\neq}$ decreases with increasing ionic size and molar volume of the solvent [38,39]. Thus similarity in shapes of the curves [15,34] in Fig. 4 indicates closeness between the mechanisms of the two transport processes.

4. Conclusion

The present work revealed that the effective size of the cations increases in aqueous 2-butanol mixtures due to preferential solvation in such a way that the sizes of the solvated cations follow their crystallographic radii. The degree of ion–solvent interaction also indicated that the alkali metal cations prefer water molecules to 2-butanol molecules in their solvation or coordination sphere. However, this association behavior can be attributed to the differences in the acetate ion–cation interactions and may not be due to specific solvent effects alone.

List of symbols

ρ	solution density
ρ_0	solvent density
η	solution viscosity
η_0	solvent viscosity
ε_r	relative permittivity
c	molarity
m	molality
Λ	molar conductance
Λ_0	limiting molar conductance
$K_{A,c}$	association constant (molarity scale)
$K_{A,m}$	association constant (molality scale)
$f_\pm$	mean activity coefficient
R_X	relaxation field effect
E_L	electrophoretic counter current
γ	fraction of solute present as unpaired ion
β	twice the Bjerrum distance
κ^{-1}	radius of ionic atmosphere
e	electric charge
K_B	Boltzmann constant
R	association distance or co-sphere diameter
ΔG^0	Gibbs energy of ion-association reaction
ΔH^0	enthalpy of ion-association reaction
ΔS^0	entropy of ion-association reaction
$\Delta H^{\#}$	activation energy of ionic movement or charge transfer
σ_A	standard deviation

Acknowledgment

The authors are grateful to the Departmental Special Assistance Scheme under the University Grants Commission, New Delhi (No. F 540/27/DRS/2007, SAP-1) for financial support.

References

[1] M.N. Roy, B. Sinha, V.K. Dakua, Pak. J. Sci. Ind. Res. 49 (2006) 153–159.
[2] A. Chatterjee, B. Das, J. Chem. Eng. Data 51 (2006) 1352–1355.
[3] M. Pal, S. Bagchi, J. Chem. Faraday Trans. I 81 (1985) 961–972.
[4] A. Mukhopadhyay, M. Pal, Ind. J. Chem. 41A (2002) 1120–1125.
[5] A. Wypych-Stasiewicz, A. Szejgis, A. Chmielewska, A. Bald, J. Mol. Liq. 130 (2007) 34–37.
[6] C.G. Janz, R.P.T. Tomkins, Non-aqueous Electrolytes Handbook, vol. 2, Academic Press, NY, 1973.
[7] D. Aurbach, Non-aqueous Electrochemistry, Marcel Dekker Inc., NY, 1999.
[8] J.A. Krom, J.T. Petty, A. Streitwieser, J. Am. Chem. Soc. 115 (1993) 8024–8030.
[9] D. Das, B. Das, D.K. Hazra, J. Sol. Chem. 31 (2002) 425–431.
[10] C. Guha, J.M. Chakraborty, S. Karanjai, B. Das, J. Phys. Chem. 107 (2003) 12814–12819.
[11] D. Das, B. Das, D.K. Hazra, J. Sol. Chem. 32 (2003) 77–83.
[12] M.N. Roy, D. Nandi, D.K. Hazra, J. Indian Chem. Soc. 70 (1993) 121–124.
[13] I. Tominic, V. Sakol, I. Mekjavic, Croat. Chem. Acta 71 (1998) 705–714.
[14] V. Sokol, I. Tominic, R. Toma, M. Visic, Croat. Chem. Acta 78 (2005) 43–47.
[15] V. Sokol, R. Tomas, M. Visic, I. Tominic, J. Sol. Chem. 35 (2006) 1687–1698.
[16] V. Sokol, R. Tomas, I. Tominic, Acta Chim. Slov. 55 (2008) 308–314.
[17] V. Sokol, R. Tomas, I. Tominic, Acta Chim. Slov. 56 (2009) 773–779.
[18] H.A. Shehata, J. Indian Chem. Soc. 70 (1993) 719–721.
[19] R.M. Fuoss, J. Phys. Chem. 82 (1978) 2427–2440.
[20] R.M. Fuoss, Paired ions: dipolar pairs as subset of diffusion pairs, Proc. Natl. Acad. Sci. U.S.A. 75 (1978) 16–20.
[21] D.D. Perrin, W.L.F. Armarego, Purification of Laboratory Chemicals, 3rd ed., Pergamon Press, Oxford, 1988.
[22] R. Kay, C. Zawoyski, D. Evans, J. Phys. Chem. 69 (1965) 4208–4215.
[23] M.N. Marsh, Recommended Reference Materials for the Realisation of Physicochemical Properties, Blackwell Scientific Publications, Blackwell Science Publications, Oxford, U.K., 1987.
[24] J.A. Dean, Lange's Handbook of Chemistry, 11th ed., McGraw-Hill Book Company, NY, 1973.
[25] B. Sinha, B.K. Sarkar, M.N. Roy, J. Chem. Thermodyn. 40 (2008) 394–400.
[26] A. Bhattacharjee, M.N. Roy, Phys. Chem. Chem. Phys. 12 (2010) 14534–14542.
[27] J.E. Lind, J.J. Zwolenik, R.M. Fuoss, J. Am. Chem. Soc. 81 (1959) 1557–1559.
[28] R.M. Fuoss, T. Shedlovsky, J. Am. Chem. Soc. 71 (1949) 1496–1498.
[29] H.S. Harned, B.B. Owen, The Physical Chemistry of Electrolyte Solutions, 3rd ed., ACS, Reinhold Publishing Corporation, NY, 1958, p. 289.
[30] H. Doe, H. Ohe, H. Matoba, A. Ichimura, T. Kitagawa, Bull. Chem. Soc. Jpn. 63 (1990) 2785–2789.
[31] A.K. Covington, T. Dickinson, Physical Chemistry of Organic Solvent Systems, Plenum Press, NY, 1973, p. 637, Chapter 5.
[32] Y. Marcus, Chem. Rev. 88 (1988) 1475–1498.
[33] J.-K. Hyun, K.P. Johnston, P.J. Rossky, J. Phys. Chem. B 105 (2001) 9302–9307.
[34] B.K. Sarkar, M.N. Roy, B. Sinha, Indian J. Chem. 48A (2009) 63–68.
[35] O.L. Hughes, H. Hartley, Philos. Mag. 15 (1933).
[36] M.B. Reynolds, C.A. Kraus, J. Am. Chem. Soc. 70 (1948) 1709–1713.
[37] R.L. Kay, J. Am. Chem. Soc. 82 (1960) 2099–2105.
[38] S.B. Brummer, G.J. Hills, J. Chem. Soc. Faraday Trans. 57 (1961) 1816–1822.
[39] S.B. Brummer, G.J. Hills, J. Chem. Soc. Faraday Trans. 57 (1961) 1823–1837.

Please cite this article in press as: R.S. Sah, et al., Ion association and solvation behavior of some alkali metal acetates in aqueous 2-butanol solutions at T = 298.15, 303.15 and 308.15 K, Fluid Phase Equilib. (2011), doi:10.1016/j.fluid.2011.05.017

Thermochimica Acta 499 (2010) 149–154

Contents lists available at ScienceDirect

Thermochimica Acta

journal homepage: www.elsevier.com/locate/tca

Solute–solvent and solvent–solvent interactions of menthol in isopropyl alcohol and its binary mixtures with methyl salicylate by volumetric, viscometric, interferometric and refractive index techniques

Radhey Shyam Sah, Prasanna Pradhan, Mahendra Nath Roy*

Department of Chemistry, North Bengal University, Darjeeling 734013, India

ARTICLE INFO

Article history:
Received 16 September 2009
Received in revised form
28 November 2009
Accepted 1 December 2009
Available online 5 December 2009

Keywords:
Solute–solvent and solvent–solvent interactions
Menthol
Isopropyl alcohol
Methyl salicylate

ABSTRACT

The apparent molar volume (V_ϕ), viscosity *B*-coefficient, isoentropic compressibility (ϕ_K) of menthol have been determined in binary solution of isopropyl alcohol and methyl salicylate (at 303.15, 313.15 and 323.15 K) from density (ρ), viscosity (η) and sound speed respectively. The apparent molar volumes have been extrapolated to zero concentration to obtain the limiting values at infinite dilution using Masson equation. The infinite dilution partial molar expansibilities have also been calculated from the temperature dependence of the limiting apparent molar volumes. Viscosity *B*-coefficients has been calculated using Jones–Dole equation. The structure-making or breaking capacity of the solute under investigation has been discussed in terms of sign of $(\delta^2 V_\phi^\circ/\delta T^2)_p$. The activation parameters of viscous flow were determined and discussed by application of transition state theory.

1. Introduction

The volumetric, viscometric and interferrometric behavior of solutes has been proved to be very useful in elucidating the various interactions occurring in pure and mixed solvents. Studies on the effect of concentration and temperature on the apparent molar volumes of solutes have been extensively used to obtain information on ion–ion, ion–solvent, and solvent–solvent interactions [1–3]. It has been found by a number of workers [4–6] that the addition of a solute could either make or break the structure of a liquid.

In this paper we have attempted to study the behavior of menthol in isopropyl alcohol (I.P.A.) and in its mixture with methyl salicylate (5, 10 and 15 mass%) at various temperatures because of their extensive use in pharmaceutical and cosmetic industries. Methyl salicylate has a long history of use in consumer products as a counterirritant and as an analgesic in the treatment and temporary management of aching and painful muscles and joints. Methyl salicylate is also used as an UV absorber and in perfumery as a modifier of blossom fragrances [7]. I.P.A. is widely used as a cleaning agent, a cost-effective preservative for biological specimens and is a major ingredient in "dry-gas" fuel additive. Menthol, an old remedy in Chinese medicine extracted from plants of the genus *Mentha*, is widely used as both a cooling agent and a counterirritant for relieving pain especially in the muscles, viscera or remote areas [8], as well as for the treatment of pruritus.

Menthol

Isopropyl alcohol

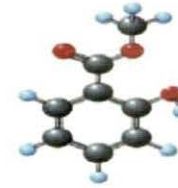

Methyl salicylate

2. Experimental

2.1. Chemicals

Menthol (Thomas Baker, >99%) was used as such without further purification. Isopropyl alcohol (Merck, >99.5%) and methyl salicylate (Sigma–Aldrich, >99%) were used with no further purification other than being dried with molecular sieves. Experimental values of viscosity (η), density (ρ), sound speed (u) and refractive indices (n_D) of the pure solvents were compared with the literature values and are listed in Table 1.

* Corresponding author. Tel.: +91 353 2776381; fax: +91 353 2699001.
E-mail address: mahendraroy2002@yahoo.co.in (M.N. Roy).

0040-6031/$ – see front matter © 2009 Elsevier B.V. All rights reserved.
doi:10.1016/j.tca.2009.12.001

Table 1
Density (ρ), viscosity (η), sound speed (u) and refractive indices (n_D) of binary mixture of methyl salicylate (1) and I.P.A. (2) at different temperatures.

Temperature (K)	$\rho \times 10^{-3}$ (kg m^{-3})		η (mPa s)		u (m s^{-1})		n_D	
	Exp	Lit	Exp	Lit	Exp	Lit	Exp	Lit
$w_1 = 0.00$								
303.15	0.7771	0.7768 [25]	1.7470	1.7430 [26]	1130.6	1127 [27]	1.3736	1.3737 [28]
313.15	0.7684	0.7680 [25]	1.3296	1.3260 [25]	–	–	–	–
323.15	0.7560	0.7557 [26]	1.0029	1.0020 [26]	–	–	–	–
$w_1 = 0.05$								
303.15	0.7909	–	1.7981	–	1146.8	–	1.3791	–
313.15	0.7828	–	1.3786	–	–	–	–	–
323.15	0.7703	–	1.0485	–	–	–	–	–
$w_1 = 0.10$								
303.15	0.8053	–	1.8464	–	1170.6	–	1.3852	–
313.15	0.7943	–	1.4369	–	–	–	–	–
323.15	0.7851	–	1.1164	–	–	–	–	–
$w_1 = 0.15$								
303.15	0.8224	–	1.9614	–	1197.7	–	1.3912	–
313.15	0.8120	–	1.5600	–	–	–	–	–
323.15	0.7993	–	1.2274	–	–	–	–	–

2.2. Measurements

Densities (ρ) were measured with an Ostwald–Sprengel type pycnometer having a bulb volume of about 25 cm^3 and an internal diameter of about 0.1 cm. The measurements were done in a thermostat bath controlled to ±0.01 K. Viscosity (η) was measured by means of suspended Ubbelohde type viscometer, calibrated at 298.15 K with triply distilled water and purified methanol using density and viscosity values from literature. The flow times were accurate to ±0.1 s, and the uncertainty in the viscosity measurements was $\pm 2 \times 10^{-4}$ mPa s. The mixtures were prepared by mixing known volume of pure liquids in airtight-stopper bottles and each solution thus prepared was distributed into three recipients to perform all the measurements in triplicate, with the aim of determining possible dispersion of the results obtained. Adequate precautions were taken to minimize evaporation loses during the actual measurements. Mass measurements were done on a Mettler AG-285 electronic balance with a precision of ±0.01 mg. The precision of density measurements was $\pm 3 \times 10^{-4}$ g cm^{-3}. Refractive index was measured with the help of Abbe-Refractometer (U.S.A.). The accuracy of refractive index measurement was ±0.0002 units. The refractometer was calibrated twice using distilled and deionized water, and calibration was checked after every few measurements.

Viscosity of the solution, η, is given by the following equation:

$$\eta = \left(\frac{Kt - L}{t}\right)\rho \tag{1}$$

where K and L are the viscometer constants and t and ρ are the efflux time of flow in seconds and the density of the experimental liquid, respectively. The uncertainty in viscosity measurements is within ±0.003 mPa s.

Details of the methods and techniques of density and viscosity measurements have been described elsewhere [9–12]. The solutions studied here were prepared by mass and the conversion of molality in molarity was accomplished [3] using experimental density values. The experimental values of concentrations (c), densities (ρ), viscosities (η), and derived parameters at various temperatures are reported in Table 2.

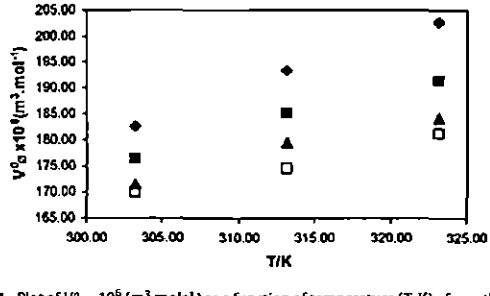

Fig. 1. Plot of $V^o_\phi \times 10^6$ (m^3 mol^{-1}) as a function of temperature (T, K) of menthol in 0% (♦), 5% (■), 10% (▲), 15% (□) mass percent of methyl salicylate + I.P.A.

3. Results and discussions

Apparent molar volumes (V_ϕ) were determined from the solution densities using the following equation:

$$V^o_\phi = \frac{M}{\rho_o} - \frac{1000(\rho - \rho_o)}{c\rho_o} \tag{2}$$

where M is the molar mass of the solute, c is the molarity of the solution; ρ_o and ρ are the densities of the solvent and the solution respectively. The limiting apparent molar volumes V^o_ϕ was calculated using a least-square treatment to the plots of V_ϕ versus $\sqrt{c}$ using the Masson equation [13].

$$V_\phi = V^o_\phi + S^*_v\sqrt{c} \tag{3}$$

where V^o_ϕ is the partial molar volume at infinite dilution and S^*_v the experimental slope. The plots of V_ϕ against square root of molar concentration ($\sqrt{c}$) were found to be linear with negative slopes. Values of V^o_ϕ and S^*_v are reported in Table 3.

The solute–solvent and solute–solute interactions can be interpreted in terms of structural changes which arise due to hydrogen bonding between various components of the solvent and solution systems. V^o_ϕ values can be used to interpret solute–solvent interactions. Table 3 reveals that V^o_ϕ values are positive and increases with rise in temperature and decreases with increase in the mass percent of methyl salicylate in the solvent mixture as depicted in Figs. 1 and 2 respectively. This indicates the presence of strong solute–solvent interactions and these interactions are strengthened with rise in temperature and weakened with an increase in the mass percent of methyl salicylate suggesting larger electrostriction at higher temperature. Similar results were obtained for some 1:1 electrolytes in aqueous DMF [14] and aqueous THF [15].

The observed result can also be explained in view of the molar volume of solute as well as solvents studied here. The partial molar volume (182.55) of menthol in pure I.P.A. is far greater than molar volume of I.P.A. (77.24) but a little extent greater than the molar

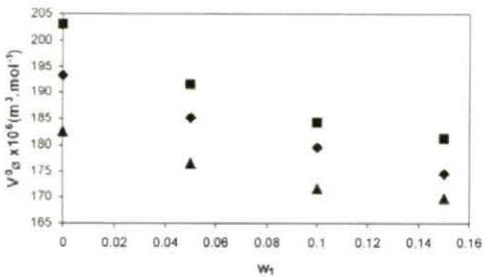

Fig. 2. Plot of $V^o_\phi \times 10^6$ ($m^3\,mol^{-1}$) as a function of mass percent of methyl salicylate in different binary mixture of methyl salicylate + I.P.A. at 303.15 K (▲), 313.15 K (♦) and 323.15 K (■).

volume of methyl salicylate. Further, the partial molar volume of menthol decreases gradually with decreasing composition of I.P.A. to the mixture. Hence I.P.A. easily fits in menthol in the mixture resulting in more solute–solvent interaction between them which is an excellent agreement with the conclusion drawn from values of V^o_ϕ as well as viscosity B-coefficient.

A schematic diagram is shown below.

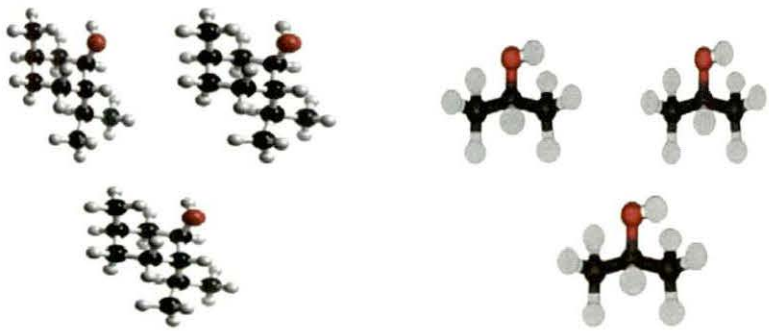

Partial Molar Volume (182.55) Molar Volume (77.24)

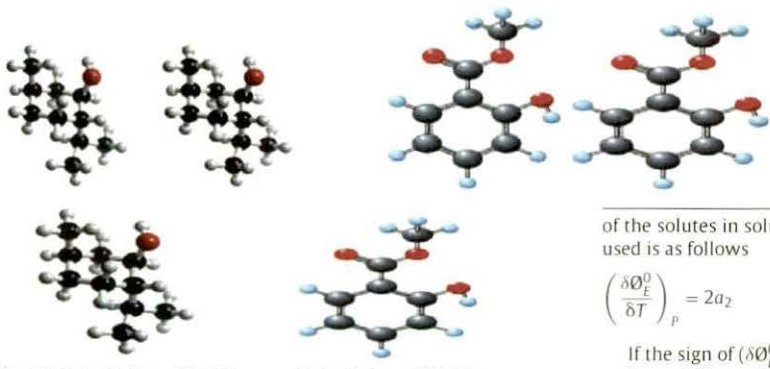

Partial Molar Volume (182.55) Molar Volume (129.49)

S^*_v values are negative at all temperatures and the values decreases with increase of temperature and increases with increase in mass percent of methyl salicylate which may be attributed to more violent thermal agitation at higher temperatures, resulting in diminishing the force of ion–ion interactions (ionic-dissociation) [16]. The magnitude of V^o_ϕ values are much greater than those of S^*_v for all the solutions which suggests that solute–solvent interactions dominate over solute–solute interactions in all the solutions and at all experimental temperatures.

The polynomial below represents the variation of V^o_ϕ with temperature

$$V^o_\phi = a_0 + a_1 T + a_2 T^2 \tag{4}$$

over the temperature range under study where T is the temperature in K. Values of coefficients of the above equation are reported in Table 4.

The apparent molar expansibilities (ϕ^0_E) can be obtained by the following equation:

$$\phi^0_E = \left(\frac{\delta V^o_\phi}{\delta T}\right)_P = a_1 + 2a_2 T \tag{5}$$

The values ϕ^0_E of for different solutions at 303.15, 313.15 and 323.15 K are reported in Table 5. Table 5 reveals that ϕ^0_E value decreases with increasing temperature and mass percent of methyl salicylate. This fact may be attributed to gradual disappearance of caging or packing effect [16,17] in the ternary solutions. According to Helper [18] the sign of $(\delta\phi^0_E/\delta T)_P$ is a better criterion in characterizing the long-range structure-making and breaking ability of the solutes in solution. The general thermodynamic expression used is as follows

$$\left(\frac{\delta\phi^0_E}{\delta T}\right)_P = 2a_2 \tag{6}$$

If the sign of $(\delta\phi^0_E/\delta T)_P$ is positive [19] the solute is a structure maker and if negative it is a structure breaker. As is evident from the values of $(\delta\phi^0_E/\delta T)_P$, menthol predominately acts as a structure breaker.

The viscosity data has been analyzed using Jones–Dole [20] equation:

$$\left(\frac{(\eta/\eta_0 - 1)}{c^{1/2}}\right) = A + Bc^{1/2} \tag{7}$$

Table 2
Molarity (c), density (ρ), viscosity (η), apparent molar volume (V_ϕ) and $(\eta/\eta_0 - 1)/c^{1/2}$ of menthol in binary mixture of different mass% (w_1) of methyl salicylate (1) and I.P.A. (2) at 303.15, 313.15 and 323.15 K.

c (mol dm^{-3})	$\rho \times 10^{-3}$ (kg m^{-3})	η (mPa s)	$V_\phi \times 10^6$ (m^3 mol^{-1})	$(\eta/\eta_0 - 1)/c^{1/2}$
$w_1 = 0.00$				
303.15 K				
0.0250	0.7776	1.7572	176.31	0.0370
0.0350	0.7778	1.7613	175.36	0.0436
0.0450	0.7780	1.7659	174.55	0.0510
0.0550	0.7783	1.7713	173.92	0.0593
0.0750	0.7788	1.7812	172.25	0.0716
0.0850	0.7791	1.7851	171.03	0.0748
313.15 K				
0.0247	0.7688	1.3401	182.60	0.0501
0.0346	0.7690	1.3443	180.77	0.0592
0.0445	0.7692	1.3493	178.95	0.0699
0.0544	0.7695	1.3545	177.14	0.0800
0.0742	0.7700	1.3638	175.43	0.0942
0.0840	0.7703	1.3684	173.20	0.1007
323.15 K				
0.0243	0.7564	1.0121	187.30	0.0590
0.0340	0.7566	1.0170	184.80	0.0760
0.0438	0.7568	1.0215	181.50	0.0886
0.0535	0.7571	1.0258	179.20	0.0989
0.0730	0.7577	1.0342	175.65	0.1157
0.0827	0.7580	1.0388	174.40	0.1246
$w_1 = 0.05$				
303.15 K				
0.0250	0.7914	1.8073	171.15	0.0322
0.0350	0.7917	1.8110	170.20	0.0384
0.0450	0.7919	1.8145	169.06	0.0431
0.0550	0.7922	1.8200	168.34	0.0519
0.0750	0.7927	1.8282	167.30	0.0612
0.0850	0.7930	1.8329	166.55	0.0664
313.15 K				
0.0247	0.7832	1.3879	176.43	0.0430
0.0346	0.7835	1.3922	174.00	0.0530
0.0445	0.7837	1.3966	172.70	0.0620
0.0544	0.7840	1.4014	171.45	0.0709
0.0741	0.7846	1.4097	169.32	0.0829
0.0840	0.7849	1.4138	168.40	0.0881
323.15 K				
0.0243	0.7707	1.0567	182.04	0.0500
0.0340	0.7709	1.0603	180.44	0.0610
0.0438	0.7711	1.0642	178.83	0.0715
0.0535	0.7714	1.0682	177.33	0.0811
0.0729	0.7719	1.0754	175.24	0.0950
0.0827	0.7721	1.0795	174.24	0.1030
$w_1 = 0.10$				
303.15 K				
0.0250	0.8058	1.8631	168.90	0.0571
0.0350	0.8060	1.8675	168.40	0.0610
0.0450	0.8062	1.8728	167.96	0.0673
0.0550	0.8065	1.8794	167.76	0.0760
0.0750	0.8069	1.8878	166.94	0.0818
0.0850	0.8072	1.8937	166.57	0.0879
313.15 K				
0.0247	0.7948	1.4511	172.80	0.0630
0.0345	0.7950	1.4572	171.06	0.0760
0.0444	0.7952	1.4605	170.24	0.0780
0.0543	0.7955	1.4673	168.94	0.0910
0.0740	0.7960	1.4767	167.40	0.1020
0.0839	0.7963	1.4821	166.88	0.1086
323.15 K				
0.0244	0.7855	1.1281	175.71	0.0670
0.0341	0.7858	1.1328	173.71	0.0800
0.0439	0.7860	1.1362	172.20	0.0850
0.0536	0.7862	1.1414	171.80	0.0970
0.0731	0.7868	1.1501	169.65	0.1120
0.0829	0.7871	1.1535	167.87	0.1160
$w_1 = 0.15$				
303.15 K				
0.0250	0.8228	1.9763	168.21	0.0480
0.0350	0.8230	1.9818	167.94	0.0554
0.0450	0.8232	1.9859	167.71	0.0588
0.0550	0.8235	1.9905	167.44	0.0632
0.0750	0.8238	1.9991	166.98	0.0702
0.0850	0.8240	2.0034	166.83	0.0734
313.15 K				
0.0247	0.8125	1.5752	169.49	0.0620
0.0346	0.8127	1.5806	168.51	0.0710
0.0444	0.8129	1.5846	167.48	0.0750
0.0543	0.8132	1.5909	166.69	0.0850
0.0741	0.8137	1.6003	165.80	0.0949
0.0840	0.8140	1.6047	165.00	0.0990
323.15 K				
0.0243	0.7997	1.2408	175.44	0.0700
0.0340	0.7999	1.2451	174.28	0.0781
0.0437	0.8001	1.2500	173.37	0.0880
0.0535	0.8003	1.2538	172.68	0.0931
0.0729	0.8007	1.2634	171.20	0.1087
0.0826	0.8010	1.2683	170.48	0.1160

where η_0 and η are the viscosities of the solvent/solvent mixtures and solution respectively. A and B are the constants estimated by a least-squares method and are reported in Table 6. The values of the A coefficient are found to decrease with temperature and increases with increase in mass percent of methyl salicylate. These results indicate the presence of very weak ion–ion interactions and these interactions further decrease with the rise of experimental temperatures and increase with an increase in mass percent of methyl salicylate. These results are in excellent agreement with those obtained from S_v^* values.

The effects of ion–solvent interactions on the solution viscosity can be inferred from the B-coefficient [21,22]. The viscosity B-coefficient is a valuable tool to provide information concerning the solvation of the solutes and their effects on the structure of the solvent. From Table 6 it is evident that the values of the B-coefficient are positive, thereby suggesting the presence of strong solute–solvent interactions, and these types of interactions are strengthened with a rise in temperature and weakened with an increase of mass percent of methyl salicylate. Similar results are obtained from V_ϕ^0 values discussed earlier.

The adiabatic compressibility (β) was evaluated from the following equation:

$$\beta = \frac{1}{u^2 \rho} \tag{8}$$

where ρ is the solution density and u is the sound speed in the solution. The apparent molal adiabatic compressibility (ϕ_K) of the solutions was determined from the relation,

$$\phi_K = \frac{M\beta}{\rho_o} + \frac{1000(\beta\rho_o - \beta_o\rho)}{m\rho\rho_o} \tag{9}$$

where β_o, β are the adiabatic compressibility of the solvent and solution respectively and m is the molality of the solution. Limiting partial molal adiabatic compressibilities (ϕ_K^o) and experimental slopes (S_K^*) were obtained by fitting ϕ_K against the square root of molality of the electrolyte ($\sqrt{m}$) using the method of least squares.

$$\phi_K = \phi_K^o + S_K^* \sqrt{m} \tag{10}$$

Values of m, u, β, ϕ_K, ϕ_K^o and S_K^* are presented in Table 7. Since the values of ϕ_K^o and S_K^* are measures of ion–solvent and ion–ion

Table 3
Limiting apparent molar volumes (V_ϕ^o) and experimental slopes (S_v^*) of menthol in binary mixture of different mass% (w_1) of methyl salicylate (1) and I.P.A. (2) at 303.15, 313.15 and 323.15 K.

Mass% of methyl salicylate	$V_\phi^o \times 10^6$ (m^3 mol^{-1})			$S_v^* \times 10^6$ (m^3 $mol^{-3/2}$ $dm^{3/2}$)		
	303.15 K	313.15 K	323.15 K	303.15 K	313.15 K	323.15 K
$w_1 = 0.00$	182.55	193.33	202.89	−38.25	−68.07	−100.44
$w_1 = 0.05$	176.45	185.26	191.37	−33.97	−58.74	−59.83
$w_1 = 0.10$	171.63	179.53	184.13	−17.15	−44.36	−55.16
$w_1 = 0.15$	169.92	174.58	181.18	−10.60	−33.01	−37.10

Table 4
Values of the coefficients of Eq. (4) of menthol in binary mixture of different mass% (w_1) of methyl salicylate (1) and I.P.A. (2) at 303.15, 313.15 and 323.15 K.

Mass % of methyl salicylate	a_0 (m^3 mol^{-1})	a_1 (m^3 mol^{-1})	a_2 (m^3 mol^{-1} K^{-2})
$w_1 = 0.00$	−723.33	4.84	−0.0061
$w_1 = 0.05$	−1381.70	9.26	−0.0136
$w_1 = 0.10$	−1824.40	10.90	−0.0164
$w_1 = 0.15$	−1734.70	11.65	−0.0177

Table 5
Limiting partial molar expansibilities of menthol in binary mixture of different mass% (w_1) of methyl salicylate (1) and I.P.A. (2) at 303.15, 313.15 and 323.15 K.

Mass % of methyl salicylate	$\varnothing_E^o$ (m^3 mol^{-1} K^{-1})			$(\delta\varnothing_E^o/\delta T)_p$, dm^3 mol^{-1} K^{-2}
	303.15 K	313.15 K	323.15 K	
$w_1 = 0.00$	1.1390	1.0170	0.8950	−0.0122
$w_1 = 0.05$	1.0170	0.7450	0.4730	−0.0272
$w_1 = 0.10$	0.9527	0.6247	0.2967	−0.0328
$w_1 = 0.15$	0.9175	0.5635	0.2095	−0.0354

interactions respectively, a perusal of Table 7 shows that the values are in agreement with those drawn from the values of V_ϕ^o and S_v^* discussed earlier.

The viscosity data has also been analyzed on the basis of transition state theory of relative viscosity of solutes as suggested by Feakins et al. [23] using the following equation

$$\Delta\mu_2^{0\#} = \Delta\mu_1^{0\#} + \frac{(1000B + \bar{V}_2^0 - \bar{V}_1^0)RT}{\bar{V}_1^0} \quad (11)$$

Table 6
Values of A and B coefficients of menthol in binary mixture of different mass% (w_1) of methyl salicylate (1) and I.P.A.(2) at 303.15, 313.15 and 323.15 K.

Mass % of methyl salicylate	A ($dm^{3/2}$ $mol^{-1/2}$)			B (dm^3 mol^{-1})		
	303.15 K	313.15 K	323.15 K	303.15 K	313.15 K	323.15 K
$w_1 = 0.00$	−0.0108	−0.0118	−0.0149	0.2965	0.3888	0.4871
$w_1 = 0.05$	−0.0101	−0.0105	−0.0126	0.2606	0.3428	0.4015
$w_1 = 0.10$	0.0187	0.0106	0.0086	0.2349	0.3376	0.3795
$w_1 = 0.15$	0.0196	0.0177	0.0144	0.1821	0.2823	0.3495

Table 7
Molality (m), sound speed (u), adiabatic compressibility (β), partial molal adiabatic compressibility ($\varnothing_K$), limiting partial adiabatic compressibility ($\varnothing_K^o$), experimental slope (S_K^*) and refractive indices of menthol in binary mixture of different mass% (w_1) of methyl salicylate (1) and I.P.A.(2) at 303.15 K.

m (mol kg^{-1})	u (m s^{-1})	$\beta \times 10^{10}$ (Pa^{-1})	$\varnothing_K \times 10^{10}$ (m^3 mol^{-1} Pa^{-1})	$\varnothing_K^o \times 10^{10}$ (m^3 mol^{-1} Pa^{-1})	$S_K^* \times 10^{10}$ (m^3 $mol^{-3/2}$ Pa^{-1} $kg^{1/2}$)	n_D
$w_1 = 0.00$						
0.0323	1135.7	9.9707	−2.0794			1.3741
0.0453	1138.2	9.9242	−2.3166			1.3744
0.0584	1141.2	9.8692	−2.6390	−0.5097	−8.7395	1.3747
0.0715	1144.4	9.8106	−2.9100			1.3750
0.0978	1151.1	9.6908	−3.2796			1.3755
0.1110	1154.2	9.6350	−3.3568			1.3757
$w_1 = 0.05$						
0.0317	1152.0	9.5213	−2.0600			1.3796
0.0445	1154.7	9.4744	−2.3500			1.3799
0.0573	1157.3	9.4282	−2.5000	−0.7934	−7.2134	1.3801
0.0702	1160.4	9.3756	−2.7132			1.3803
0.0960	1166.8	9.2658	−3.0300			1.3807
0.1090	1170.3	9.2080	−3.1700			1.3809
$w_1 = 0.10$						
0.0312	1176.4	8.9674	−2.0200			1.3852
0.0437	1178.8	8.9278	−2.1500			1.3858
0.0563	1181.7	8.8825	−2.3300	−0.8666	−6.2585	1.3861
0.0689	1184.6	8.8368	−2.4700			1.3865
0.0943	1191.2	8.7328	−2.8000			1.3870
0.1071	1194.9	8.6776	−2.9416			1.3872
$w_1 = 0.15$						
0.0305	1203.4	8.3926	−1.6900			1.3920
0.0428	1205.6	8.3602	−1.7300			1.3924
0.0551	1208.2	8.3219	−1.8900	−0.9136	−4.1905	1.3928
0.0675	1210.8	8.2833	−2.0000			1.3932
0.0924	1216.7	8.2000	−2.1935			1.3937
0.1048	1219.7	8.1572	−2.2800			1.3940

Table 8
Values of $\Delta\mu_1^{0\#}$, $\Delta\mu_2^{0\#}$, $T\Delta S_2^{0\#}$ and $\Delta H_2^{0\#}$ of menthol in binary mixture of different mass% (w_1) of methyl salicylate (1) and I.P.A. (2) at 303.15, 313.15 and 323.15 K.

Parameter	303.15 K	313.15 K	323.15 K
$w_1 = 0.00$			
$\Delta\mu_1^{0\#}$, kJ mol^{-1}	66.92	68.45	69.92
$\Delta\mu_2^{0\#}$, kJ mol^{-1}	13.16	16.84	20.70
$T\Delta S_2^{0\#}$, kJ mol^{-1}	−114.35	−118.12	−121.89
$\Delta H_2^{0\#} \times 10^3$ kJ mol^{-1}	−101.19	−101.28	−101.19
$w_1 = 0.05$			
$\Delta\mu_1^{0\#}$, kJ mol^{-1}	67.03	68.58	70.07
$\Delta\mu_2^{0\#}$, kJ mol^{-1}	11.60	14.83	17.18
$T\Delta S_2^{0\#}$, kJ mol^{-1}	−84.55	−87.34	−90.13
$\Delta H_2^{0\#} \times 10^3$ kJ mol^{-1}	−72.94	−72.51	−72.95
$w_1 = 0.10$			
$\Delta\mu_1^{0\#}$, kJ mol^{-1}	67.13	68.73	70.31
$\Delta\mu_2^{0\#}$, kJ mol^{-1}	10.45	14.18	15.17
$T\Delta S_2^{0\#}$, kJ mol^{-1}	−89.70	−92.66	−76.26
$\Delta H_2^{0\#} \times 10^3$ kJ mol^{-1}	−79.26	−78.48	−61.10
$w_1 = 0.15$			
$\Delta\mu_1^{0\#}$, kJ mol^{-1}	67.31	68.97	70.58
$\Delta\mu_2^{0\#}$, kJ mol^{-1}	8.68	12.08	14.63
$T\Delta S_2^{0\#}$, kJ mol^{-1}	−90.13	−93.10	−96.07
$\Delta H_2^{0\#} \times 10^3$ kJ mol^{-1}	−81.45	−81.02	−81.45

where $\bar{V}_1^0$ and $\bar{V}_2^0$ are the partial molar volumes of the solvent and the solute respectively. The contribution per mole of the solute to the free energy of activation of viscous flow ($\Delta\mu_2^{0\#}$) of the solutions was determined from the above relation and is listed in Table 8. The free energy of activation of viscous flow of the pure solvent ($\Delta\mu_1^{0\#}$) is given by the relation:

$$\Delta\mu_1^0 = \Delta G_1^0 = \frac{RT\ln(\eta_0\bar{V}_1^0)}{hN_0} \quad (12)$$

where the symbols have their usual significance. The values of $\Delta\mu_2^{0\#}$ and $\Delta\mu_1^{0\#}$ are reported in Table 8. From Table 8 it is evident that $\Delta\mu_1^{0\#}$ is almost constant over all solvent composition and temperature, implying that $\Delta\mu_2^{0\#}$ is mainly dependent on the viscosity B-coefficients and $(\bar{V}_2^0 - \bar{V}_1^0)$ terms. According to Feakins et al., $\Delta\mu_2^{0\#} > \Delta\mu_1^{0\#}$ for electrolytes having positive B-coefficients and indicates a stronger solute–solvent interactions, thereby suggesting that the formation of transition state is accompanied by the rupture and distortion of the intermolecular forces in solvent structure [24]. The smaller values of $\Delta\mu_2^{0\#}$ supports the increased structure breaking tendency of the solute as discussed earlier. The entropy of activation for solution has been calculated using the following relation [23].

$$\Delta S_2^{0\#} = \frac{-\mathrm{d}(\Delta\mu_2^{0\#})}{\mathrm{d}T} \quad (13)$$

where $\Delta S_2^{0\#}$ has been determined from the negative slope of the plots of $\Delta\mu_2^{0\#}$ against T by using a least square treatment.

The activation enthalpy ($\Delta H_2^{0\#}$) has been calculated using the relation [23]:

$$\Delta H_2^{0\#-} = \Delta\mu_2^{0\#} + T\Delta S_2^{0\#} \quad (14)$$

The value of $\Delta S_2^{0\#}$ and $\Delta H_2^{0\#}$ are listed in Table 8 and are found to be negative for all the solutions at all experimental temperatures which suggest that the transition state is associated with bond-breaking and increase in order which supports our earlier discussions.

4. Conclusion

The values of apparent molar volume (V_ϕ^o), viscosity B-coefficients and isoentropic compressibility (ϕ_K^0) indicate the presence of strong solute–solvent interactions and these interactions are strengthened at higher temperature and weakened with increasing mass percent of methyl salicylate in the binary solution.

Acknowledgement

The authors are grateful to the Departmental Special Assistance Scheme, Department of Chemistry, NBU under the University Grants Commission, New Delhi (No. 540/27/DRS/2007, SAP-1) for financial support in order to continue this research work.

References

[1] J.M. Mc Dowall, C.A. Vincent, J. Chem. Soc. Faraday Trans. 1.70 (1974) 1862–1868.
[2] M.R.J. Deck, K.J. Bird, A.J. Parker, Aust. J. Chem. 28 (1975) 955–963.
[3] M.N. Roy, B. Sinha, R. Dey, A. Sinha, Int. J. Thermophys. 26 (2005) 1549–1563.
[4] R.H. Stokes, R. Mills, Int. Encyclopedia of Physical Chemistry and Chemical Physics Vol. 3, 1965.
[5] P.S. Nikam, H. Mehdi, J. Chem. Eng. Data 33 (1988) 165–169.
[6] D. Nandi, M.N. Roy, D.K. Hazra, J. Indian Chem. Soc. 70 (1993) 305–310.
[7] S. Ismadji, J. Chem. Eng. Data 53 (2008) 2207–2210.
[8] G. Yosipovitch, C. Szolar, X.Y. Hui, H. Maibach, Arch. Dermatol. Res. 288 (1996) 245–248.
[9] M.N. Roy, A. Sinha, B. Sinha, J. Solution Chem. 34 (2005) 1311–1325.
[10] M.N. Roy, B. Sinha, V.K. Dakua, J. Chem. Eng. Data 51 (2006) 590–594.
[11] M.N. Roy, A. Sinha, Fluid Phase Equilib. 243 (2006) 133–141.
[12] M.N. Roy, M. Das, Russ. J. Phys. Chem. 80 (2006) S163–S171.
[13] D.O. Masson, Philos. Mag. 8 (1929) 218–226.
[14] E. Garland-Paneda, C. Yanes, J.J. Calventa, A. Maestre, J. Chem. Soc. Faraday Trans. 90 (1994) 575–578.
[15] M.N. Roy, A. Jha, R. Dey, J. Chem. Eng. Data 46 (2001) 1327–1329.
[16] F.J. Millero, Structure and Transport Process in Water and Aqueous Solutions, R.A. Horne, New York, 1972.
[17] M.L. Parmar, D.S. Banyal, Indian J. Chem. 44A (2005) 1582–1588.
[18] L.G. Hepler, Can. J. Chem. 47 (1969) 4613–4617.
[19] B.K. Sarkar, B. Sinha, M.N. Roy, Russian J. Phys. Chem. 82 (2008) 960–966.
[20] G. Jones, M. Dole, J. Am. Chem. Soc. 51 (1929) 2950–2964.
[21] F.J. Millero, Chem. Rev. 71 (1971) 147–176.
[22] F.J. Millero, A. Losurdo, C. Shin, J. Phys. Chem. 82 (1978) 784–792.
[23] D. Feakins, D.J. Freemantle, K.G. Lawrence, J. Chem. Soc. Faraday Trans. 1.70 (1974) 795–806.
[24] B. Samantaray, S. Mishra, U.N. Dash, J. Teach. Res. Chem. 11 (2005) 87–96.
[25] C.H. Tu, C.Y. Liu, W.F. Wang, Y.T. Chou, J. Chem. Eng. Data 45 (2000) 450–456.
[26] C. Yang, H. Lai, Z. Liu, P. Ma, J. Chem. Eng. Data 51 (2006) 584–589.
[27] K.R. Babu, R. Venkateswarlu, G.K. Raman, Asian J. Chem. 1 (1989) 147–152.
[28] T.M. Aminabhavi, M.I. Aralaguppi, S.B. Harogoppad, R.H. Balundgi, J. Chem. Eng. Data 38 (1993) 31–39.

J. Chem. Eng. Data 2009, 54, 2429–2435

Ion Pair and Triple Ion Formation by Some Tetraalkylammonium Iodides in Binary Mixtures of Carbon Tetrachloride + Nitrobenzene†

Mahendra Nath Roy,* Pran Kumar Roy, Radhey Shyam Sah, Prasanna Pradhan, and Biswajit Sinha*

Department of Chemistry, University of North Bengal, Darjeeling-734013, India

Electrical conductances of tetraalkylammonium iodides, R_4NI (R = butyl to heptyl), in different mass % (20 to 80) of carbon tetrachloride (CCl_4) + nitrobenzene ($PhNO_2$) have been measured at 298.15 K. Limiting molar conductances Λ_0, association constants K_A, and cosphere diameter R for ion pair formation in the mixed solvent mixtures have been evaluated using the Lee–Wheaton conductivity equation. However, the deviation of the conductometric curves (Λ versus $\sqrt{c}$) from linearity for the electrolytes in 80 mass % of CCl_4 + $PhNO_2$ indicated triple ion formation, and therefore corresponding conductance data have been analyzed by the Fuoss–Kraus theory of triple ions. Limiting ionic molar conductances $\lambda_0^{\pm}$ have been calculated by the reference electrolyte method along with a numerical evaluation of ion pair and triple ion formation constants ($K_P \approx K_A$ and K_T); the results have been discussed in terms of solvent properties and configurational theory.

Introduction

Mixed solvents enable the variation of properties such as dielectric constant or viscosity, and therefore the ion–ion and ion–solvent interactions can be better studied. Furthermore, different quantities strongly influenced by solvent properties can be derived from concentration dependence of the electrolyte conductivity. Consequently, a number of conductometric[1] and related studies of different electrolytes in nonaqueous solvents, especially mixed organic solvents, have been made for their optimal use in high-energy batteries[2] and for understanding organic reaction mechanisms.[3] Ionic association of electrolytes in solution depends upon the mode of solvation of its ions,[4–8] which in turn depends on the nature of the solvent or solvent mixtures. Such solvent properties as viscosity and the relative permittivity have been taken into consideration as these properties help in determining the extent of ion association and the solvent–solvent interactions. Thus, extensive studies on electrical conductances in various mixed organic solvents have been performed in recent years[9–13] to examine the nature and magnitude of ion–ion and ion–solvent interactions. Also, tetraalkylammonium salts are characterized by their low surface charge density, and they show little or no solvation in solution.[14,15] As such, they are frequently selected as desired electrolytes in conductance studies. In continuation of our investigation on electrical conductances,[8,10,11] the present work deals with the conductance measurements of some tetraalkylammonium iodides, R_4NI (R = butyl to heptyl), in binary mixtures of CCl_4—a nonpolar aprotic liquid—and $PhNO_2$—a polar aprotic liquid—at 298.15 K.

Experimental Section

Materials. CCl_4 (carbon tetrachloride, CAS: 56-23-5) and $PhNO_2$ (nitrobenzene, CAS: 98-95-3) were purchased from Merck, India, and purified as reported earlier.[16] The mole percent purities for the liquids used as checked by GC (HP6890) using an FID detector were better than 99. The salts Bu_4NI (*N,N,N*-tributyl-1-butanaminium iodide, CAS: 311-28-4), Pen_4NI (*N,N,N*-tripentyl-1-pentanaminium iodide, CAS: 2498-20-6), Hex_4NI (*N,N,N*-trihexyl-1-hexanaminium iodide, CAS: 2138-24-1), and $Hept_4NI$ (*N,N,N*-triheptyl-1-heptanaminium iodide, CAS: 3535-83-9) of puriss grade were purchased from Aldrich, Germany, and purified by dissolving in mixed alcohol medium and recrystallized from solvent ether medium.[17] After filtration, the salts were dried in a oven for a few hours.

Table 1. Density ρ, Viscosity η, and Dielectric Constant ε for CCl_4 (1) + $PhNO_2$ (2) at T = 298.15 K

	$(\rho \cdot 10^{-3})/(kg \cdot m^{-3})$		$(\eta)/(mPa \cdot s)$		
solvent mixture	expt	lit.	expt	lit.	ε_r
$w_1 = 0.00$	1.1982	1.1985[40] 1.1983[41]	1.686	1.686[41]	34.69[18]
$w_1 = 0.20$	1.2614		1.613		29.66[a]
$w_1 = 0.40$	1.3314		1.411		23.90[a]
$w_1 = 0.60$	1.4067		1.224		17.45[a]
$w_1 = 0.80$	1.4910		1.099		10.22[a]
$w_1 = 1.00$	1.5843	1.5844[41]	0.902	0.9017[41]	2.25[41]

[a] Obtained by interpolation of literature data from ref 18.

Apparatus and Procedure. Binary solvent mixtures were prepared by mixing a required volume of CCl_4 and $PhNO_2$ with earlier conversion of required mass of each liquid into volume at 298.15 K using experimental densities. A stock solution for each salt was prepared by mass, and the working solutions were obtained by mass dilution. The uncertainty of molarity of different salt solutions is evaluated to ± 0.0001 mol·dm^{-3}.

The values of relative permittivity ε_r of the solvent mixtures were obtained by interpolation of the solvent permittivity data from the literature[18] by cubic spline fitting. The physical properties of the binary solvent mixtures at 298.15 K are listed in Table 1. Densities were measured with an Ostwald–Sprengel-type pycnometer having a bulb volume of about 25 cm^3 and an internal diameter of the capillary of about 0.1 cm. The pycnometer was calibrated at 298.15 K with doubly distilled

* Corresponding authors. Tel.: +91-353-2776381. E-mail: mahendraroy2002@yahoo.co.in and biswachem@gmail.com.

† Part of the "William A. Wakeham Festschrift".

10.1021/je800885h CCC: $40.75
Published on Web 05/11/2009

water and benzene.[19] The pycnometer with experimental liquid was equilibrated in a glass-walled thermostatted water bath maintained at ± 0.01 K of the desired temperature. The pycnometer was then removed from the thermostat, properly dried, and weighed in an electronic balance with a precision of ± 0.01 mg. Adequate precautions were taken to avoid evaporation losses during the time of measurements. An average of triplicate measurement was taken into account. The uncertainty of density values is $\pm 3 \cdot 10^{-4}$ g·cm^{-3}. Solvent viscosities were measured by means of a suspended Ubbelohde-type viscometer, calibrated at 298.15 K with doubly distilled water and purified methanol using density and viscosity values from the literature.[20−22] A thoroughly cleaned and perfectly dried viscometer filled with experimental liquid was placed vertically in the glass-walled thermostat maintained to ± 0.01 K. After attainment of thermal equilibrium, efflux times of flow were recorded with a stopwatch correct to ± 0.1 s. At least three repetitions of each data reproducible to ± 0.1 s were taken to average the flow times. The uncertainty of viscosity values is ± 0.003 mPa·s. The details of the methods and measurement techniques had been described elsewhere.[11,23] The conductance measurements were carried out in a systronic 308 conductivity bridge (accuracy ± 0.01 %) using a dip-type immersion conductivity cell, CD-10, having a cell constant of approximately (0.1 ± 10) %. Measurements were made in a water bath maintained within T = (298.15 ± 0.01) K, and the cell was calibrated by the method proposed by Lind et al.[24] The conductance data were reported at a frequency of 1 kHz and were uncertain to ± 0.3 %.

Results and Discussion

The concentrations and molar conductances Λ of R_4NI (R = butyl to heptyl) in different binary solvent mixtures of CCl_4 and $PhNO_2$ are given in Table 2.

For the solvent mixtures in the range of moderate relative permittivity (ε_r = 29.66 to 17.45), the conductance curves (Λ versus $\sqrt{c}$) were linear, and extrapolation of $\sqrt{c} = 0$ evaluated the starting limiting molar conductances for the electrolytes; however, as the relative permittivity ε_r droped to 10.22 for the solvent mixture containing 80 mass % of CCl_4 in $PhNO_2$, nonlinearity (Figure 1) was observed in conductance curves. Thus the conductance data, in the solvent mixtures (w_1 = 0.20 to 0.60) wherein higher clusters other than ion pair formation was not expected, were analyzed by the Lee−Wheaton conductance equation[25] in the form

$$\Lambda = \alpha_i\left\{\Lambda_0[1 + C_1\beta\kappa + C_2(\beta\kappa)^2 + C_3(\beta\kappa)^3] - \frac{\rho\kappa}{1+\kappa R}\left[1 + C_4\beta\kappa + C_5(\beta\kappa)^2 + \frac{\kappa R}{12}\right]\right\} \quad (1)$$

The mass action law association[26] is

$$K_A = (1 - \alpha_i)\gamma_A/\alpha_i^2 c_i \gamma_\pm^2 \quad (2)$$

and the equation for the mean ionic activity coefficient

$$\gamma_\pm = \exp\left[-\frac{q\kappa}{1+\kappa R}\right] \quad (3)$$

where C_1 to C_5 are least-squares fitting coefficients as described by Pethybridge and Taba;[25] Λ_0 is the limiting molar conductivity; K_A is the association constant; α_i is the dissociation degree; q is the Bjerrum parameter; γ is the activity coefficient; and $\beta = 2q$. The distance parameter R is the least distance that two free ions can approach before they merge into an ion pair. The Debye parameter κ, the Bjerrum parameter q, and ρ[25] are defined by the expressions

$$\kappa = 16000\pi N_A q c_i \alpha_i \quad (4)$$

$$q = \frac{e^2}{8\varepsilon_0\varepsilon_r kT} \quad (5)$$

$$\rho = \frac{Fe}{299.79 \cdot 3\pi\eta} \quad (6)$$

where the symbols have their usual significance.[27]

Equation 1 was resolved by an iterative procedure. For a definite R value, the initial values of Λ_0 and K_A were obtained by the Kraus−Bray method.[28] The parameters Λ_0 and K_A were made to approach gradually their best values by a sequence of alternating linearization and least-squares optimizations by the Gauss−Siedel method[29] until satisfying the criterion for convergence. The best value of a parameter is the one when eq 1 is best fitted to the experimental data corresponding to minimum standard deviation σ_Λ for a sequence of predetermined R values, and standard deviation σ_Λ was calculated by the following equation

$$\sigma_\Lambda^2 = \sum_{i=1}^{n} \frac{[\Lambda_i(\text{calcd}) - \Lambda_i(\text{obsd})]^2}{n - m} \quad (7)$$

where n is the number of experimental points and m is the number of fitting parameters. The conductance data were analyzed by fixing the distance of closest approach R with two-parameter fit (m = 2). As for the electrolytes studied in the solvent mixtures (w_1 = 0.20 to 0.60), no significant minima were observed in the σ_Λ versus R curves, and the R values were arbitrarily preset at the center to center distance of the solvent-separated pair[8]

$$R = a + d \quad (8)$$

where a is the sum of the crystallographic radii of the cation and anion and d is the average distance corresponding to the side of a cell occupied by a solvent molecule. The definitions of d and related terms have already been described in the literature.[8] R was generally varied by a step of 0.1 Å, and the iterative process was continued with eq 1.

Table 3 reveals that the limiting molar conductances Λ_0 for the electrolytes decrease with the increase of CCl_4 content in the solvent mixtures. This fact is in line with the decrease of the relative permittivity ε_r of the solvent mixtures.[14,30] Although the decreasing trend of viscosity for the solvent mixtures with increasing content of CCl_4 suggests concomitant increase in limiting molar conductances[14,30] for the electrolytes, we observed an opposite trend. This trend suggests predominance of relative permittivity ε_r over the solvent viscosity η_0 in effecting the electrolytic conductances of the electrolytes under study in these media. In a particular solvent mixture, the limiting molar conductances Λ_0 of the electrolytes under investigation decrease as the size of the alkyl group increases, in contraposition to the conductance behavior of the alkali metal cations, as tetraalkylammonium salts are characterized by their low surface charge density.[14,15]

The decreasing trend of Walden products $\Lambda_0\eta_0$ in Table 3 is mainly in accordance with the concomitant decrease of both the solvent viscosity and limiting molar conductance of the electrolytes. The ionic conductances $\lambda_0^\ddagger$ for the various R_4N^+ cations (R = butyl to hexyl) in different solvent mixtures (w_1 = 0.20 to 0.60) were calculated using tetrabutylammonium tetraphenyl borate (Bu_4NBPh_4) as a reference electrolyte following the scheme as suggested by B. Das et al.[31] We calculated its limiting molar conductances $\lambda_0^\ddagger$ in our solvent compositions by interpolation of conductance data from the literature[18] using

Table 2. Concentrations c and Molar Conductances Λ of R_4NI (R = Butyl to Heptyl) in Different Binary Solvent Mixtures of CCl_4 (1) + $PhNO_2$ (2) at T = 298.15 K

Bu_4NI		Pen_4NI		Hex_4NI		$Hept_4NI$	
$(c \cdot 10^4)$ / (mol·dm^{-3})	(Λ) / (S·cm^2·mol^{-1})	$(c \cdot 10^4)$ / (mol·dm^{-3})	(Λ) / (S·cm^2·mol^{-1})	$(c \cdot 10^4)$ / (mol·dm^{-3})	(Λ) / (S·cm^2·mol^{-1})	$(c \cdot 10^4)$ / (mol·dm^{-3})	(Λ) / (S·cm^2·mol^{-1})
			$w_1 = 0.20$				
8.3	39.50	8.3	38.60	8.4	36.38	8.3	35.20
15.3	37.00	15.3	36.00	15.3	34.66	15.3	33.20
21.2	35.80	21.2	34.90	21.2	33.14	21.2	32.33
26.2	34.68	26.2	34.20	26.3	32.14	26.2	31.22
30.6	34.00	30.6	33.00	30.64	31.66	30.6	30.72
34.4	33.50	34.4	33.00	34.5	30.50	34.4	30.20
37.8	32.80	37.8	31.70	37.8	30.30	37.8	29.89
40.8	32.10	40.8	31.30	40.8	29.80	40.8	29.30
45.9	31.70	43.5	30.60	43.5	29.40	45.9	29.00
50.1	30.50	48.1	29.70	46.0	29.37	50.1	28.40
53.6	30.00	51.9	29.27	50.1	28.92	53.6	28.19
57.8	29.40	55.1	28.66	51.9	28.49	56.5	27.70
61.2	29.20	57.8	28.52	55.1	28.29	59.0	27.62
64.0	28.59	61.2	28.08	57.9	27.82	61.2	27.28
66.3	28.34	64.0	27.80	60.2	27.23	63.1	27.25
68.3	28.26	66.3	27.58	63.2	27.22	65.6	27.00
69.9	28.01	68.3	27.37	65.7	27.11	67.6	26.76
71.4	28.00	70.5	27.23	67.1	26.98	69.4	26.51
72.3	27.80	72.3	26.96	69.5	26.62	70.9	26.36
73.8	27.76	74.2	26.95	71.5	26.44	72.7	26.28
			$w_1 = 0.40$				
4.4	38.80	4.4	36.89	4.4	35.50	4.6	34.61
8.1	37.00	6.3	36.00	6.3	35.25	6.6	33.82
11.3	35.80	8.1	35.20	8.0	34.18	8.4	32.71
13.9	34.56	9.7	34.56	9.7	33.86	10.1	32.31
16.3	33.37	11.2	34.00	11.1	33.39	11.6	31.84
18.3	32.83	13.9	32.90	12.8	32.47	13.1	31.35
20.1	32.30	16.2	32.34	13.8	32.10	14.4	30.91
23.1	31.50	18.2	31.43	14.9	32.04	15.7	30.54
25.6	30.43	20.0	30.70	17.1	31.23	17.9	29.82
27.6	30.19	21.6	30.50	19.0	30.86	19.9	29.66
29.3	29.81	23.0	30.14	20.7	30.30	21.6	29.16
31.4	29.32	24.3	29.38	22.2	29.75	23.2	28.61
33.1	28.97	26.5	29.30	23.5	29.21	24.6	28.60
34.4	28.44	28.4	29.06	24.7	29.16	25.9	28.24
35.6	28.36	29.9	28.68	25.8	28.77	27.0	27.99
36.9	27.91	31.2	28.22	27.7	28.41	29.0	27.54
37.9	27.66	32.9	27.94	29.3	27.64	30.7	27.37
39.0	27.40	34.3	27.69	30.7	27.73	32.1	26.95
39.9	27.29	35.5	27.35	31.9	27.48	33.4	26.81
40.7	27.29	36.7	26.94	33.4	26.93	34.5	26.40
			$w_1 = 0.60$				
1.7	36.41	1.7	34.60	1.7	33.30	1.7	32.30
2.5	34.82	2.4	33.05	2.4	32.51	2.4	31.60
3.2	34.12	3.1	32.50	3.1	31.40	3.1	30.80
3.8	32.94	3.8	31.40	3.7	30.48	3.8	30.05
4.4	32.12	4.3	30.70	4.3	30.20	4.3	29.73
4.9	31.31	4.9	30.00	4.8	29.70	4.9	28.93
5.4	30.94	5.4	29.50	5.3	29.00	5.4	28.67
5.9	30.44	5.8	29.10	5.8	28.60	5.8	28.11
6.3	29.80	6.3	28.90	6.2	28.40	6.3	28.00
7.1	29.21	6.7	28.50	6.6	28.00	6.7	27.70
7.8	28.20	7.0	27.96	7.4	27.56	7.0	27.20
8.4	27.66	7.7	27.70	7.7	27.14	7.7	26.87
8.9	27.18	8.3	26.94	8.3	26.71	8.4	26.33
9.5	26.81	8.9	26.63	8.9	26.30	8.9	25.94
9.9	26.50	9.4	26.08	9.3	25.88	9.4	25.74
10.7	25.86	9.8	25.71	9.8	25.80	10.2	24.96
11.4	25.42	10.6	25.40	10.6	25.26	11.3	24.02
11.9	25.31	11.3	24.60	11.2	24.87	11.8	23.82
12.6	24.62	11.8	24.51	11.8	24.46	12.3	23.54
13.2	24.54	12.3	24.29	12.2	24.24	12.9	23.29
			$w_1 = 0.80$				
1.7	4.07	1.7	3.72	1.7	3.72	1.7	3.64
2.4	3.57	2.4	3.27	2.4	3.20	2.4	3.38
3.1	3.26	3.1	2.96	3.1	2.95	3.1	3.09
3.8	3.03	3.8	2.71	3.8	2.75	3.8	2.90
4.3	2.93	4.3	2.49	4.3	2.61	4.3	2.72
4.9	2.81	4.9	2.36	4.9	2.50	4.9	2.63
5.4	2.72	5.4	2.25	5.4	2.40	5.4	2.51
5.8	2.59	5.8	2.16	5.8	2.31	5.8	2.43
6.3	2.55	6.3	2.10	6.3	2.28	6.3	2.36
7.0	2.45	7.0	2.00	7.0	2.21	6.7	2.29
7.7	2.33	7.7	1.87	7.7	2.13	7.0	2.23

Table 2. (Continued)

Bu_4NI		Pen_4NI		Hex_4NI		$Hept_4NI$	
$(c \cdot 10^4)$	(Λ)	$(c \cdot 10^4)$	(Λ)	$(c \cdot 10^4)$	(Λ)	$(c \cdot 10^4)$	(Λ)
(mol·dm^{-3})	(S·cm^2·mol^{-1})	(mol·dm^{-3})	(S·cm^2·mol^{-1})	(mol·dm^{-3})	(S·cm^2·mol^{-1})	(mol·dm^{-3})	(S·cm^2·mol^{-1})
8.4	2.26	8.3	1.82	8.4	2.05	7.7	2.17
8.9	2.19	8.9	1.74	8.9	1.98	8.4	2.08
9.4	2.15	9.4	1.72	9.4	1.95	8.9	2.02
10.2	2.05	9.8	1.68	10.2	1.87	9.4	1.97
10.9	2.01	10.6	1.66	10.9	1.81	9.8	1.94
11.6	1.94			11.6	1.77	10.6	1.87
12.1	1.90			12.1	1.75	11.3	1.82
12.7	1.86			12.5	1.70	11.8	1.78
13.3	1.82			13.1	1.66	12.3	1.75

cubic spline fitting. The $\lambda_0^{\pm}$ values were in turn utilized for the calculation of Stokes' radii r_s according to the classical expression[32]

$$r_s = \frac{F^2}{6\pi N_A \lambda_0^{\pm} \eta_0} \tag{9}$$

Ionic Walden products $\lambda_0^{\pm}\eta_0$, Stokes' radii r_s, and crystallographic radii r_c are presented in Table 4. The trends in ionic

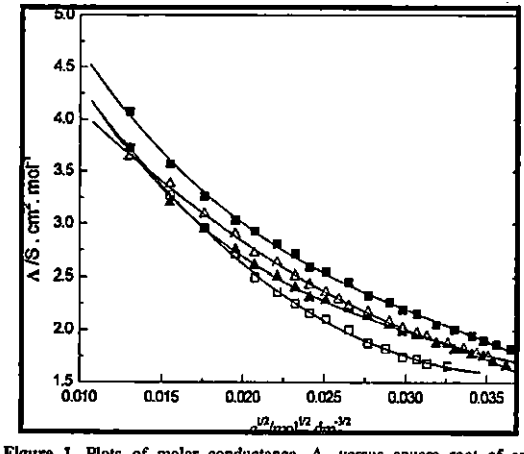

Figure 1. Plots of molar conductance, Λ, versus square root of salt concentration, $c^{1/2}$, in $w_1 = 0.80$ of CCl_4 (1) + $PhNO_2$ (2) at $T = 298.15$ K. ■, Bu_4NI; □, Pen_4NI; ▲, Hex_4NI; △, $Hept_4N$.

Table 3. Limiting Molar Conductance Λ_0, Association Constant K_A, Cosphere Diameter R, and Standard Deviations σ of Experimental Λ from Equation 1 and Walden Products for the Electrolytes in Different Binary Solvent Mixtures of CCl_4 (1) + $PhNO_2$ (2) at $T = 298.15$ K

w_1	Λ_0 (S·cm^2·mol^{-1})	K_A	R Å	$\Lambda_0\eta_0$ (S·cm^2·mol^{-1}·mPa·s)	σ
			Bu_4NI		
0.20	46.23	159.9	12.0	74.57	0.24
0.40	45.71	301.1	12.4	64.49	0.22
0.60	44.94	330.5	12.7	54.99	0.25
			Pen_4NI		
0.20	42.53	90.9	11.9	69.77	0.21
0.40	42.35	246.1	13.4	59.75	0.26
0.60	41.51	1075.3	12.6	50.79	0.26
			Hex_4NI		
0.20	41.74	126.5	11.9	67.33	0.23
0.40	41.31	231.9	12.3	58.28	0.25
0.60	39.01	816.2	12.6	47.74	0.24
			$Hept_4NI$		
0.20	39.59	99.6	11.9	63.86	0.12
0.40	39.30	195.8	12.3	55.44	0.14
0.60	38.51	851.9	12.6	47.13	0.16

Table 4. Limiting Ionic Conductance $\lambda_0^{\pm}$, Ionic Walden Product $\lambda_0^{\pm}\eta_0$, Stokes' Radii r_s, and Crystallographic Radii r_c at $T = 298.15$ K

ion	$\lambda_0^{\pm}$ (S·cm^2·mol^{-1})	$\lambda_0^{\pm}\eta_0$ (S·cm^2·mol^{-1}·mPa·s)	r_s Å	r_c[a] Å
		$w_1 = 0.20$		
Bu_4N^+	13.38	21.58	3.79	4.94
Pen_4N^+	9.68	15.61	5.25	5.29
Hex_4N^+	8.89	14.34	5.71	5.60
$Hept_4N^+$	8.74	10.87	7.53	5.88
I^-	32.85	52.99	1.76	2.16
		$w_1 = 0.40$		
Bu_4N^+	14.97	21.12	3.93	4.94
Pen_4N^+	11.61	16.38	5.09	5.29
Hex_4N^+	10.57	14.91	5.60	5.60
$Hept_4N^+$	8.56	12.08	6.95	5.88
I^-	30.74	43.37	1.87	2.16
		$w_1 = 0.60$		
Bu_4N^+	15.83	18.82	4.15	4.94
Pen_4N^+	12.40	15.18	5.26	5.29
Hex_4N^+	9.90	12.16	6.56	5.60
$Hept_4N^+$	9.40	11.50	6.89	5.88
I^-	29.11	35.62	2.32	2.16

[a] r_c values are taken from ref 14.

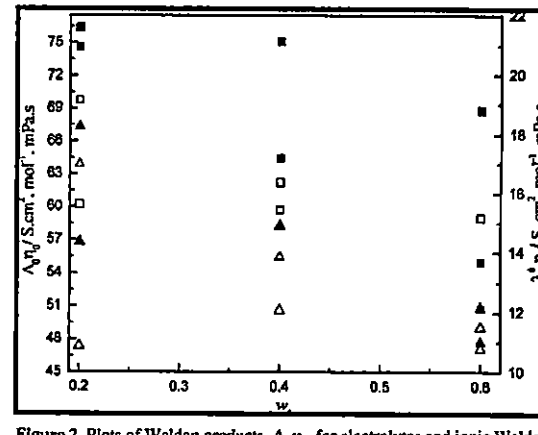

Figure 2. Plots of Walden products, $\Lambda_0\eta_0$, for electrolytes and ionic Walden products, $\lambda_0^{\pm}\eta_0$, versus w_1 of CCl_4 (1) + $PhNO_2$ (2) mixtures at $T = 298.15$ K. ■, Bu_4NI or Bu_4N^+; □, Pen_4NI or Pen_4N^+; ▲, Hex_4NI or Hex_4N^+; △, $Hept_4N$ or $Hept_4N^+$.

Walden products $\lambda_0^{\pm}\eta_0$ and Walden products $\Lambda_0\eta_0$ for all the electrolytes in the solvent mixtures ($w_1 = 0.20$ to 0.60) are depicted in Figure 2. It shows that Walden products $\Lambda_0\eta_0$ for all electrolytes decrease almost linearly as the CCl_4 content increases in the solvent mixtures, but the trend in ionic Walden products $\lambda_0^{\pm}\eta_0$ for R_4N^+ ions is rather irregular. However, the I^- ion shows a similar trend with the electrolytes in this regard.

Table 5. Calculated Limiting Molar Conductance Λ_0, Slope and Intercepts of Equation 10, Maximum Concentration c, Ion Pair Formation Constant K_P, Triple Ion Formation Constant K_T, Ion Pair Concentration c_P, and Triple Ion Concentration c_T for R_4NI (R = Butyl to Heptyl) in 80 Mass % of CCl_4 (1) + $PhNO_2$ (2) at $T = 298.15$ K

Λ_0 / (S·cm²·mol⁻¹)	slope	intercept·10²	c^a·10⁴ / (mol·dm⁻³)	K_P·10⁵	K_T	c_P·10³	c_T·10⁶
			Bu_4NI				
50.04	9.069 (± 0.003)	6.164 (± 0.002)	13.3	6.6	220.6	1.24	13.1
			Pen_4NI				
46.22	5.824 (± 0.002)	5.265 (± 0.003)	10.6	7.7	165.8	1.01	6.5
			Hex_4NI				
43.44	7.121 (± 0.004)	5.408 (± 0.001)	13.1	6.4	194.4	1.23	11.5
			$Hept_4NI$				
42.88	15.422 (± 0.001)	5.235 (± 0.001)	12.3	6.7	441.7	1.12	23.3

[a] Maximum concentrations used in calculations.

Thus, it seems that the I^- ion plays a predominating role in characterizing the conductance behavior of the electrolytes under study in these media. The position of the curves in Figure 2, $\Lambda_0\eta_0$ or $\lambda_\delta^+\eta_0$ versus w_1, suggests a relationship $Bu_4N^+ < Pen_4N^+ < Hex_4N^+ < Hept_4N^+$ for Stokes' radius just similar to their ionic radii order. For tetraalkylammonium ions, the Stokes' radii are either lower or comparable to their crystallographic radii r_c, particularly for smaller ions. This suggests that these ions are comparatively less solvated than alkali metal ions due to their intrinsic low surface charge density.

The conductance data for all the electrolytes in 80 mass % of CCl_4 in $PhNO_2$ ($\varepsilon_r = 10.22$) were analyzed by the classical Fuoss–Kraus theory of triple ion formation in the form[33,34]

$$\Lambda g(c)\sqrt{c} = \frac{\Lambda_0}{\sqrt{K_P}} + \frac{\Lambda_0^T K_T}{\sqrt{K_P}}\left(1 - \frac{\Lambda}{\Lambda_0}\right)c \qquad (10)$$

where $g(c)$ is a factor that lumps together all the intrinsic interaction terms and is defined by

$$g(c) = \frac{\exp\{-(2.303/\Lambda_0^{1/2})\beta(c\Lambda^{1/2})\}}{\{1 - (S/\Lambda_0^{3/2})(c\Lambda)^{1/2}\}(1 - \Lambda/\Lambda_0)^{1/2}} \qquad (11)$$

$$\beta = 1.8247\cdot10^6/(\varepsilon T)^{3/2} \qquad (12)$$

$$S = \alpha\Lambda_0 + \beta = \frac{0.8204\cdot10^6}{(\varepsilon T)^{3/2}}\Lambda_0 + \frac{82.501}{\eta(\varepsilon T)^{1/2}} \qquad (13)$$

In the above equations, Λ_0 is the sum of the molar conductance of the simple ions at infinite dilution; Λ_δ^T is the sum of the conductances of the two triple ions $R_4N(I_2)^-$ and $(R_4N)_2^+I$ for R_4NI salts; and $K_P \approx K_A$ and K_T are the ion pair and triple ion formation constants. To make eq 10 applicable, the symmetrical approximation of the two possible constants of triple ions equal to each other has been adopted, and Λ_0 values for the studied electrolytes in 80 mass % of CCl_4 in $PhNO_2$ have been calculated using respective Λ_0 and η_0 values in 60 mass % of CCl_4 in $PhNO_2$ according to the Walden rule.[14,30] Λ_δ^T is calculated by setting the triple ion conductance equal to $2/3\Lambda_0$.[35] The ratio $\Lambda_\delta^T/\Lambda_0$ was thus set equal to 0.667 during linear regression analysis of eq 10.

Linear regression analysis of eq 10 for the electrolytes with an average regression constant, $R^2 = 0.9653$, gives intercepts and slopes. These permit the calculation of other derived parameters such as K_P and K_T listed in Table 5. A perusal of Table 5 shows that the major portion of the electrolytes exists as ion pairs with a minor portion as triple ions. Using the K_P values, the interionic distance parameter a_{IP} has been calculated with the aid of the Bjerrum's theory of ionic association[36] in the form

Table 6. Interionic Distance Parameter a_{IP} and Interionic Distance for Triple Ion a_{TI} in 80 mass % of CCl_4 in $PhNO_2$ at $T = 298.15$ K

electrolyte	a_{IP}/Å	a_{TI}/Å	$1.5a_{IP}$/Å
Bu_4NI	3.01	3.95	4.51
Pen_4NI	2.99	4.32	4.48
Hex_4NI	3.02	3.92	4.53
$Hept_4NI$	3.01	3.62	4.51

$$K_P = \frac{4\pi N_A}{1000}\left[\frac{e^2}{\varepsilon_r kT}\right]^3 Q(b) \qquad (14)$$

$$Q(b) = \int_2^b y^{-4}\exp(y)dy \qquad (15)$$

$$b = \frac{e^2}{a_{IP}\varepsilon_r kT} \qquad (16)$$

The a_{IP} values obtained are given in Table 6. The $Q(b)$ and b values have been calculated by the literature procedure.[36] Table 6 reveals that a_{IP} values are almost similar for all the electrolytes though the actual ionic sizes varied by (0.28 to 0.35) Å. This may be due to easy penetration by the I^- ion to some extent into the void spaces between the alkyl chains, as suggested by Abbott and Schiffrin.[37] Thus, an increase in chain length for tetraalkylammonium ions does not affect the distance of closest approach between the two ions. The a_{IP} are much less in comparison with the crystallographic radii (r_c) suggesting probable contact ion pairs for the iodides in solution.[14] This will cause a decrease in the degree of freedom for the cations in the ion pair resulting in their loss of configurational entropy of the contact pair. Generally, K_P values do not change significantly for quaternary ammonium ions with the alkyl chain consisting of more than 3 carbon atoms. The small changes in the K_P may thus be related to entropic contributions. The interionic distance a_{TI} for the triple ion can be calculated using the expressions[33]

$$K_T = \frac{2\pi N_A a_{TI}^3}{1000} I(b_3) \qquad (17)$$

$$b_3 = \frac{e^2}{a_{TI}\varepsilon_r kT} \qquad (18)$$

$I(b_3)$ is a double integral tabulated in the literature[33] for a range of values of b_3. Since $I(b_3)$ is a function of a_{TI}, a_{TI} values have

been calculated by an iterative computer program. The a_{TI} values (Table 6) for the electrolytes are greater than the corresponding a_{IP} values but are much less than the expected theoretical value $1.5a_{IP}$. This is probably due to repulsive forces between the two anions or cations in the triple ions $R_4N(I_2)^-$ and $(R_4N)_2^+I$ as suggested by Hazra et al.[38]

A perusal of Table 5 shows that the major portion of the electrolytes exists as ion pairs with a minor portion as triple ions. The tendency of triple ion formation can be judged from the K_T/K_P ratios, which are highest for $Hept_4NI$. These ratios suggest that strong association between the ions is due to the Coulombic interactions as well as to covalent forces in the solution. At very low permittivity of the solvent ($\varepsilon_r < 15$),[30] electrostatic interactions are very strong permitting the ion pair to attract free anions/cations from solution bulk and from triple ions[33,38] which acquire the charge of the combining ion, i.e.

$$\begin{aligned} &M^+ + A^- \leftrightarrow M^+...A^- \leftrightarrow MA \\ &MA + A^- \leftrightarrow AMA^- \\ &MA + M^+ \leftrightarrow MAM^+ \qquad [M = R_4N \text{ and } A = I] \end{aligned} \tag{19}$$

The effect of ternary association[39] thus removes some nonconducting species MA from solution and replaces them by triple ions which increase the conductance manifested by nonlinearity observed in conductance curves for the electrolytes in 80 mass % of CCl_4 in $PhNO_2$.

The ion pair and triple ion concentrations (c_P and c_T, respectively) of the electrolytes at the highest electrolyte concentration have been derived using eqs[38] 20 to 23 and are listed in Table 5.

$$\alpha = (K_P c)^{-1/2} \tag{20}$$

$$\alpha_T = \frac{K_T}{K_P^{0.5}} c^{1/2} \tag{21}$$

$$c_P = c(1 - \alpha - 3\alpha_T) \tag{22}$$

$$c_T = \frac{K_T}{K_P^{1/2}} c^{3/2} \tag{23}$$

While the highest c_P value was found for Bu_4NI, the highest c_T value was found for $Hept_4NI$.

Note Added after ASAP Publication: This paper was published ASAP on May 11, 2009. A change was made to an author name. The revised paper was reposted on May 18, 2009.

Literature Cited

(1) Janz, C. G.; Tomkins, R. P. T. *Non-aqueous Electrolytes Handbook*; Academic Press: New York, 1973; Vol. 2.

(2) Aurbach, D. *Non-aqueous Electrochemistry*; Marcel Dekker, Inc: New York, 1999.

(3) Krom, J. A.; Petty, J. T.; Streitwieser, A. Carbon acidity. 86. Lithium and cesium ion-pair acidities of diphenylamine in tetrahydrofuran. The aggregation of lithium and cesium diphenylamide. A new method for the determination of aggregation constants in dilute solution. *J. Am. Chem. Soc.* **1993**, *115*, 8024–8030.

(4) Das, D.; Das, B.; Hazra, D. K. Conductance of Some 1:1 Electrolytes in *N, N*-Dimethylacetamide at 25°C. *J. Solution Chem.* **2002**, *31*, 425–431.

(5) Guha, C.; Chakraborty, J. M.; Karanjai, S.; Das, B. The Structure and Thermodynamics of Ion Association and Solvation of Some Thiocyanates and Nitrates in 2- Methoxyethanol Studied by Conductometry and FTIR Spectroscopy. *J. Phys. Chem. B* **2003**, *107*, 12814–12819.

(6) Das, D.; Das, B.; Hazra, D. K. Electrical Conductance of Some Symmetrical Tetraalkylammonium and Alkali Salts in *N, N*-Dimethylacetamide at 25°C. *J. Solution Chem.* **2003**, *32*, 77–83.

(7) Roy, M. N.; Nandi, D.; Hazra, D. K. Conductance Studies of alkali Metal Chlorides and Bromides in aqueous binary Mixtures of Tetrahydrofuran at 25°C. *J. Indian Chem. Soc.* **1993**, *70*, 121–124.

(8) Roy, M. N.; Sinha, B.; Dakua, V. K.; Sinha, A. Electrical conductances of some ammonium and tetraalkylammonium halides in aqueous binary mixtures of 1,4-dioxane at 298.15 K. *Pak. J. Scl. Ind. Res.* **2006**, *49*, 153–159.

(9) Das, B.; Saha, N. Electrical Conductances of Some Symmetrical Tetraalkylammonium Salts in Methanol, Acetonitrile, and Methanol (1) + Acetonitrile (2) Mixtures at 298.15 K. *J. Chem. Eng. Data* **2000**, *45*, 2–5.

(10) Roy, M. N.; Pradhan, P.; Das, R. K.; Guha, P. G.; Sinha, B. Ion-Pair and Triple-Ion Formation by Some Tetraalkylammonium Iodides in Binary Mixtures of 1,4-Dioxane + Tetrahydrofuran. *J. Chem. Eng. Data* **2008**, *53*, 1417–1420.

(11) Chanda, R.; Roy, M. N. Study of ion–solvent interactions of some tetraalkylammonium halides in THF + CCl_4 mixtures by conductance measurements. *Fluid Phase Equilib.* **2008**, *269*, 134–138.

(12) Chen, Z.; Hojo, M. Relationship between Triple Ion Formation Constants and the Salt Concentration of the Minimum in the Conductometric Curves in Low-Permittivity Solvents. *J. Phys. Chem. B* **1997**, *101*, 10896–10902.

(13) Parvatalu, D.; Srivastava, A. K. Ionic Conductivity in Binary Solvent Mixtures. 6. Behavior of Selected 1:1 Electrolytes in 80 mass Propylene Carbonate + *p*-Xylene at 25°C. *J. Chem. Eng. Data* **2003**, *48*, 608–611.

(14) Covington, A. K.; Dickinson, T. *Physical chemistry of organic solvent systems*; Plenum: New York, 1973.

(15) Krumgalz, B. S. Separation of limiting equivalent conductances into ionic contributions in non-aqueous solutions by indirect methods. *J. Chem. Soc., Faraday Trans. I* **1983**, *79*, 571–587.

(16) Hirsch, E.; Fuoss, R. M. Electrolyte-Solvent Interaction. VIII. Tetrabutylammonium Salts in Nitrobenzene-Carbon Tetrachloride Mixtures at 25°C. *J. Am. Chem. Soc.* **1960**, *82*, 1018–1022.

(17) Perrin, D. D.; Armarego, W. L. F. *Purification of laboratory chemicals*, 3rd ed.; Pergamon Press: Oxford, 1988.

(18) Fuoss, R. M.; Hirsch, E. Single Ion Conductances in Non-aqueous Solvents. *J. Am. Chem. Soc.* **1960**, *82*, 1013–1017.

(19) Sinha, B.; Dakua, V. K.; Roy, M. N. Apparent Molar Volumes and Viscosity *B*-Coefficients of Some Amino Acids in Aqueous Tetramethylammonium Iodide Solutions at 298.15 K. *J. Chem. Eng. Data* **2007**, *52*, 1768–1772.

(20) Marsh, K. N. *Recommended reference materials for the realization of physicochemical properties*; Blackwell Scientific Publications: Oxford, U. K, 1987.

(21) Dean, J. A. *Lange's handbook of chemistry*, 11th ed.; McGraw-Hill Book Company: New York, 1973.

(22) Chatterjee, A.; Das, B. Electrical Conductances of Tetrabutylammonium Bromide, Sodium Tetraphenylborate, and Sodium Bromide in Methanol (1) + Water (2) Mixtures at (298.15, 308.15, and 318.15) K. *J. Chem. Eng. Data* **2006**, *51*, 1352–1355.

(23) Roy, M. N.; Sinha, B.; Dakua, V. K. Excess Molar Volumes and Viscosity Deviations of Binary Liquid Mixtures of 1,3-Dioxolane and 1,4-Dioxane with Butyl Acetate, Butyric Acid, Butylamine, and 2-Butanone at 298.15 K. *J. Chem. Eng. Data* **2006**, *51*, 590–594.

(24) Lind, J. E., Jr.; Zwolenik, J. J.; Fuoss, R. M. Calibration of Conductance Cells at 25° with Aqueous Solutions of Potassium Chloride. *J. Am. Chem. Soc.* **1959**, *81*, 1557–1559.

(25) Pethybridge, A. D.; Taba, S. S. Precise conductimetric studies on aqueous solutions of 2:2 electrolytes. Part 2-Analysis of data for $MgSO_4$ in terms of new equations from Fuoss and from Lee and Wheaton. *J. Chem. Soc., Faraday Trans. I* **1980**, *76*, 368–376.

(26) Lee, W. H.; Wheaton, R. J. Conductance of symmetrical, unsymmetrical and mixed electrolytes. Part 2-Hydrodynamic terms and complete conductance equation. *J. Chem. Soc., Faraday Trans. II* **1978**, *74*, 1456–1482.

(27) Bester-Rogac, M.; Neueder, R.; Barthel, J. Conductivity of Sodium Chloride in Water + 1,4-Dioxane Mixtures at Temperatures from 5 to 35°C I. Dilute Solutions. *J. Solution Chem.* **1999**, *28*, 1071–1086.

(28) Krauss, C. A.; Bray, W. C. A general relation between the concentration and the conductance of ionized substances in various solvents. *J. Am. Chem. Soc.* **1913**, *35*, 1315–1434.

(29) Balaguruswami, E. *Numerical Methods*; Tata McGraw-Hill Publishing Company: New Delhi, 2007; p 259.

(30) Bockris, J. O.; Reddy, A. N. *Modern Electrochemistry*, 2nd ed.; Plenum Press: New York, 1998; pp 552.

(31) Chakraborty, J. M.; Das, B. Electrical Conductances and Viscosities of Tetrabutylammonium Thicyanate in Acetonitrile in the Temparature Range 25–45°C. *Z. Phys. Chem.* **2004**, *218*, 219–230.

(32) Robinson, R. A.; Stokes, R. H. *Electrolyte Solutions*; Butterworth: London, 1959; Chapter 6, pp 130.

(33) Fuoss, R. M.; Krauss, C. A. Properties of Electrolytic Solutions. IV. The Conductance Minimum and the Formation of Triple Ions Due to the Action of Coulomb Forces. *J. Am. Chem. Soc.* **1933**, *55*, 2387–2399.

(34) Fuoss, R. M.; Accascina, F. *Electrolytic Conductance*; Interscience: New York, 1959.

(35) Delsignore, M.; Farber, H. Petrucci. Ionic conductivity and microwave dielectric relaxation of $LiAsF_6$ and $LiClO_4$ in dimethyl carbonate. *J. Phys. Chem.* **1985**, *89*, 4968–4973.

(36) Fuoss, R. M.; Krauss, C. A. Properties of Electrolytic Solutions. III. The Dissociation Constant. *J. Am. Chem. Soc.* **1933**, *55*, 1019–1028.

(37) Abbott, A. P.; Schiffrin, D. J. Conductivity of tetra-alkylammonium salts in polyaromatic solvents. *J. Chem. Soc., Faraday Trans.* **1990**, *86*, 1453–1459.

(38) Nandi, D.; Roy, M. N.; Hazra, D. K. Electrical conductances for tetraalkylammonium bromides, $LiBF_4$ and $LiAsF_6$ in tetrahydrofuran at 25°C. *J. Indian Chem. Soc.* **1993**, *70*, 305–310.

(39) Sinha, A.; Roy, M. N. Conductivity studies of sodium iodide in pure tetrahydrofuran and aqueous binary mixtures of tetrahydrofuran and 1,4-dioxane at 298.15 K. *Phys. Chem. Liq.* **2007**, *45*, 67–77.

(40) Sadek, H.; Fuoss, R. M. Electrolyte-solvent Interaction. IV. Tetrabutylammonium Bromide in Methanol-Carbon Tetrachloride and Methanol-Heptane Mixtures. *J. Am. Chem. Soc.* **1954**, *76*, 5897–5901.

(41) Singh, S.; Rattan, V. K.; Kapoor, S.; Kumar, R.; Rampal, A. Thermophysical Properties of Binary Mixtures of Cyclohexane + Nitrobenzene, Cyclohexanone + Nitrobenzene, and Cyclohexane + Cyclohexanone at (298.15, 303.15, and 308.15) K. *J. Chem. Eng. Data* **2005**, *50*, 288–292.

Received for review November 20, 2008. Accepted April 17, 2009. The authors are grateful to the Departmental Special Assistance Scheme under the University Grants Commission, New Delhi (No. F 540/27/DRS/2007, SAP-1), for financial support.

JE800885H

Physics and Chemistry of Liquids
Vol. 49, No. 2, March–April 2011, 133–144

Taylor & Francis
Taylor & Francis Group

Volumetric, viscometric, interferrometric and refractometric properties of 2-methoxyethanol + diethylether + dichloromethane ternary system and its corresponding binaries at 298.15 K

Radhey Shyam Sah and Mahendra Nath Roy*

Department of Chemistry, North Bengal University, Darjeeling 734013, India

(*Received 22 March 2009; final version received 1 May 2009*)

Density, viscosity, speed of sound and refractive index of the binary mixture of 2-methoxyethanol (2-ME) + diethylether, 2-ME + dichloromethane (DCM) and diethyl ether + DCM and the ternary mixture of 2-ME + diethylether + DCM have been measured at 298.15 K and atmospheric pressure over the entire composition range. These results are used to calculate excess molar volume (V^E), viscosity deviation ($\Delta\eta$), deviation in isentropic compressibility (ΔK_S), excess Gibbs free energy of activation (ΔG^{*E}) and excess molar refraction (ΔR) for the above systems. The calculated quantities are further fitted to the Redlich–Kister equation to estimate the binary fitting parameters and root mean square deviations from the regression lines. These excess properties have been used to discuss the presence of significant interactions between the component molecules in the binary and ternary mixtures. The excess or deviation properties were found to be either negative or positive depending on the molecular interactions and the nature of liquid mixtures and have been discussed in terms of molecular interactions and structural changes.

Keywords: excess molar volume; viscosity deviation; ultrasonic speed; refractive index

1. Introduction

The thermodynamics of ternary liquid mixtures has not received much attention as has the thermodynamics of binary mixtures because it becomes more difficult and time consuming with the addition of each component beyond a binary mixture. It is also possible to investigate molecular packing, molecular motion, various types and extent of intermolecular interaction influenced by the size, shape and chemical nature of component molecules and microscopic structure of liquids.

The study of alkoxy alkanols is of interest not only because of their wide use as industrial solvents but also from the more theoretical point of investigating the effect of the simultaneous presence of etheric and hydroxyl groups on the interaction of such molecules. Since ethers are used as oxygenating agents in gasoline technology, the thermodynamics involving ethers and other liquid mixtures have been intensively studied [1–4]. Dichloromethane (DCM) is a very interesting solvent with appreciable

*Corresponding author. Email: mahendraroy2002@yahoo.co.in

ISSN 0031-9104 print/ISSN 1029-0451 online

DOI: 10.1080/00319100903012395
http://www.informaworld.com

industrial use in pharmaceutical industry, as a paint stripping agent, aerosols and as adhesives etc. and also as it is a solvent exhibiting high density and low viscosity.

Considering all of these aspects, we undertook investigations on the thermodynamic and transport properties of binary and ternary mixtures involving 2-methoxyethanol (2-ME), diethyl ether (DEE) and DCM.

In this paper are reported excess molar volume (V^E), viscosity deviations ($\Delta\eta$), deviations in isentropic compressibility (ΔK_S), excess molar refraction (ΔR) and Gibbs excess free energy of activation for viscous flow (ΔG^*) for three binary mixtures 2-ME + DEE, 2-ME + DCM, DEE + DCM and their corresponding ternary mixtures at 298.15 K over the entire range of composition. The excess or deviation properties of binary mixtures were fitted to Redlich–Kister polynomial equation to obtain their coefficients and have been interpreted in terms of molecular interactions and structural effects.

2. Experimental

2.1. *Chemicals*

2-ME (S.D. Fine Chemicals, AR, India) was purified as described in the literature [5]. DCM (Sigma-Aldrich, 99.9%, HPLC grade) was dried over calcium hydride and distilled. Diethylether (S.D. Fine Chemicals, AR grade, India) was used as purchased. The purity of each substance was evaluated by comparing experimental values of density, viscosity and refractive index with those reported in the literature when available, as presented in Table 1.

2.2. *Measurements*

Densities (ρ) were measured with an Ostwald–Sprengel type pycnometer having a bulb volume of about 25 cm^3 and an internal diameter of the capillary of about 0.1 cm. The measurements were done in a thermostat bath controlled to ±0.01 K. Viscosity (η) was measured by means of suspended Ubbelohde type viscometer, calibrated at 298.15 K with triply distilled water and purified methanol using density and viscosity values from the literature. The flow times were accurate to ±0.1 s, and the uncertainty in the viscosity measurements was $\pm 2 \times 10^4$ mPa s. The mixtures were prepared by mixing known volume of pure liquids in airtight-stopper bottles and each solution thus prepared was distributed into three recipients to perform all the

Table 1. Density (ρ), viscosity (η), sound speed (u) and refractive index (n_D) of pure liquids at 298.15 K.

	$\rho \times 10^{-3}$ (kg m^{-3})		η (mPa s)		u (ms^{-1})		n_D	
Pure components	This work	Lit.	This work	Lit.	This work	Lit.	This work	Lit.
2-Methoxyethanol	0.9608	0.9601[a]	1.5470	1.573[d]	1339.40	1341[a]	1.4005	1.3996[d]
Dichloromethane	1.3162	1.3163[b]	0.4652	0.406[e]	1071.30	1035[b]	1.4210	1.4228[b]
Diethylether	0.7091	0.7083[c]	0.2337	–	982.30	983[e]	1.3515	–

[a]See ref [22]; [b]See ref [23]; [c]See ref [24]; [d]See ref [25]; [e]See ref [26].

measurements in triplicate, with the aim of determining possible dispersion of the results obtained. Adequate precautions were taken to minimize evaporation loses during the actual measurements. The reproducibility in mole fractions was within ±0.0002. The mass measurements were done on a Mettler AG-285 electronic balance with a precision of ±0.01 mg. The precision of density measurements was $\pm 3 \times 10^{-4}\,g\,cm^{-3}$.

Ultrasonic speeds of sound (u) were determined by a multi-frequency ultrasonic interferometer (Mittal enterprise, New Delhi 9, M-81) working at 1 MHz, calibrated with triply distilled and purified water, methanol and benzene at 303.15 K. The precision of ultrasonic speed measurements was $\pm 0.2\,ms^{-1}$. The details of the methods and techniques have been described in earlier papers [6–9]. Refractive index was measured with the help of Abbe-Refractometer (USA). The accuracy of refractive index measurement was ±0.0002 units. The refractometer was calibrated twice using distilled and deionised water and calibration was checked after every few measurements.

3. Results and discussion

The experimental values of densities and excess molar volumes of binary mixtures 2-ME + DEE, 2-ME + DCM and DEE + DCM at 298.15 K are listed in Table 2.

Table 2. Densities, viscosities, excess molar volumes, viscosity deviations and excess Gibbs energy of activation for binary mixtures of 2-methoxyethanol, dichloromethane and diethylether at 298.15 K.

x_1	$\rho \times 10^{-3}$ (kg m^{-3})	η (mPa s)	$V^E \times 10^6$ (m^3 mol^{-1})	$\Delta\eta$ (mPa s)	$\Delta G^* \times 10^{-3}$ (Jmol^{-1})
(x_1) *2-Methoxyethanol* + (1 − x_1) *diethylether*					
0.0000	0.7091	0.2337	0.0000	0.0000	0.00
0.0976	0.7321	0.2661	−0.5400	−0.0958	−167.00
0.1958	0.7562	0.3070	−1.0400	−0.1838	−280.00
0.2944	0.7824	0.3630	−1.5900	−0.2574	−309.82
0.3936	0.8083	0.4399	−1.9000	−0.3107	−276.00
0.4933	0.8360	0.5713	−2.2000	−0.3103	−175.00
0.5936	0.8650	0.6782	−2.4500	−0.3351	−96.00
0.6944	0.8927	0.8546	−2.3700	−0.2910	31.00
0.7957	0.9201	1.0645	−2.1100	−0.2142	80.00
0.8976	0.9445	1.3300	−1.4400	−0.0825	70.60
1.0000	0.9608	1.5470	0.0000	0.0000	0.00
(x_1) *2-Methoxyethanol* + (1 − x_1) *dichloromethane*					
0.0000	1.3162	0.4652	0.0000	0.0000	0.00
0.1103	1.2779	0.5177	−0.4500	−0.0668	−75.08
0.2181	1.2419	0.5832	−0.8942	−0.1180	−113.11
0.3235	1.2056	0.6707	−1.2004	−0.1445	−88.49
0.4266	1.1702	0.7669	−1.4324	−0.1598	−53.00
0.5274	1.1359	0.8908	−1.5990	−0.1450	−3.13

(*Continued*)

Table 2. Continued.

x_1	$\rho \times 10^{-3}$ (kg m^{-3})	η (mPa s)	$V^E \times 10^6$ (m^3 mol^{-1})	$\Delta\eta$ (mPa s)	$\Delta G^* \times 10^{-3}$ (Jmol^{-1})
0.6260	1.1013	1.0294	−1.6165	−0.1130	48.00
0.7225	1.0671	1.1678	−1.5248	−0.0790	77.00
0.8170	1.0331	1.2950	−1.2940	−0.0540	80.00
0.9095	0.9977	1.4276	−0.8000	−0.0214	49.05
1.0000	0.9608	1.5470	0.0000	0.0000	0.00
(x_1) *Diethylether* + (1 − x_1) *dichloromethane*					
0.0000	1.3162	0.4652	0.0000	0.0000	0.00
0.1130	1.2193	0.4351	−0.3915	−0.0039	50.00
0.2227	1.1347	0.4106	−0.7090	−0.0031	91.00
0.3294	1.0592	0.3839	−0.8800	−0.0050	124.40
0.4331	0.9934	0.3585	−1.0670	−0.0064	134.44
0.5341	0.9343	0.3342	−1.1633	−0.0074	127.97
0.6322	0.8806	0.3106	−1.1290	−0.0083	113.09
0.7278	0.8313	0.2890	−0.9383	−0.0077	89.81
0.8209	0.7842	0.2687	−0.6520	−0.0065	63.00
0.9116	0.7471	0.2496	−0.5070	−0.0046	20.24
1.0000	0.7091	0.2337	0.0000	0.0000	0.00

3.1. *Excess molar volume*

The ρ values have been used to calculate the excess molar volumes (V^E) for binary ($n=2$) and ternary ($n=3$) mixture using the following equation [10]:

$$V^E = \sum_{i=1}^{n} x_i M_i (1/\rho - 1/\rho_i), \tag{1}$$

where ρ is the density of the mixture and M_i, x_i and ρ_i are the molecular weight, mole fraction and viscosity of the ith component in the mixture, respectively.

Figure 1 summarizes details of the experimental binary excess molar volume data over the entire range of composition.

V^E is the resultant of contributions from several opposing effects. These may be divided arbitrarily into three types, namely, chemical, physical and structural. Physical contributions, which are non-specific interactions between the real species present in the mixture, contribute a positive term to V^E. The negative values to V^E are contributed by the chemical or specific intermolecular interactions that result in a volume decrease. The structural contributions are mostly negative and arise from several effects, especially from interstitial accommodation and changes of free volume [11].

From Table 2 and Figure 1 it is evident that V^E values are negative for binary mixtures of 2-ME + DEE, 2-ME + DCM and DEE + DCM. These phenomena are the results of difference in energies of interaction between molecules being in solutions and packing effects.

The negative values of V^E indicate that the packing degree is enhanced in these mixed liquids with respect to the pure species and to their ideal mixtures, suggesting that specific intermolecular interactions such as hydrogen bonding and dipolar interactions of any kind between the component molecules are more effective

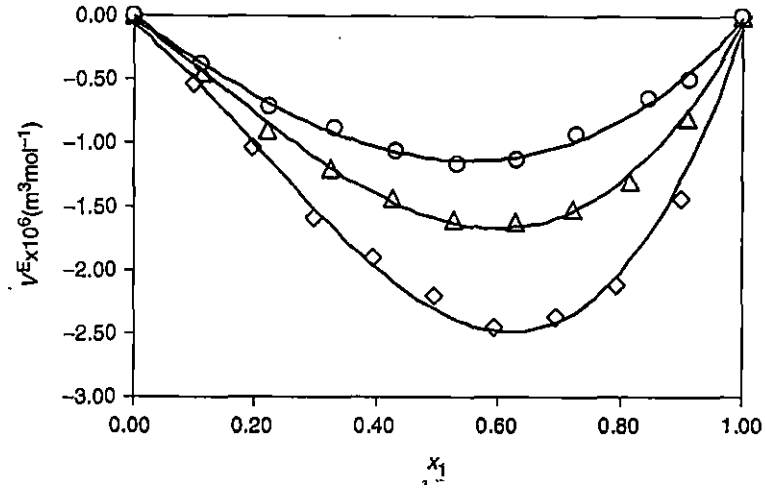

Figure 1. Plot of excess molar volumes $V^E \times 10^6$ (m3 mol^{-1}) against (x_1) for the three binary subsystems at 298.15K. ◇ (x_1)2-ME+(1−x_1) DEE; △ (x_1)2-ME+(1 − x_1) DCM; ○ (x_1) DEE+(1 − x_1) DCM.

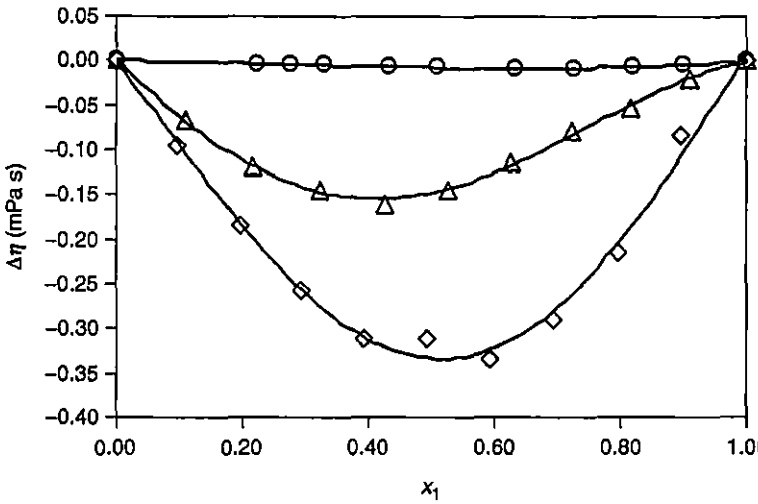

Figure 2. Plot of viscosity deviations, $\Delta\eta$ (mPa s) against mole fraction (x_1) for the three binary subsystems at 298.15K. ◇ (x_1)2-ME+(1 − x_1) DEE; △ (x_1)2-ME+(1 − x_1) DCM; ○(x_1)DEE+(1 − x_1) DCM.

and operative. Therefore, the attractive interactions (which are generally responsible for structure-making effects) seem to be the prevailing forces in the liquid structure [12] of these solutions with respect to repulsive phenomena due to sterical hindrances and unfavourable interactions between polar and apolar groups (structure-breaking effects). Another negative contribution to V^E comes from the geometrical fitting of unlike molecules into each other's structure due to differences in shape and size of the component molecules.

Table 3. Densities, viscosities, excess molar volumes, viscosity deviations and excess Gibbs energy of activation for ternary mixtures of 2–methoxyethanol, diethylether and dichloromethane at 298.15 K.

x_1	x_2	$\rho \times 10^{-3}$ kg m^{-3}	η (mPa s)	$V^E \times 10^6$ (m^3 mol^{-1})	$\Delta\eta$ (mPa s)	$\Delta G^* \times 10^{-3}$ (J mol^{-1})
(x_1) *2-Methoxyethanol* + (x_2) *diethylether* + (1 − x_1x_2) *dichloromethane*						
0.4933	0.5067	0.8338	0.5713	−1.9657	−0.3103	−35.00
0.4702	0.4829	0.8723	0.5616	−4.0630	−0.3005	−62.34
0.4442	0.4562	0.9084	0.5541	−5.4352	−0.2861	−97.18
0.4148	0.4260	0.9434	0.5476	−6.2341	−0.2677	−146.79
0.3810	0.3913	0.9832	0.5306	−6.9236	−0.2562	−193.65
0.3421	0.3513	1.0266	0.5158	−7.3003	−0.2382	−260.69
0.2966	0.3047	1.0741	0.5026	−7.2811	−0.2130	−298.59
0.2429	0.2494	1.1256	0.4926	−6.7043	−0.1776	−316.29
0.1782	0.1830	1.1842	0.4857	−5.5657	−0.1299	−285.48
0.0991	0.1018	1.2493	0.4799	−3.5475	−0.0689	−158.19
0.0000	0.0000	1.3241	0.4652	−0.4003	0.0000	−0.12

Table 3 lists experimental values of densities (ρ) and viscosities (η) of ternary mixture of 2-ME + DEE + DCM at 298.15 K. The excess molar volume depends on the balance between two opposing contribution (a) a positive term from the rupture of hydrogen bond and physical dipole–dipole interaction between components in solution and (b) a negative term from formation of hydrogen bonded complex and packing effect between solvents. The experimental data in the present investigation suggests that factor (b), which is responsible for negative excess volume, dominates over the entire range of composition. From Table 3 it is evident that the magnitude of negative deviation of V^E values of ternary mixture is more than that of their corresponding binary mixtures, suggesting that specific intermolecular interactions between the component molecules are more prominent and operative.

3.2. *Viscosity deviation*

The measured η values for binary systems at 298.15 K are listed in Table 2 and are grephically depicted in Figure 2. The viscosity deviations ($\Delta\eta$) [13] from linear dependence for binary ($n = 2$) and ternary ($n = 3$) mixtures can be calculated as:

$$\Delta\eta = \eta - \sum_{i=1}^{n} x_i\eta_i, \tag{2}$$

where η is the viscosity of the mixture and x_i and η_i are the mole fraction and viscosity of pure component i, respectively. The values of $\Delta\eta$ are negative over the entire range of mole fraction for 2-ME + DEE, 2-ME + DCM and DEE + DCM systems. It is observed in many systems that there is no simple correlation between the strength of the interactions and the observed properties. Rastogi *et al.* [14] therefore suggested that the observed excess property is a combination of an interaction and a non-interaction part. The non-interaction part in the form of size effect can be comparable to the interaction part and may be sufficient to reverse the trend set by the latter.

The values of viscosity deviations ($\Delta\eta$) for the ternary mixture are listed in Table 3. For the ternary mixture, the viscosity deviations are negative over the entire range of composition. These can be interpreted qualitatively by considering the effect of intermolecular interaction and shape of components.

3.3. *Deviation in isentropic compressibility*

Isentropic compressibility, K_S, and deviation in isentropic compressibility, ΔK_S, for binary ($n=2$) and ternary ($n=3$) mixtures were calculated using the following relations:

$$K_S = (u^2\rho)^{-1} \tag{3}$$

$$\Delta K_S = K_S - \sum_{i=1}^{n} x_i K_{Si}, \tag{4}$$

where u and K_S are the speed of sound and isentropic compressibility of the mixture and K_{Si}, the isentropic compressibility of the ith component in the mixture, respectively. It is evident from Table 4 and Figure 3 that for the binary mixtures, the ΔK_S values are negative over all composition range. These results can be explained in terms of molecular interactions [15,16] between unlike molecules. It appears from the sign and magnitude of ΔK_S that specific interaction exists between mixing components. These results are in excellent agreement with those of V^E discussed earlier.

The values of ΔK_S for the ternary mixture are negative over all composition range and are given in Table 5, which suggests that specific interactions exist between mixing components [17].

3.4. *Deviation in molar refraction*

The molar refraction, $[R]$, can be evaluated from Lorentz–Lorenz relation [18] and gives more information than n_D about the mixture phenomenon because it takes into account the electronic perturbation of molecular orbital during the liquid mixture process and $[R]$ is also directly related to the dispersion forces

$$[R] = (n_D^2 - 1/n_D^2 + 2)(M/\rho), \tag{5}$$

where $[R]$, n_D^2, and M are, correspondingly, the molar refraction, the refractive index and the molar mass of the mixture, respectively. Deviation from molar refraction for binary ($n=2$) and ternary ($n=3$) was calculated from the following relation:

$$\Delta R = [R] - \sum_{i=1}^{n} (x_i[R]_i), \tag{6}$$

where x_i and $[R]_i$ are mole fraction and molar refraction for the pure components, respectively. The values of ΔR for binary mixtures (Table 4 and Figure 4) and ternary mixture (Table 5) were found to be negative over the entire range of composition.

Table 4. Ultrasonic speed, isentropic compressibility, deviation in isentropic compressibility, refractive indices and excess molar refraction for binary mixtures of 2-methoxyethanol, dichloromethane and diethylether at 298.15 K.

x_1	u (ms^{-1})	$K_s \times 10^{12}$ (Pa^{-1})	$\Delta K_s \times 10^{12}$ (Pa^{-1})	n_D	$\Delta R \times 10^{-6}$ ($m^3 mol^{-1}$)
(x_1) *2-Methoxyethanol* + (1 − x_1) *diethylether*					
0.0000	982.30	1461.52	0.00	1.3515	0.0000
0.0976	1017.70	1318.92	−56.55	1.3562	−0.0570
0.1958	1053.40	1191.72	−97.26	1.3616	−0.0890
0.2944	1089.10	1077.55	−124.47	1.3674	−0.1280
0.3936	1124.80	977.80	−136.79	1.3727	−0.1640
0.4933	1160.50	888.22	−138.49	1.3786	−0.1840
0.5936	1196.20	807.91	−130.44	1.3846	−0.2070
0.6944	1231.90	738.17	−111.35	1.3897	−0.2140
0.7957	1267.60	676.38	−83.84	1.3948	−0.1920
0.8976	1303.30	623.32	−47.11	1.3990	−0.1284
1.0000	1339.40	580.16	0.00	1.4005	0.0000
(x_1) *2-Methoxyethanol* + (1 − x_1) *dichloromethane*					
0.0000	1071.30	662.00	0.00	1.4210	0.0000
0.1103	1104.91	640.97	−12.00	1.4190	−0.0883
0.2181	1137.46	622.34	−21.80	1.4157	−0.2260
0.3235	1166.54	609.52	−26.00	1.4130	−0.3134
0.4266	1196.12	597.28	−29.80	1.4105	−0.3808
0.5274	1222.20	589.35	−29.48	1.4080	−0.4373
0.6260	1247.93	583.06	−27.70	1.4062	−0.4360
0.7225	1270.90	580.17	−22.70	1.4050	−0.3881
0.8170	1292.52	579.39	−15.74	1.4033	−0.3310
0.9095	1315.96	578.77	−8.79	1.4020	−0.1960
1.0000	1339.40	580.16	0.00	1.4005	0.0000
(x_1) *Diethylether* + (1 − x_1) *dichloromethane*					
0.0000	1.4210	662.00	0.00	1.4210	0.0000
0.1130	1.4106	575.31	−177.00	1.4106	−0.0320
0.2227	1.4015	575.07	−265.00	1.4015	−0.0586
0.3294	1.3930	621.73	−303.63	1.3930	−0.0758
0.4331	1.3859	686.30	−322.00	1.3859	−0.0827
0.5341	1.3794	775.98	−313.00	1.3794	−0.0840
0.6322	1.3732	897.03	−270.46	1.3732	−0.0782
0.7278	1.3671	1013.53	−230.39	1.3671	−0.0647
0.8209	1.3603	1148.43	−169.92	1.3603	−0.0452
0.9116	1018.01	1291.50	−99.36	1.3568	−0.0272
1.0000	982.30	1461.52	0.00	1.3515	0.0000

3.5. *Excess Gibb's free energy of activation*

On the basis of the theories of absolute reaction rates [19], the excess Gibbs energy of activation for viscous flow was calculated from equation [20] for binary ($n = 2$) and ternary ($n = 3$) systems.

$$\Delta G^* = RT\left[\ln \eta V - \sum_{i=1}^{n} (x_i \ln \eta_i V_i)\right], \tag{7}$$

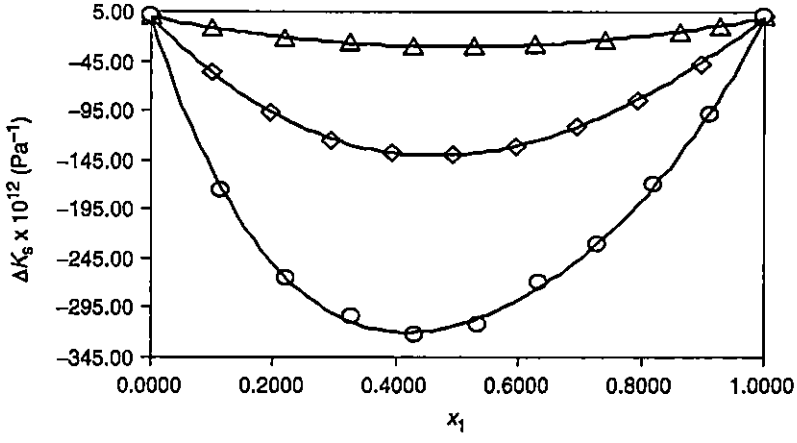

Figure 3. Plot of deviation in isentropic compressibility $\Delta K_s \times 10^{12}$ (Pa^{-1}) against mole fraction (x_1) for the three binary subsystems at 298.15K. ◇ (x_1) 2-ME + (1 − x_1) DEE; Δ (x_1)2-ME + (1 − x_1) D.C.M; ○ (x_1) DEE + (1 − x_1) DCM.

Table 5. Ultrasonic speed, isentropic compressibility, deviation in isentropic compressibility, refractive indices and excess molar refraction for ternary mixtures of 2-methoxyethanol, diethylether and dichloromethane at 298.15 K.

x_1	x_2	u (ms^{-1})	$K_s \times 10^{12}$ (Pa^{-1})	$\Delta K_s \times 10^{12}$ (Pa^{-1})	n_D	$\Delta R \times 10^{-6}$ (m^3 mol^{-1})
(x_1) *2-Methoxyethanol* + (x_2) *diethylether* + (1 − x_1x_2) *dichloromethane*						
0.4933	0.5067	1260.90	890.5	−136.17	1.4668	0.0000
0.4702	0.4829	1293.77	834.9	−150.00	1.4475	−0.4136
0.4442	0.4562	1296.88	806.5	−152.00	1.4294	−0.7550
0.4148	0.4260	1249.41	826.0	−147.00	1.4139	−0.9582
0.3810	0.3913	1208.62	830.3	−134.00	1.3986	−1.1149
0.3421	0.3513	1171.32	827.0	−117.00	1.3835	−1.2055
0.2966	0.3047	1148.04	806.4	−100.00	1.3668	−1.2957
0.2429	0.2494	1125.02	785.9	−84.00	1.3525	−1.1946
0.1782	0.1830	1109.57	746.9	−61.00	1.3377	−0.9935
0.0991	0.1018	1090.98	706.5	−34.00	1.3244	−0.5604
0.0000	0.0000	1071.30	658.0	0.00	1.3090	0.0000

where R, T, V_i and V are the universal gas constant, experimental temperature in absolute scale, and the molar volumes of the pure component and the mixtures, respectively. The calculated values of ΔG^* for binary mixtures are reported in Table 2 and represented graphically in Figure 5 and those for ternary mixtures are reported in Table 3.

The excess properties (V^E, $\Delta\eta$, ΔK_S, ΔR, ΔG^*) for the binary mixtures were fitted to the Redlich–Kister polynomial equation [21]:

$$Y^E = x_1x_2 \sum_{i=0}^{K} A_i(x_1 - x_2)^i, \tag{8}$$

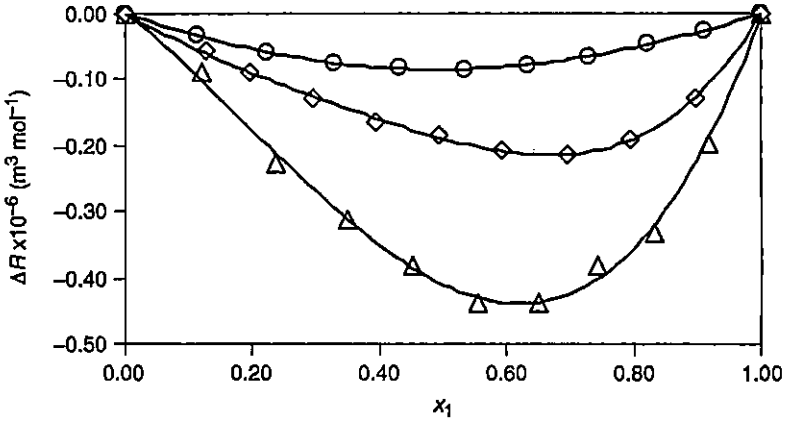

Figure 4. Plot of molar refraction $\Delta R \times 10^{-6}$ ($m^3 mol^{-1}$) against mole fraction (x_1) for the three binary subsystems at 298.15K. ◇ (x_1) 2-ME+(1 − x_1) DEE; Δ (x_1)2-ME+(1 − x_1) DCM; o (x_1) DEE+(1 − x_1) DCM.

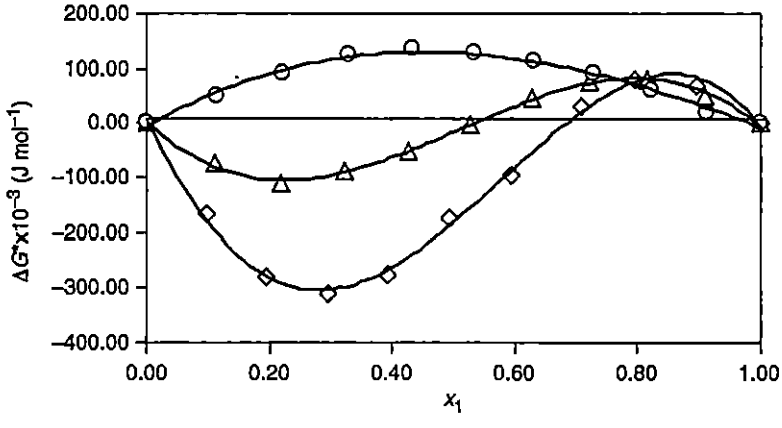

Figure 5. Plot of deviation of excess Gibbs energy of activation $\Delta G^* \times 10^{-3}$($Jmol^{-1}$) against mole fraction (x_1) for the three binary subsystems at 298.15K. ◇ (x_1) 2-ME+(1 − x_1) DEE; Δ (x_1)2-ME+(1 − x_1) DCM; o (x_1) DEE+(1 − x_1) DCM.

where Y^E refers to an excess property, x_1 is the mole fraction of IAA and x_2 is that of the other component. The coefficients (A_i) were obtained by fitting Equation (8) to experimental results using a least-squares regression method. In each case, the optimal number of coefficients was ascertained from an approximation of the variation in the standard deviation. The estimated values along with the standard deviations are summarized for all mixtures in Table 6. The standard deviation was calculated using the equation:

$$\sigma = \left[(Y^{E}_{exp} - Y^{E}_{calcd})^2/(n-m)\right]^{1/2}, \quad (9)$$

where n is the number of data points and m is the number of coefficients.

Table 6. Redlich-Kister coefficients and standard deviations (σ) for the binary mixtures at 298.15 K.

Excess property	A_0	A_1	A_2	A_3	A_4	A_5	σ
(x_1) *2-Methoxyethanol* + (1 − x_1) *diethylether*							
$V^E \times 10^6$ ($m^3 mol^{-1}$)	−8.9561	−4.5284	−2.8712	−2.1783			0.0361
$\Delta\eta$ (mPa s)	−1.4062	−0.2284	0.5879	−0.1309	−1.4100	0.9561	0.0039
$\Delta G^* \times 10^{-3}$ ($Jmol^{-1}$)	−726.6322	2050.1837	260.3553	−529.6563			8.1111
$\Delta K_s \times 10^{12}$ (Pa^{-1})	−554.1238	90.0715	−35.7869	−13.8799			0.3714
$\Delta R \times 10^{-6}$ ($m^3 mol^{-1}$)	−0.7534	−0.4545	−0.4509	−0.1894	0.2568		0.0019
(x_1) *2-Methoxyethanol* + (1 − x_1) *dichloromethane*							
$V^E \times 10^6$ ($m^3 mol^{-1}$)	−6.2185	−2.3247	−1.4405	−1.2546			0.0124
$\Delta\eta$ (mPa s)	−0.5735	0.4051	0.1382	−0.2725			0.0025
$\Delta G^* \times 10^{-3}$ ($J mol^{-1}$)	−58.5601	1071.7461	−56.7858	−292.8441			3.6397
$\Delta K_s \times 10^{12}$ (Pa^{-1})	−118.1758	3.3582	−20.3350				0.4595
$\Delta R \times 10^{-6}$ ($m^3 mol^{-1}$)	−1.6550	−0.9392					0.0108
(x_1) *Diethylether* + (1 − x_1) *dichloromethane*							
$V^E \times 10^6$ ($m^3 mol^{-1}$)	−4.51045	−1.01182					0.0364
$\Delta\eta$ (mPa s)	−0.03317	−0.00694	−0.00822				0.0002
$\Delta G^* \times 10^{-3}$ ($Jmol^{-1}$)	417.5670	88.7335	−12.3521	−92.0735	82.5724		1.3980
$\Delta K_s \times 10^{12}$ (Pa^{-1})	−1249.4508	340.0011	−336.8316				4.6221
$\Delta R \times 10^{-6}$ ($m^3 mol^{-1}$)	−0.33878	0.01127	0.02961				0.0012

Acknowledgements

The authors are grateful to the Departmental Special Assistance Scheme under the University Grants Commission, New Delhi (No. 540/6/DRS/2007, SAP-2) for financial support.

References

[1] J. Canosa, A. Rodriguez, and J. Tojo, Fluid Phase Equilibr. **156**, 57 (1999).
[2] A. Rodriguez, J. Canosa, and J. Tojo, J. Chem. Thermodyn. **31**, 1009 (1999).
[3] T.M. Letcher and P.U. Govender, Fluid Phase Equilibr. **140**, 207 (1997).
[4] A. Arce, E. Rodil, and A. Soto, J. Chem. Eng. Data **42**, 721 (1997).
[5] N.V. Sastry and S.R. Patel, Int. J. Thermophys. **21**, 1153 (2000).
[6] M.N. Roy, A. Choudhury, and A. Sinha, J. Teach. Res. Chem. **11**, 12 (2004).
[7] D.K. Hazra, M.N. Roy, and B. Das, Indian J. Chem. Technol. 1, 93 (1994).
[8] M.N. Roy, A. Jha, and R. Dey, J. Chem. Eng. Data **46**, 1327 (2001).
[9] M.N. Roy, A. Sinha, and B. Sinha, J. Sol. Chem. **34**, 1319 (2005).
[10] P.S. Nikam, L.N. Shirsat, and M. Hasan, J. Indian Chem. Soc. **77**, 244 (2000).

[11] S.J. Kharat and P.S. Nikam, J. Mol. Liq. **131–132**, 81 (2007).
[12] H. Erying and M.S. John, *Significant Liquid Structur* (Wiley, New York, 1969).
[13] S. Glasstone, K.J. Laidner, and H. Eyring, *The Theory of Rate Processes* (McGraw-Hill, New York, 1941).
[14] R.P. Rastogi, J. Nath, and J. Misra, J. Phys. Chem. **71**, 1277 (1967).
[15] M.J.W. Povey, S.A. Hindle, J.D. Kennedy, Z. Stec, and R.G. Taylor, Phys. Chem. Chem. Phys. **5**, 73 (2003).
[16] C. Lafuente, B. Giner, A. Villares, I. Gascon, and P. Cea, Int. J. Thermophys. **25**, 1746 (2004).
[17] T.M. Aminbhavi, H.T.S. Phyade, M.I. Aralaguppi, and R.S. Khinnavar, J. Chem. Eng. Data **38**, 540 (1993).
[18] V.Minkin, O. Osipov and Y.Zhdanov, editors, Dipole Moments in Organic Chemistry (Plenum Press, New York, London, 1970).
[19] A.W. Quin, D.F. Hoffmann, and P. Munk, J. Chem. Eng. Data **37**, 55 (1992).
[20] S. Glasstone, K.J. Laidler, and H. Eyring, *The Theory of Rate Process: The Kinetics of Chemical Reactions, Viscosity, Diffusion and Electrochemical Phenomena* (McGraw-Hill, New York, 1941).
[21] D.S. Gill, T.S. Kaur, H. Kaur, I.M. Joshi, and J. Singh, J. Chem. Soc. Faraday Trans. **89**, 1737 (1993).
[22] I. Mozo, I.G. Fuente, J.A González, J.C. Cobos, and N. Riesco, J. Chem. Eng. Data **53**, 1404 (2008).
[23] T.M. Aminabhavi and K. Banerjee, J. Chem. Eng. Data **43**, 1096 (1998).
[24] G. Savaroglu and E. Aral, Pramana J. Phys. **66**, 435 (2006).
[25] S. Aznarez, M. Katz, and E.L. Arancibia, J. Sol. Chem. **31**, 639 (2002).
[26] A. Pal and G. Dass, J. Mol. Liq. **89**, 327 (2000).

Journal of Molecular Liquids 144 (2009) 149–154

Contents lists available at ScienceDirect

Journal of Molecular Liquids

journal homepage: www.elsevier.com/locate/molliq

Ion–solvent and ion–ion interactions of sodium molybdate and sodium tungstate in mixtures of ethane-1,2-diol and water at 298.15, 308.15 and 318.15 K

Prasanna Pradhan, Radhey Shyam Sah, Mahendra Nath Roy *

Department of Chemistry, North Bengal University, Darjeeling-734013, India

ARTICLE INFO

Article history:
Received 3 June 2008
Received in revised form 31 October 2008
Accepted 3 November 2008
Available online 11 November 2008

Keywords:
Ethane-1,2-diol
Sodium tungstate
Sodium molybdate
Apparent molar volume

ABSTRACT

Apparent molar volume (V_ϕ) and viscosity B-coefficients were estimated for sodium molybdate and sodium tungstate in aqueous binary mixture of ethane-1,2-diol from measured solution density (ρ) and viscosity (η) at 298.15, 308.15 and 318.15 K at various electrolyte concentrations. The experimental density data were evaluated by Masson equation and the derived data were interpreted in terms of ion–solvent and ion–ion interactions. The viscosity data has been analyzed using Jones–Dole equation and the derived parameters, B and A, have also been interpreted in terms of ion–solvent and ion–ion interactions respectively. The structure-making or breaking capacity of the electrolyte under investigation has been discussed in terms of sign of $(\delta^2 V\ ^0_\phi/\delta T^2)_P$. The activation parameters of viscous flow were also determined and were discussed by the application of transition state theory.

1. Introduction

Studies on densities (ρ) and viscosities (η) of electrolyte solutions are of great importance in characterizing the properties and structural aspects of solutions. The addition of an electrolyte to an aqueous organic solution alters the pattern of ion solvation and causes phenomenal changes in the behavior of the dissolved electrolyte. Hence studies on the limiting apparent molar volume and viscosity-B coefficients of electrolyte provide us valuable information regarding ion–ion, ion–solvent and solvent–solvent interactions [1–3]. It has been found by a number of workers [4–6] that the addition of an electrolyte could either make or break the structure of a liquid. As the viscosity of a liquid depends on the intermolecular forces, the structural aspects of the liquid can be inferred from the viscosity of solutions at various electrolyte concentrations and temperature.

In this paper we have attempted to report the limiting apparent molar volume (V^0_ϕ), experimental slopes (S^*_v) and viscosity B-coefficients for sodium molybdate and sodium tungstate in aqueous binary mixture of ethane-1,2-diol at 298.15, 308.15 and 318.15 K. The mixture of ethane-1,2-diol with water was chosen because of its diverse application in pharmaceutical and cosmetic industries [7,8]. However, the experiment was not performed in pure ethane-1,2-diol due to the insolubility of the electrolytes. Since both molybdate and tungstate ions have similar structure [9] and sodium ion being a common cation for both the electrolyte under investigation, the present work enables us to have a qualitative comparison of the role of anion in aqueous binary mixture of ethane-1,2-diol in terms of various derived parameters obtained from viscosity (η) and density (ρ) measurement.

2. Experimental section

2.1. Materials

Ethane-1,2-diol (E. Merck, India) was purified by standard methods [10]. The purity of the solvent was checked by measuring the viscosity (η) and density (ρ) at 298.15 K which was in good agreement with the literature values. Doubly distilled, degassed and deionised water with a specific conductance of $1\times10^{-6}\ \Omega^{-1}\ cm^{-1}$ was used. Sodium tungstate and sodium molybdate (E. Merck, India) were purified by re-crystallizing twice from conductivity water and then dried in a vacuum dessicator over P_2O_5 for 24 h before use. The purity of the solvents was ascertained by GLC and also by comparing experimental values of viscosity (η) and density (ρ) whenever available with those reported in the literature and is listed in Table 1.

2.2. Measurements

Densities (ρ) were measured with an Ostwald–Sprengel type pycnometer having a bulb volume of about 25 cm^3 and an internal diameter of about 0.1 cm. The measurements were done in a thermostat bath controlled to ±0.01 K. Viscosity (η) was measured by means of suspended Ubbelohde type viscometer, calibrated at 298.15 K with triply

* Corresponding author. Fax: +91 353 2581546.
E-mail addresses: praspradhan_03@yahoo.com (P. Pradhan), sahradhey@yahoo.com (R.S. Sah), mahendraroy2002@yahoo.co.in (M.N. Roy).

0167-7322/$ – see front matter © 2008 Published by Elsevier B.V.
doi:10.1016/j.molliq.2008.11.001

Table 1
Density (ρ, kg m^{-3}) and viscosity (η, mPa s) of aqueous binary mixtures of ethane-1,2-diol in 0.0312, 0.0677, 0.1106 mole fractions (x_1) of ethane-1,2-diol at different temperatures

Temperature (K)	$\rho\times10^{-3}$ kg m^{-3}		η mPa s	
	This work	Lit	This work	Lit
x_1=0.0312				
298.15	1.0110	1.0116 [32]	1.1284	–
308.15	1.0071	1.0080 [32]	0.8922	–
318.15	1.0036	1.0038 [32]	0.7564	–
x_1=0.0677				
298.15	1.0238	1.0279 [32]	1.4244	–
308.15	1.0207	1.0239 [32]	1.1371	–
318.15	1.0167	1.0195 [32]	0.9440	–
x_1=0.1106				
298.15	1.0372	1.0432 [32]	1.8286	–
308.15	1.0352	1.0390 [32]	1.4302	–
318.15	1.0290	1.0343 [32]	1.1472	–

distilled water and purified methanol using density and viscosity values from literature. The flow times were accurate to ±0.1 s, and the uncertainty in the viscosity measurements was $\pm2\times10^{-4}$ mPa s. The mixtures were prepared by mixing known volume of pure liquids in airtight-stopper bottles and each solution thus prepared was distributed into three recipients to perform all the measurements in triplicate, with the aim of determining possible dispersion of the results obtained. Adequate precautions were taken to minimize evaporation loses during the actual measurements. The reproducibility in mole fractions was within ±0.0002. The mass measurements were done on a Mettler AG-285 electronic balance with a precision of ±0.01 mg. The precision of density measurements was $\pm3\times10^{-4}$ g cm^{-3}. Viscosity of the solution, η, is given by the following equation:

$$\eta = (Kt - L/t)\rho \tag{1}$$

where K and L are the viscometer constants and t and ρ are the efflux time of flow in seconds and the density of the experimental liquid, respectively. The uncertainty in viscosity measurements is within ±0.003 mPa s.

Details of the methods and techniques of density and viscosity measurements have been described elsewhere [11–14]. The electrolyte solutions studied here were prepared by mass and the conversion of molality into molarity was accomplished [3] using experimental density values. The experimental values of concentrations (c), densities (ρ), viscosities (η), and derived parameters at various temperatures are reported in Table 2.

3. Results and discussion

The apparent molar volumes (V_ϕ) were determined from the solution densities using the following Eq. [3]:

$$V_\phi = M/\rho_0 - 1000(\rho-\rho_0)/c\rho_0 \tag{2}$$

where M is the molar mass of the solute, c is the molarity of the solution; ρ_0 and ρ are the densities of the solvent and the solution respectively. The limiting apparent molar volumes V_ϕ^0 was calculated using a least-squares treatment to the plots of V_ϕ versus $\sqrt{c}$ using the following Masson equation [15]:

$$V_\phi = V_\phi^0 + S_v^*\sqrt{c} \tag{3}$$

where V_ϕ^0 is the apparent molar volume at infinite dilution and S_v^* is the experimental slope. The plots of V_ϕ against square root of molar concentration ($\sqrt{c}$) were found to be linear as depicted graphically in Figs. 1–6 with negative slopes. Values of V_ϕ^0 and S_v^* are reported in Table 3.

As the systems under study are characterized by hydrogen bonding, the ion–solvent and ion–ion interactions can be interpreted in terms of structural changes, which arise due to hydrogen bonding between various components of the solvent and solution systems. V_ϕ^0 can be used to interpret ion–solvent interactions. A perusal of Table 3 reveals that the V_ϕ^0 values are positive and increases with rise in temperature and decreases with increase in the amount of ethane-1,2-diol in the solvent mixture. This indicates the presence of strong ion–solvent interactions and these interactions are strengthened with rise in temperature and weakened with an increase in the amount of ethane-1,2-diol in the solvent mixture under study, suggesting larger electrostriction at higher temperature and in lower amount of ethane-1,2-diol in the mixture. Similar results were obtained for some 1:1 electrolytes in aqueous dimethylformamide [16] and aqueous tetrahydrofuran [17].

It is evident from Table 3 that the S_v^* values are negative for all temperatures for aqueous mixtures of ethane-1,2-diol. Furthermore S_v^* values decrease with the increase of experimental temperature which may be attributed to more violent thermal agitation at higher temperatures, resulting in diminishing the force of ion–ion interactions (ionic-dissociation) [18]. The S_v^* values increase with an increase in the amount of ethane-1,2-diol in the aqueous mixture which results in a decrease in solvation of ions, i.e., more and more solute is accommodated in the void space left in the packing of large associated solvent molecules with the addition of ethane-1,2-diol to the mixture. A quantitative comparison of the magnitude of values shows that V_ϕ^0 values are much greater in magnitude than those of S_v^* for all the solutions. This suggests that ion–solvent interactions dominate over ion–ion interactions in all the solutions and at all experimental temperatures.

The variation of V_ϕ^0 with temperature of sodium molybdate and sodium tungstate in solvent mixture follows the polynomial,

$$V_\phi^0 = a_0 + a_1T + a_2T^2 \tag{4}$$

over the temperature range under study where T is the temperature in K.

Values of coefficients of the above equation for sodium molybdate and sodium tungstate for aqueous ethane-1,2-diol mixtures are reported in Table 4.

The apparent molar expansibilities (ϕ_E^0) can be obtained by the following equation:

$$\phi_E^0 = \left(\delta V_\phi^0/\delta T\right)_P = a_1 + 2a_2T \tag{5}$$

The values of ϕ_E^0 for different solutions of the studied electrolytes at 298.15, 308.15 and 318.15 K are reported in Table 5. From the table it is evident that the values of ϕ_E^0 for sodium molybdate increases with a rise in temperature and decreases with the increase in the amount of ethane-1,2-diol in the mixture which can be ascribed to the absence of caging or packing effects [19]. However for sodium tungstate the ϕ_E^0 values were found to be rather complicated to explain.

During the past few years it has been emphasized by a number of workers that S_v^* is not the sole criterion for determining the structure-making or breaking tendency of any solute. Hepler [20] developed a technique of examining the sign of $(\delta\phi_E^0/\delta T)_P$ for the solute in terms of long-range structure-making and breaking capacity of the electrolytes in the mixed solvent systems. The general thermodynamic expression used is as follows

$$\left(\delta\phi_E^0/\delta T\right)_P = 2a_2 \tag{6}$$

If the sign of $(\delta\phi_E^0/\delta T)_P$ is positive or small negative [21] the electrolyte is a structure maker and when the sign of $(\delta\phi_E^0/\delta T)_P$ is negative, it is a structure breaker. As is evident from Table 5, the electrolyte under investigation generally acts as a structure breaker.

Table 2
Concentration (c), density (ρ), viscosity (η), apparent molar volume (V_Φ), and $\alpha=(\eta/\eta_0-1)/c^{1/2}$ of sodium molybdate and sodium tungstate in different aqueous binary mixtures of ethane-1,2-diol in 0.0312, 0.0677, 0.1106 mole fractions (x_1) of ethane-1,2-diol at different temperatures

c mol dm^{-3}	$\rho\times10^{-3}$ kg m^{-3}	η mPa s	$V_\Phi\times10^{6}$ m^3 mol^{-1}	α	c mol dm^{-3}	$\rho\times10^{-3}$ kg m^{-3}	η mPa s	$V_\Phi\times10^{6}$ m^3 mol^{-1}	α
Sodium molybdate $x_1=0.0312$					Sodium tungstate $x_1=0.0312$				
298.15 K					298.15 K				
0.0250	1.0143	1.1429	109.228	0.0850	0.0250	1.0163	1.1471	116.278	0.1050
0.0350	1.0159	1.1493	101.895	0.0900	0.0350	1.0186	1.1582	110.767	0.1410
0.0450	1.0174	1.1549	97.665	0.1050	0.0450	1.0210	1.1669	106.845	0.1610
0.0550	1.0191	1.1619	93.236	0.1267	0.0550	1.0233	1.1750	104.213	0.1760
0.0750	1.0223	1.1748	90.621	0.1502	0.0750	1.0281	1.1902	100.921	0.2000
0.0850	1.0239	1.1820	89.663	0.1630	0.0850	1.0305	1.1998	99.7900	0.2170
308.15 K					308.15 K				
0.0249	1.0099	0.9044	127.605	0.0870	0.0249	1.0120	0.9094	133.908	0.1220
0.0348	1.0115	0.9102	114.742	0.1080	0.0349	1.0143	0.9173	121.999	0.1507
0.0448	1.0131	0.9183	107.597	0.1380	0.0448	1.0167	0.9245	115.189	0.1711
0.0548	1.0147	0.9256	103.106	0.1598	0.0548	1.0191	0.9325	110.818	0.1929
0.0747	1.0178	0.9383	98.545	0.1889	0.0747	1.0238	0.9472	105.575	0.2255
0.0846	1.0195	0.9442	94.498	0.2003	0.0846	1.0262	0.9543	103.732	0.2391
318.15 K					318.15 K				
0.0248	1.0060	0.7672	144.585	0.0910	0.0248	1.0081	0.7724	149.569	0.1346
0.0347	1.0076	0.7743	125.053	0.1273	0.0347	1.0105	0.7799	130.293	0.1667
0.0447	1.0093	0.7801	114.206	0.1485	0.0446	1.0130	0.7868	119.589	0.1903
0.0547	1.0110	0.7867	105.545	0.1712	0.0546	1.0154	0.7937	112.722	0.2110
0.0747	1.0144	0.7991	96.4701	0.2065	0.0744	1.0204	0.8076	104.345	0.2484
0.0847	1.0161	0.8047	92.9767	0.2195	0.0844	1.0228	0.8146	101.635	0.2649
Sodium molybdate $x_1=0.0677$					Sodium tungstate $x_1=0.0677$				
298.15 K					298.15 K				
0.0250	1.0274	1.4451	94.8690	0.0100	0.0250	1.0306	1.4460	101.479	0.0960
0.0350	1.0290	1.4527	91.4636	0.1130	0.0350	1.0331	1.4553	97.1661	0.1158
0.0450	1.0307	1.4633	86.8985	0.1350	0.0450	1.0355	1.4646	96.866	0.1330
0.0550	1.0324	1.4720	82.8316	0.1480	0.0550	1.0380	1.4738	94.961	0.1479
0.0750	1.0357	1.4906	81.3094	0.1746	0.0750	1.0428	1.4934	95.189	0.1770
0.0850	1.0374	1.4997	79.8219	0.1860	0.0850	1.0453	1.5016	94.153	0.1860
308.15 K					308.15 K				
0.0249	1.0236	1.1540	115.626	0.0960	0.0249	1.0267	1.1563	131.329	0.1070
0.0349	1.0252	1.1630	106.010	0.1236	0.0349	1.0292	1.1653	118.732	0.1330
0.0448	1.0268	1.1710	100.402	0.1419	0.0448	1.0317	1.1732	111.443	0.1500
0.0548	1.0283	1.1788	96.9554	0.1578	0.0548	1.0341	1.1797	107.973	0.1600
0.0747	1.0315	1.1940	93.3839	0.1841	0.0747	1.0390	1.1992	103.259	0.1998
0.0846	1.0330	1.2033	91.9710	0.2010	0.0847	1.0415	1.2065	101.803	0.2097
318.15 K					318.15 K				
0.0248	1.0193	0.9583	136.063	0.0950	0.0248	1.0224	0.9608	139.942	0.1130
0.0347	1.0208	0.9667	120.549	0.1280	0.0347	1.0248	0.9694	127.007	0.1444
0.0446	1.0223	0.9739	113.695	0.1487	0.0446	1.0272	0.9763	119.833	0.1619
0.0546	1.0240	0.9808	105.996	0.1659	0.0546	1.0297	0.9840	113.528	0.1816
0.0744	1.0271	0.9947	99.814	0.1962	0.0744	1.0346	0.9988	107.263	0.2127
0.0843	1.0287	1.0019	97.666	0.2104	0.0843	1.0371	1.0068	104.668	0.2290
Sodium molybdate $x_1=0.1106$					Sodium tungstate $x_1=0.1106$				
298.15 K					298.15 K				
0.0250	1.0410	1.8517	85.2862	0.0940	0.0250	1.0446	1.8553	85.2862	0.0924
0.0350	1.0428	1.8624	81.6000	0.1108	0.0350	1.0471	1.8648	81.6000	0.1057
0.0450	1.0443	1.8731	80.7124	0.1253	0.0450	1.0498	1.8760	80.7124	0.1221
0.0550	1.0462	1.8845	76.2873	0.1401	0.0550	1.0520	1.8874	76.2873	0.1370
0.0750	1.0495	1.9066	74.7013	0.1640	0.0750	1.0572	1.9109	74.7013	0.1643
0.0850	1.0513	1.9190	73.6711	0.1775	0.0850	1.0603	1.9214	73.6711	0.1740
308.15 K					308.15 K				
0.0249	1.0385	1.4522	105.289	0.1070	0.0249	1.0240	1.4521	105.289	0.0976
0.0349	1.0401	1.4597	99.2167	0.1184	0.0349	1.0447	1.4615	99.2167	0.1170
0.0449	1.0416	1.4695	95.8562	0.1368	0.0449	1.0471	1.4687	95.8562	0.1270
0.0548	1.0431	1.4793	95.3671	0.1532	0.0549	1.0496	1.4798	95.3671	0.1480
0.0748	1.0460	1.5002	93.5430	0.1847	0.0748	1.0544	1.4979	93.5430	0.1731
0.0848	1.0483	1.5095	84.7810	0.1960	0.0847	1.0570	1.5089	84.7810	0.1892
318.15 K					318.15 K				
0.0248	1.0321	1.1679	114.771	0.1148	0.0248	1.0356	1.1660	114.771	0.1040
0.0347	1.0336	1.1756	105.395	0.1330	0.0347	1.0380	1.1746	105.395	0.1282
0.0446	1.0353	1.1840	98.2377	0.1520	0.0446	1.0405	1.1831	98.238	0.1483
0.0545	1.0369	1.1924	93.4467	0.1686	0.0545	1.0430	1.1914	93.447	0.1651
0.0743	1.0401	1.2106	90.0550	0.2029	0.0743	1.0479	1.2075	90.055	0.1928
0.0842	1.0418	1.2193	87.2167	0.2166	0.0842	1.0505	1.2157	87.217	0.2059

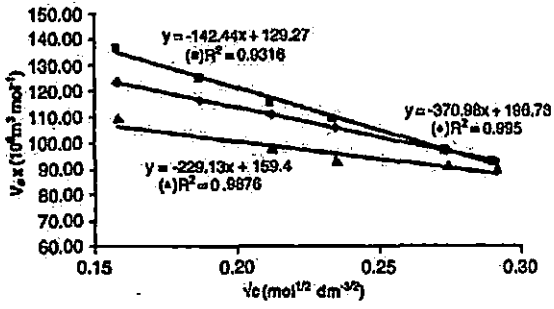

Fig. 1. The apparent molar volume of sodium molybdate in the mixture of aqueous ethane-1,2-diol (x_1 = 0.0312) as a function of square root of concentration at 298.15 (▲), 308.15 (♦) and 318.15 K (■). The lines represent the linear fits.

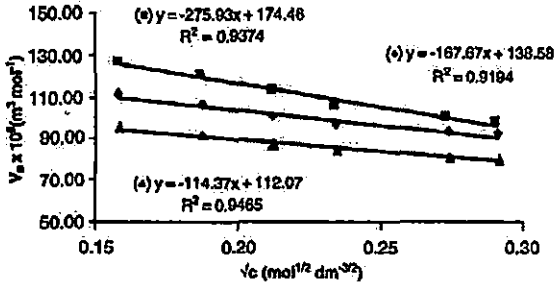

Fig. 2. The apparent molar volume of sodium molybdate in the mixture of aqueous ethane-1,2-diol (x_1 = 0.0677) as a function of square root of concentration at 298.15 (▲), 308.15 (♦) and 318.15 K (■).The lines represent the linear fits.

Thus it may be concluded that the electrolytes are characterized by the absence of caging effect [18,22].

The viscosity data of solutions for the electrolytes in 0.0312, 0.0677, 0.1106 mole fraction (x_1) of ethane-1,2-diol + water mixtures have been analyzed using Jones–Dole [23] equation:

$$(\eta/\eta_0 - 1)/c^{1/2} = A + Bc^{1/2} \quad (7)$$

where η_0 and η are the viscosities of the solvent/solvent mixtures and solution respectively. A and B are the constants estimated by least-squares method and are reported in Table 6. From the table it is evident that the values of the A coefficient are negative for all the solutions under investigation at all experimental temperatures. These results indicate the presence of weak ion–ion interactions, and these interactions further decrease with the rise of experimental temperatures suggesting an increase in ion–solvation while these interactions increase with an increase of ethane-1,2-diol in the mixture. Interestingly, values are found to be more negative for sodium molybdate and

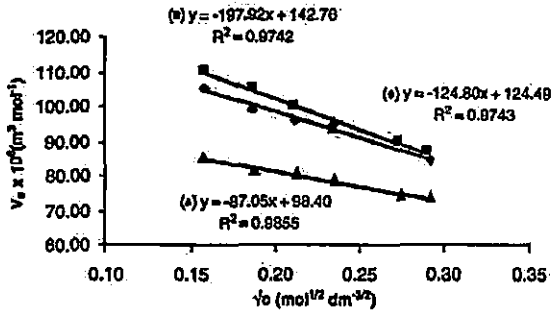

Fig. 3. The apparent molar volume of sodium molybdate in the mixture of aqueous ethane-1,2-diol (x_1 = 0.1106) as a function of square root of concentration at 298.15 (▲), 308.15 (♦) and 318.15 K (■).The lines represent the linear fits.

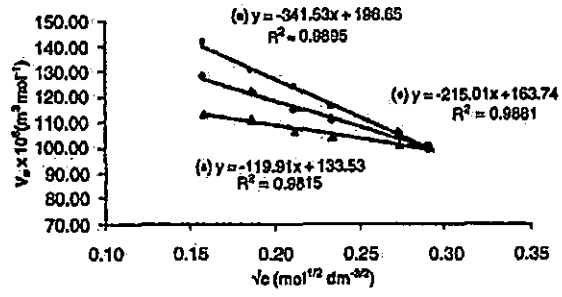

Fig. 4. The apparent molar volume of sodium tungstate in the mixture of aqueous ethane-1,2-diol (x_1 = 0.0312) as a function of square root of concentration at 298.15 (▲), 308.15 (♦) and 318.15 K (■).The lines represent the linear fits.

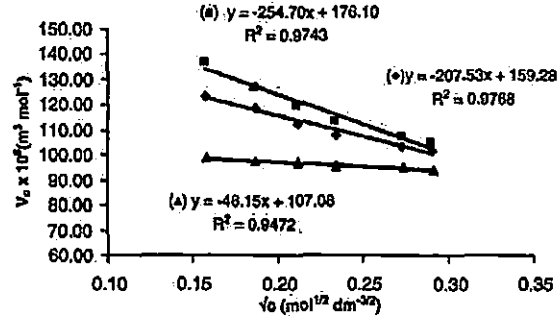

Fig. 5. The apparent molar volume of sodium tungstate in the mixture of aqueous ethane-1,2-diol (x_1 = 0.0677) as a function of square root of concentration at 298.15 (▲), 308.15 (♦) and 318.15 K (■).The lines represent the linear fits.

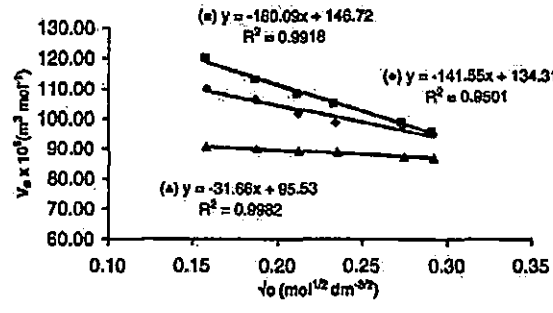

Fig. 6. The apparent molar volume of sodium tungstate in the mixture of aqueous ethane-1,2-diol (x_1 = 0.1106) as a function of square root of concentration at 298.15 (▲), 308.15 (♦) and 318.15 K (■).The lines represent the linear fits.

Table 3
Limiting apparent molar volumes (V_ϕ^0) and experimental slopes (S_v^*) of sodium molybdate and sodium tungstate in different aqueous binary mixtures of ethane-1,2-diol in 0.0312, 0.0677, 0.1106 mole fractions of ethane-1,2-diol at different temperatures

Mole fraction of ethane-1,2-diol	$V_\phi^0 \times 10^6$ m^3 mol^{-1}			$S_v^* \times 10^6$ m^3 mol$^{-3/2}$ dm$^{3/2}$		
	298.15 K	308.15 K	318.15 K	298.15 K	308.15 K	318.15 K
Sodium molybdate						
0.0312	129.27	159.40	196.73	−142.44	−229.13	−370.98
0.0677	112.07	138.58	174.46	−114.37	−167.67	−275.93
0.1106	98.401	123.80	142.76	−87.05	−124.49	−197.92
Sodium tungstate						
0.0312	133.53	163.74	196.65	−119.91	−215.01	−341.53
0.0677	107.08	159.28	176.10	−46.15	−207.53	−254.70
0.1106	95.53	134.31	146.72	−31.66	−141.55	−180.09

Table 5
Limiting partial molar expansibilities for sodium molybdate and sodium tungstate in different aqueous binary mixtures of ethane-1,2-diol in 0.0312, 0.0677, 0.1106 mole fractions of ethane-1,2-diol at different temperatures

Mole fraction of ethane-1,2-diol	ϕ_E^0 (m^3 mol^{-1} K^{-1})			$(\partial\phi_E^0/\partial T)_p$ (m^3 mol^{-1} K^{-2})
	298.15 K	308.15 K	318.15 K	
Sodium molybdate				
0.0312	2.6530	3.3730	4.0930	0.0720
0.0677	2.1820	3.1200	4.0580	0.0938
0.1106	−2.8619	−2.2179	−1.5739	−0.0644
Sodium tungstate				
0.0312	2.8861	3.1561	3.4261	0.0270
0.0677	6.9890	3.4510	0.0870	−0.3538
0.1106	5.1957	2.5597	−0.0763	−0.2636

hence it may be concluded that sodium molybdate is more soluble in aqueous ethane-1,2-diol solutions than sodium tungstate.

The effects of ion–solvent interactions on the solution viscosity can be inferred from the *B*-coefficient [24,25]. The viscosity *B*-coefficient is a valuable tool to provide information concerning the solvation of the solutes and their effects on the structure of the solvent. From Table 6 it is evident that the values of the *B*-coefficient of sodium molybdate and sodium tungstate in the studied solvent systems are positive, thereby suggesting the presence of strong ion–solvent interactions, and these type of interactions are strengthened with a rise in temperature and weakened with an increase of ethane-1,2-diol in the mixture. These conclusions are in excellent agreement with those drawn from V_ϕ^0 values discussed earlier.

It has been reported in a number of studies [26,27] that d*B*/d*T* is a better criterion for determining the structure-making/breaking nature of any solute rather than simply the value of the *B*-coefficient. It is found from Table 6 that the values of the *B*-coefficient increase with a rise in temperature (positive d*B*/d*T*) suggesting the structure-breaking tendency of sodium molybdate and sodium tungstate in the solvent systems. A similar result was reported in a study [28] of viscosity of some salts in propionic acid and ethanol mixtures.

The viscosity data have also been analyzed on the basis of transition state theory of relative viscosity of the electrolytes, suggested by Feakins et al. [29] using the following equation

$$\Delta\mu_2^{0*} = \Delta\mu_1^{0*} + \left(1000B + \overline{V}_2^0 - \overline{V}_1^0\right)RT/\overline{V}_1^0 \tag{8}$$

where $\overline{V}_1^0$ and $\overline{V}_2^0$ are the partial molar volumes of the solvent and the solute respectively. The contribution per mole of the solute to the free energy of activation of viscous flow ($\Delta\mu_2^{0*}$) of the solutions was determined from the above relation and is listed in Table 7. The free energy of activation of viscous flow of the pure solvent ($\Delta\mu_1^{0*}$) is given by the relation:

$$\Delta\mu_1^{0*} = \Delta G_1^{0*} = RT\ln\left(\eta_0\overline{V}_1^0\right)/hN_0 \tag{9}$$

where *N* is the Avogadro's number and the other symbols have their usual significance. The values of $\Delta\mu_2^{0*}$ and $\Delta\mu_1^{0*}$ are reported in Table 7. From Table 7 it is evident that $\Delta\mu_1^{0*}$ is practically constant at all the solvent composition and at all temperatures, implying that $\Delta\mu_2^{0*}$ is mainly dependent on the viscosity *B*-coefficients and $(\overline{V}_2^0 - \overline{V}_1^0)$ terms. Also $\Delta\mu_2^{0*}$ values were found to positive at all the experimental temperatures and hence the formation of the transition state is less favorable in the presence of these anions. A similar result was reported for sodium molybdate and sodium tungstate in aqueous acetonitrile solutions [21]. According to Feakins et al. [29] $\Delta\mu_2^{0*} > \Delta\mu_1^{0*}$ for electrolytes having positive *B*-coefficients and indicates a stronger ion–solvent interactions, thereby suggesting that the formation of transition state is accompanied by the rupture and distortion of the intermolecular forces in solvent structure [30]. The smaller values of $\Delta\mu_2^{0*}$ indicate the increased structure breaking tendency of the electrolyte. Thus from the values of $\Delta\mu_2^{0*}$ it can be inferred that both tungstate and molybdate ions have similar structure breaking tendencies. The entropy of activation for electrolytic solutions has been calculated using the following relation [29].

$$\Delta S_2^{0*} = -d(\Delta\mu_2^{0*})/dt \tag{10}$$

where ΔS_2^{0*} has been determined from the negative slope of the plots of $\Delta\mu_2^{0*}$ against *T* by using a least square treatment.

Table 4
Values of the coefficients of Eq. (4) for sodium molybdate and sodium tungstate in different aqueous binary mixtures of ethane-1,2-diol in 0.0312, 0.0677, 0.1106 mole fractions of ethane-1,2-diol

Mole fraction of ethane-1,2-diol	a_0 (m^3 mol^{-1})	a_1 (m^3 mol^{-1} K^{-1})	a_2 (m^3 mol^{-1} K^{-2})
Sodium molybdate			
0.0312	2538.441	−18.8138	0.0360
0.0677	3630.617	−25.7845	0.0469
0.1106	−3617.255	22.0628	−0.0322
Sodium tungstate			
0.0312	473.1154	−5.164	0.0135
0.0677	17,701.946	−112.475	0.1769
0.1106	−13,169.706	83.788	−0.1318

Table 6
Values of *A* and *B* coefficients for sodium molybdate and sodium tungstate in different aqueous binary mixtures of ethane-1,2-diol in 0.0312, 0.0677, 0.1106 mole fractions of ethane-1,2-diol at different temperatures

Mole fraction of ethane-1,2-diol	*A*, dm$^{3/2}$ mol$^{-1/2}$			*B*, dm^3 mol^{-1}		
	298.15 K	308.15 K	318.15 K	298.15 K	308.15 K	318.15 K
Sodium molybdate						
0.0312	−0.0478	−0.0504	−0.0535	0.7272	0.8746	0.9493
0.0677	−0.0067	−0.0211	−0.0329	0.6606	0.7610	0.8445
0.1106	−0.0056	−0.0083	−0.0108	0.6226	0.6977	0.7792
Sodium tungstate						
0.0312	−0.0118	−0.0145	−0.0165	0.7891	0.8733	0.9720
0.0677	−0.0122	−0.0135	−0.0176	0.6842	0.7678	0.8494
0.1106	−0.0102	−0.0126	−0.0139	0.6311	0.6834	0.7608

Table 7
Values of V_1^{0*}, V_2^{0*}, $\Delta\mu_1^{0*}$, $\Delta\mu_2^{0*}$, $T\Delta S_2^{0*}$ and ΔH_2^{0*} for sodium molybdate and sodium tungstate in different aqueous binary mixtures of ethane-1,2-diol in 0.0312, 0.0677, 0.1106 mole fractions (x_1) of ethane-1,2-diol at different temperatures

Parameter	Mole fraction of ethane-1,2-diol x_1=0.0312			Mole fraction of ethane-1,2-diol x_1=0.0677			Mole fraction of ethane-1,2-diol x_1=0.1106		
	298.15 K	308.15 K	318.15 K	298.15 K	308.15 K	318.15 K	298.15 K	308.15 K	318.15 K
$V_1^0\times10^6$, $m^3\,mol^{-1}$	19.1855	20.8527	22.8122	18.9456	20.5749	22.5182	18.7008	20.2867	22.2491
$\Delta\mu_1^{0*}$, kJ mol^{-1}	27.0272	27.5454	28.2401	27.5736	28.1325	28.7919	28.1606	28.6840	29.2758
Sodium molybdate									
$V_2^{0*}\times10^6$, $m^3\,mol^{-1}$	129.27	159.40	196.73	112.07	138.58	174.46	98.401	123.80	142.76
$\Delta\mu_2^{0*}$, kJ mol^{-1}	42.1900	45.6418	49.5068	40.6222	43.7739	47.6317	39.5501	42.6376	44.5292
$T\Delta S_2^{0*}$, kJ mol^{-1}	−109.1229	−112.7829	−116.4429	−104.5015	−108.0065	−111.5115	−74.239	−76.729	−79.2193
$\Delta H_2^{0*}\times10^3$, kJ mol^{-1}	−66.9329	−67.1411	−66.936	−63.8793	−64.2326	−63.8798	−34.6889	−34.0914	−34.6901
Sodium tungstate									
$V_2^{0*}\times10^6$, $m^3\,mol^{-1}$	133.53	163.74	196.65	107.08	139.28	176.10	95.53	134.31	146.72
$\Delta\mu_2^{0*}$, kJ mol^{-1}	42.8203	46.1784	49.5238	40.0002	46.3590	47.8301	39.1810	43.9108	44.9781
$T\Delta S_2^{0*}$, kJ mol^{-1}	−99.8802	−103.2302	−106.5802	−116.4275	−120.3325	−124.2375	−86.3144	−89.2094	−92.1044
$\Delta H_2^{0*}\times10^3$, kJ mol^{-1}	−57.0599	−57.0518	−57.0519	−76.4273	−73.9726	−76.4074	−47.1334	−45.2986	−47.1263

The activation enthalpy (ΔH_2^{0*}) has been calculated using the relation [29]:

$$\Delta H_2^{0*} = \Delta\mu_2^{0*} + T\Delta S_2^{0*} \quad (11)$$

the value of ΔS_2^{0*} and ΔH_2^{0*} are listed in Table 7 and they are found to be negative for all the electrolytic solutions and at all experimental temperatures suggesting that the transition state is associated with bond formation and increase in order. Although a detailed mechanism for this cannot be easily advanced, it may be suggested that the slip-plane is in the disordered state [29,31].

4. Conclusion

In summary it can be concluded that both sodium molybdate and sodium tungstate show similar trend of ion–solvent and ion–ion interactions, which can be ascribed to the similar structure of tungstate and molybdate ions [7]. From the values of apparent molar volume (V_ϕ^0) and viscosity B-coefficients it may be concluded that ion–solvent interaction increases with increasing temperature and decreases with increasing amount of ethane-1,2-diol in the aqueous mixture. Also the structure breaking tendencies of the two electrolytes were found to be similar.

Acknowledgement

The authors are grateful to the Departmental Special Assistance Scheme under the University Grants Commission, New Delhi (No. 540/6/DRS/2002, SAP-1) for financial support.

References

[1] J.M. Mc Dowall, C.A. Vincent, J. Chem. Soc., Faraday Trans. 1 (1974) 1862–1868.
[2] M.R.J. Dack, K.J. Bird, A.J. Parker, Aust. J. Chem. 28 (1975) 955–963.
[3] M.N. Roy, B. Sinha, R. Dey, A. Sinha, Int. J. Thermophys. 26 (2005) 1549–1563.
[4] R.H. Stokes, R. Mills, Int. Encyclopedia of Physical Chemistry and Chemical Physics, , 1965.
[5] P.S. Nikam, H. Mehdi, J. Chem.Eng.Data 33 (1988) 165–169.
[6] D. Nandi, M.N. Roy, D.K. Hazra, J. Indian Chem. Soc. 70 (1993) 305–310.
[7] R. Jasinki, High Energy Battery, Plenum, New York, 1967.
[8] C.G. Janz, R.P.T. Tomkins, Non-aqueous Electrolytes Handbook, vol. 2, Academic, New York, 1973.
[9] J.D. Lee, Concise Inorganic Chemistry, fifth ed.Blackwell Science Ltd, Oxford, 1999.
[10] D.D. Perrin, W.L.F. Amarego, Purification of Laboratory Chemicals, third ed., 1988 Great Britain.
[11] M.N. Roy, A. Sinha, B. Sinha, J. Solution Chem. 34 (2005) 1311–1325.
[12] M.N. Roy, B. Sinha, V.K. Dakua, J. Chem. Eng. Data 51 (2006) 590–594.
[13] M.N. Roy, A. Sinha, Fluid Phase Equilibr. 243 (2006) 133–141.
[14] M.N. Roy, M. Das, Russ. J. Phys. Chem. 80 (2006) S163–S171.
[15] D.O. Masson, Phila. Mag. 8 (1929) 218–226.
[16] E. Garcia-Paneda, C. Yanes, J.J. Calvente, A. Maestre, J. Chem. Soc., Faraday Trans. 94 (1994) 575–577.
[17] M.N. Roy, A. Jha, R. Dey, J. Chem. Eng. Data 46 (2001) 1327–1329.
[18] F.J. Millero, Structure and Transport Process in Water and Aqueous Solutions, R.A. Horne, New York, 1972.
[19] P.R. Misra, B. Das, Ind. J. Chem. 16 (1978) 348–353.
[20] L.G. Hepler, Can. J. Chem. 47 (1969) 4613–4617.
[21] B.K. Sarkar, B. Sinha, M.N. Roy, Russ. J. Phys. Chem 82 (2008) 960–966.
[22] M.L. Parmar, D.S. Banyal, Indian J. Chem. 44A (2005) 1582–1588.
[23] G. Jones, M. Dole, J. Am. Chem. Soc. 51 (1929) 2950–2964.
[24] F.J. Millero, Chem. Rev. 71 (1971) 147–176.
[25] F.J. Millero, A. Lo Surdo, C. Shin, J. Phys. Chem. 82 (1978) 784–792.
[26] R. Gopal, M.A. Siddiqi, J. Phys. Chem. 72 (1969) 1814–1817.
[27] N. Saha, B. Das, J. Chem. Eng. Data 42 (1997) 227–229.
[28] S.M. Contreras, J. Chem. Eng. Data 46 (2001) 1149–1152.
[29] D. Feakins, D.J. Freemantle, K.G. Lawrence, J. Chem. Soc., Faraday Trans.1 70 (1974) 795–806.
[30] B. Samantaray, S. Mishra, U.N. Dash, J. Teach. Res. Chem. 11 (2005) 87–93.
[31] Mithlesh, M. Singh, J. Indian. Chem. Soc. 83 (2006) 803–809.
[32] Piping and Fluid Mechanics Engineering Volume Expansivity of Ethylene Glycol vs Temperature(http://www.Engeneeringtoolbox.com/24%20146.html).

ЖУРНАЛ ФИЗИЧЕСКОЙ ХИМИИ, 2009, том 83, № 11, с. 2076–2084

ФИЗИЧЕСКАЯ ХИМИЯ РАСТВОРОВ

УДК 532.78

ION–SOLVENT AND ION–ION INTERACTIONS OF PHOSPHOMOLYBDIC ACID IN AQUEOUS SOLUTION OF CATECHOL AT 298.15, 308.15 AND 318.15K

© 2009 M. N. Roy, R. S. Sah, P. Pradhan, and P. K. Roy

Department of Chemistry, North Bengal University, Darjeeling-734013, India

E-mail: mahendraroy2002@yahoo.co.in

Received 22 July 2008

Abstract – Apparent molar volume ($V_\varnothing$) and viscosity B-coefficients were measured for phosphomolybdic acid in aqueous solution of catechol from solution density (ρ) and viscosity (η) at 298.15, 308.15 and 318.15K at various solute concentrations. The experimental density data were evaluated by Masson equation and the derived data were interpreted in terms of ion-solvent and ion-ion interactions. The viscosity data have been analyzed using Jones–Dole equation and the derived parameters, B and A, have been interpreted in terms of ion–solvent and ion–ion interactions respectively. The structure-making or breaking capacity of the solute under investigation has been discussed in terms of sign of $(\delta^2 V_\varnothing^\circ/\delta T^2)_P$. The activation parameters of viscous flow were determined and discussed by application of transition state theory.

INTRODUCTION

Studies on densities (ρ) and viscosities (η) of solutions are of great importance in characterizing the properties and structural aspects of solutions. Hence studies on the limiting apparent molar volume and viscosity B-coefficients of electrolyte provide us valuable information regarding ion–ion, ion–solvent and solvent–solvent interactions [1–3]. It has been found by a number of workers [4–6] that the addition of a solute could either make or break the structure of a liquid. As the viscosity of a liquid depends on the intermolecular forces, the structural aspects of the liquid can be inferred from the viscosity of solutions at various solute concentrations and temperature.

In this paper we have attempted to report the limiting apparent molar volume ($V_\varnothing^\circ$), experimental slopes (S_v^*) and viscosity B-coefficients for phosphomolybdic acid in aqueous catechol solution at 298.15, 308.15 and 318.15K. Phosphomolybdic acid is widely used to stain connective tissues by dyes. It has been found that phosphomolybdic acid forms salts with connective tissues containing basic groups and hence the polyvalent phosphomolybdic acid appears to form a bridge between the basic group of the substrate and the basic group of the dye. In other words, addition of phosphomolybdic acid to connective tissues changes its acidophilia to basophilia. Phosphomolybdic acid not only yields an intense staining of connective tissue fibers by dyes with basic groups but also reduces the staining of cytoplasm, thus producing a specific staining of connective tissue fiber [7].

EXPERIMENTAL

Commercial sample of catechol was purified by repeated crystallization from mixture of chloroform–methanol. The sample was dissolved in chloroform in hot condition, filtered and to the filtrate dried and distilled methanol was added drop wise. Fine plate like crystal separated and was recovered by rapid filtration and ready for use. Phosphomolybdic acid of analytical grade was purchased from Thomas Baker and was used without further purification. Doubly distilled, degassed and deionised water with a specific conductance of 1×10^{-6} Ω^{-1} cm^{-1} was used for all measurements. Experimental values of viscosity (η), density (ρ) and pH are listed in Table 1.

Table 1. Experimental value of density (ρ, kg m^{-3}) and viscosity (η, mPa s) of aqueous catechol mixtures at different temperatures

T, K	$\rho \times 10^{-3}$, kg m^{-3}	η, mPa s	pH
0.05 M			
298.15	0.99650	0.9003	6.16
308.15	0.99371	0.7350	5.31
318.15	0.99222	0.6135	
0.1 M			
298.15	0.99797	0.9132	4.20
308.15	0.99509	0.7475	4.16
318.15	0.99303	0.6375	4.13
0.15 M			
298.15	0.99910	0.9227	3.97
308.15	0.99621	0.7602	3.89
318.15	0.99429	0.6528	3.82

Densities (ρ) were measured with an Ostwald–Sprengel type pycnometer having a bulb volume of about 25 cm^3 and an internal diameter of about 0.1 cm. The measurements were done in a thermostat bath controlled to ±0.01 K. the viscosity (η) was measured by means of suspended Ubbelohde type viscometer, calibrated at 298.15 K with triply distilled water and purified methanol using density and viscosity values from literature. The flow times were accurate to ±0.1s, and the uncertainty in the viscosity measurements was $\pm 2 \times 10^{-4}$ mPa s. The mixtures were prepared by mixing known volume of pure liquids in airtight-stopper bottles and each solution thus prepared was distributed into three recipients to perform all the measurements in triplicate, with the aim of determining possible dispersion of the results obtained. Adequate precautions were taken to minimize evaporation loses during the actual measurements. The reproducibility in mole fractions was within ±0.0002 units. The mass measurements were done on a Mettler AG-285 electronic balance with a precision of ±0.01 mg. The precision of density measurements was $\pm 3 \times 10^{-4}$ g cm^{-3}. Viscosity of the solution, η, is given by the following equation:

$$\eta = (Kt - L/t)\rho, \quad (1)$$

where K and L are the viscometer constants and t and ρ are the efflux time of flow in seconds and the density of the experimental liquid, respectively. The uncertainty in viscosity measurements is within ±0.003 mPa s.

Details of the methods and techniques of density and viscosity measurements have been described elsewhere[8–11] .The electrolyte solutions studied here were prepared by mass and the conversion of molality in molarity was accomplished [3] using experimental density values. The experimental values of concentrations(c), densities (ρ), viscosities (η), and derived parameters at various temperatures are reported in Table 2.

RESULTS AND DISCUSSION

The apparent molar volumes ($V_\varnothing$) were determined from the solution densities using the following equation [3]:

$$V_\varnothing^\circ = M/\rho_0 - 1000(\rho - \rho_0)/c\rho_0, \quad (2)$$

where M is the molar mass of the solute, c is the molarity of the solution; ρ_0 and ρ are the densities of the solvent and the solution respectively. The limiting apparent molar volumes $V_\varnothing^\circ$ was calculated using a least-square treatment to the plots of $V_\varnothing$ versus $c^{1/2}$ using the following Masson equation [12].

$$V_\varnothing = V_\varnothing^\circ + S_v^* c^{1/2}, \quad (3)$$

where $V_\varnothing^\circ$ is the partial molar volume at infinite dilution and S_v^* the experimental slope. The plots of $V_\varnothing$ against square root of molar concentration ($c^{1/2}$) were found to be linear with negative slopes. Values of $V_\varnothing^\circ$ and S_v^* are reported in Table 3.

As the systems under study are characterized by hydrogen bonding, the ion–solvent and ion–ion interactions can be interpreted in terms of structural changes which arise due to hydrogen bonding between various components of the solvent and solution systems. $V_\varnothing^\circ$ can be used to interpret ion–solvent interactions. Table 3 reveals that $V_\varnothing^\circ$ values are positive and increases with rise in temperature and decreases with increase in the amount of catechol in the solvent mixture. This indicates the presence of strong ion-solvent interactions and these interactions are strengthened with rise in temperature and weakened with an increase in the amount of catechol in the solvent mixture under study, suggesting larger electrostriction at higher temperature and in lower amount of catechol in the mixture. Similar results were obtained for some 1:1 electrolytes in aqueous DMF [13] and aqueous THF [14].

It is evident from Table 3 that the S_v^* values are negative at all temperatures for aqueous mixtures of catechol. Furthermore S_v^* values decreases with the increase of experimental temperature which may be attributed to more violent thermal agitation at higher temperatures, resulting in diminishing the force of ion–ion interactions (ionic dissociation) [15] . A quantitative comparison of the magnitude of values shows that $V_\varnothing^\circ$ values are much greater in magnitude than those of S_v^* for all the solutions. This suggests that ion–solvent interactions dominate over ion–ion interactions in all the solutions and at all experimental temperatures.

The variation of $V_\varnothing^\circ$ with temperature of phosphomolybdic acid in solvent mixture follows the polynomial,

$$V_\varnothing^\circ = a_0 + a_1 T + a_2 T^2 \quad (4)$$

over the temperature range under study where T is the temperature in K. Values of coefficients of the above equation for phosphomolybdic acid in aqueous catechol mixtures are reported in Table 4.

The apparent molar expansibilities ($\varnothing_E^\circ$) can be obtained by the following equation:

$$\varnothing_E^\circ = (\delta V_\varnothing^\circ/\delta T)_P = a_0 + 2a_2 T. \quad (5)$$

The values $\varnothing_E^\circ$ of for different solutions of the studied electrolytes at 298.15, 308.15 and 318.15 K are reported in Table 5. Table 5 reveals that $\varnothing_E^\circ$ value increases as concentration increases up to 0.05 mol dm^{-3} of catechol mixtures but thereafter $\varnothing_E^\circ$ value decreases slightly with increasing temperature. This fact may be attributed to gradual disappearance of caging or pack-

Table 2. Concentration (c), density (ρ), viscosity (η), apparent molar volume ($V_\varnothing$), $(\eta/\eta_0 - 1)/c^{1/2}$ and pH of phosphomolybdic acid in different aqueous catechol mixtures at different temperatures (c_c is concentration of catechol in aqueous solution)

c, mol dm^{-3}	$\rho \times 10^{-3}$, kg m^{-3}	η, mPa s	$V_\varnothing \times 10^6$, m^3 mol^{-1}	$(\eta/\eta_0 - 1)/c^{1/2}$	pH
		$c_c = 0$, 298.15 K			
0.0025	1.0003	0.8970	963.4739	0.0754	2.56
0.0050	1.0042	0.9013	807.3489	0.1213	2.29
0.0074	1.0085	0.9059	709.8034	0.1585	2.13
0.0099	1.0125	0.9099	693.5894	0.1829	1.99
0.0124	1.0169	0.9146	649.6547	0.2107	1.91
0.0154	1.0223	0.9205	593.0401	0.2432	1.83
		$c_c = 0$, 308.15 K			
0.0025	0.9972	0.7234	980.4210	0.0260	2.50
0.0049	1.0008	0.7275	880.5810	0.0980	2.20
0.0074	1.0048	0.7318	803.2913	0.1500	2.02
0.0098	1.0091	0.7365	725.1210	0.1961	1.89
0.0123	1.0135	0.7404	677.6658	0.2239	1.80
0.0151	1.0189	0.7454	617.4291	0.2571	1.72
		$c_c = 0$, 318.15 K			
0.0024	0.9949	0.6042	1117.8019	0.2110	2.40
0.0049	0.9989	0.6170	874.4041	0.4530	2.08
0.0073	1.0032	0.6280	745.7746	0.5860	1.90
0.0098	1.0072	0.6378	717.0760	0.6720	1.79
0.0122	1.0114	0.6469	678.2216	0.7400	1.69
0.0151	1.0169	0.6583	614.9841	0.8200	1.59
		$c_c = 0.05$ M, 298.15 K			
0.0024	1.0007	0.9071	504.8713	0.0860	2.73
0.0048	1.0053	0.9116	431.7338	0.1330	2.36
0.0076	1.0107	0.9162	391.3216	0.1637	2.14
0.0101	1.0156	0.9190	365.7746	0.1727	2.03
0.0125	1.0205	0.9229	339.9873	0.1940	1.92
0.0149	1.0252	0.9270	329.7652	0.2145	1.83
		$c_c = 0.05$ M, 308.15 K			
0.0024	0.9978	0.7396	530.2752	0.1280	2.66
0.0048	1.0023	0.7458	472.4611	0.2130	2.29
0.0076	1.0075	0.7516	434.2549	0.2600	2.08
0.0101	1.0123	0.7569	412.4919	0.2970	1.98
0.0125	1.0170	0.7604	387.1231	0.3100	1.85
0.0148	1.0217	0.7663	373.6044	0.3492	1.77
		$c_c = 0.05$ M, 318.15 K			
0.0024	0.9962	0.6217	569.2613	0.2750	2.58
0.0048	1.0004	0.6307	518.5812	0.4060	2.22
0.0076	1.0055	0.6421	484.1216	0.5364	1.99
0.0102	1.0094	0.6514	458.6212	0.6171	1.91
0.0126	1.0132	0.6583	424.2826	0.6560	1.83
0.0150	1.0174	0.6657	411.1519	0.7000	1.73

Table 2. (Contd.)

c, mol dm^{-3}	$\rho \times 10^{-3}$, kg m^{-3}	η, mPa s	$V_{\varnothing} \times 10^{6}$, m^3 mol^{-1}	$(\eta/\eta_0 - 1)/c^{1/2}$	pH
		$c_c = 0.1$ M, 298.15K			
0.0024	1.0022	0.9199	510.1307	0.1490	2.53
0.0048	1.0065	0.9254	491.9397	0.1930	2.26
0.0076	1.0116	0.9306	471.7912	0.2180	2.09
0.0101	1.0162	0.9343	456.3825	0.2300	1.99
0.0125	1.0207	0.9375	440.5892	0.2380	1.91
0.0149	1.0253	0.9411	423.4132	0.2500	1.85
		$c_c = 0.1$ M, 308.15 K			
0.0024	0.9992	0.7524	562.0561	0.1340	2.58
0.0048	1.0034	0.7577	526.5677	0.1970	2.24
0.0076	1.0084	0.7634	501.1550	0.2440	2.04
0.0101	1.0130	0.7682	487.9350	0.2762	1.94
0.0125	1.0173	0.7716	476.8405	0.2881	1.83
0.0149	1.0219	0.7752	460.9899	0.3040	1.75
		$c_c = 0.1$ M, 318.15 K			
0.0024	0.9970	0.6441	600.0121	0.2020	2.42
0.0048	1.0011	0.6518	572.6434	0.3230	2.14
0.0076	1.0060	0.6604	551.5000	0.4120	1.94
0.0101	1.0104	0.6662	533.7240	0.4480	1.85
0.0125	1.0148	0.6731	514.6262	0.5000	1.75
0.0150	1.0192	0.6806	498.5364	0.5540	1.70
		$c_c = 0.15$ M, 298.15K			
0.0024	1.0034	0.9309	480.5001	0.1820	2.52
0.0050	1.0081	0.9354	462.5995	0.1940	2.25
0.0076	1.0128	0.9400	458.5057	0.2150	2.09
0.0102	1.0174	0.9434	445.8924	0.2230	1.97
0.0125	1.0217	0.9474	439.3518	0.2402	1.88
0.0151	1.0265	0.9512	428.7236	0.2520	1.81
		$c_c = 0.15$ M, 308.15 K			
0.0024	1.0002	0.7644	576.6336	0.1140	2.45
0.0050	1.0047	0.7673	560.6523	0.1320	2.16
0.0076	1.0092	0.771	548.4545	0.1630	1.99
0.0102	1.0135	0.7737	537.4861	0.1767	1.87
0.0125	1.0175	0.7770	535.1857	0.1990	1.78
0.0151	1.0221	0.7807	524.5887	0.2208	1.70
		$c_c = 0.15$ M, 318.15 K			
0.0024	0.9983	0.1040	592.5463	0.1040	2.40
0.0050	1.0027	0.1450	565.5505	0.1450	2.09
0.0076	1.0072	0.1700	550.8687	0.1700	1.89
0.0102	1.0116	0.1960	540.2304	0.1960	1.79
0.0125	1.0156	0.2270	533.9527	0.2270	1.70
0.0151	1.0204	0.2490	513.5327	0.2490	1.62

Table 3. Limiting apparent molar volumes ($V^\circ_\varnothing$) and experimental slopes (S^*_v) for phosphomolybdic acid at different temperatures (c_c is concentration of catechol in aqueous solution)

c_c, mol dm^{-3}	$V^\circ_\varnothing \times 10^6$, m^3 mol^{-1}			$-S^*_v \times 10^6$, m^3 mol$^{-3/2}$dm$^{3/2}$		
	298.15 K	308.15 K	318.15 K	298.15 K	308.15 K	318.15 K
0.00	1163.5	1227.3	1368.4	4757.8	4980.3	6440.7
0.05	607.33	626.22	673.7	2372.1	2128.5	2185.7
0.1	571.38	622.56	668.44	1174.5	1335.1	1371.7
0.15	513.4	609.94	639.48	674.12	697.1	1000.7

ing effect [15, 16] in the ternary solutions. During the past few years it has been emphasized by a number of workers that S^*_v is not the sole criterion for determining the structure-making or breaking tendency of any solute. According to Helper [17] the sign of $(\delta\varnothing^\circ_E/\delta T)_P$ is a better criterion in characterizing the long–range structure-making and breaking ability of the solutes in solution. The general thermodynamic expression used is as follows

$$(\delta\varnothing^\circ_E/\delta T)_P = 2a_2. \quad (6)$$

If the sign of $(\delta\varnothing^\circ_E/\delta T)_P$ is positive or small negative [18] the solute is a structure maker otherwise it is a structure breaker. As is evident from Table 5, phosphomolybdic acid predominately acts as a structure maker and its structure making ability decreases to some extent as the molarity of catechol increases in the solvent mixture. A similar result was observed in the study of nicotinamide in aqueous tetrabutylammonium bromide solution [19]. The small negative values of $(\delta\varnothing^\circ_E/\delta T)_P$ at 0.1 and 0.15 mol dm^{-3} aqueous catechol solution are probably due to higher structure promoting ability of catechol than phosphomolybdic acid with comparatively higher $V^\circ_\varnothing$ value in aqueous solution [20] originating from hydrophobic hydration with greater degree of hydrogen bonding than the bulk water [21].

Table 4. Values of the coefficients of equation (4) for phosphomolybdic acid in different aqueous catechol mixtures

$c_c$mol dm^{-3}	a_0, m^3 mol^{-1}	a_1, m^3 mol^{-1} K^{-1}	a_2, m^3 mol^{-1} K^{-2}
0.00	34772.46	−227.96	0.3865
0.05	13182.24	−84.81	0.1430
0.1	−3389.23	21.18	−0.0265
0.15	−33143.04	212.76	−0.3350

Partial molar volume $\Delta V^\circ_\varnothing$ of transfer from water to different aqueous catechol solution has been determined using the following relation [22, 23]

$$\Delta V^\circ_\varnothing = V^\circ_\varnothing(\text{aqueous catechol solution}) - V^\circ_\varnothing(\text{water}). \quad (7)$$

The $V^\circ_\varnothing$ value is independent from solute–solute interaction and provides information regarding solute and co-solute interaction [22]. Table 3 shows that the values of $V^\circ_\varnothing$ is positive at all experimental temperatures and increases with the concentration of catechol in the ternary mixture. The concentration dependence of the thermodynamic properties of the solute in aqueous solution can be explained in terms of overlap of hydration co-sphere. According to the co-sphere model as developed by Friedman and Krishnan [24], the effect of the overlap of hydration co-sphere is destructive. The overlap of hydration co-spheres of two ionic species results in an increase in volume but that of hydration co-sphere of hydrophobic–hydrophobic group and ion–hydrophobic group results in a net volume decrease. The positive value of $\Delta V^\circ_\varnothing$ indicate that hydrophobic–hydrophobic and ion–hydrophobic group interaction are predominant and the overall effect of the hydration co-sphere of phosphomolybdic acid and catechol reduce the effect of electrostriction of water by phosphomolybdic acid molecule and these effect increases with the molarity of catechol in the ternary mixture as shown in the Fig. 1($\Delta V^\circ_\varnothing$ vs. molarity of catechol in solution). In addition, standard partial molar volume of the solute has been explained by a simple model [25, 26].

$$V^\circ_\varnothing = V_{\varnothing vw} + V_{\varnothing void} - V_{\varnothing s}, \quad (8)$$

where $V_{\varnothing vw}$ is the vander wall volume, $V_{\varnothing void}$ is the volume associated with void or empty space and $V_{\varnothing s}$ the shrinkage volume due to electrostriction. Considering the $V_{\varnothing vw}$ and $V_{\varnothing void}$ have the same magnitude in water

and in aqueous catechol solution for the same solute [27]. The increase in $V_\varnothing^\circ$ values and the concomitant positive $\Delta V_\varnothing^\circ$ can be attributed to the decrease in shrinkage volume of water by phosphomolybdic acid in presence of catechol. This fact suggests that catechol has a dehydrating effect on the hydrated phosphomolybdic acid.

The viscosity data of aqueous and aqueous catechol solution have been analyzed using Jones–Dole [28] equation:

$$(\eta/\eta_0 - 1)/c^{1/2} = A + Bc^{1/2}, \quad (9)$$

where η_0 and η are the viscosities of the solvent–solvent mixtures and solution respectively. A and B are the constants estimated by a least-squares method and are reported in Table 6. From the table it is evident that the values of the A coefficient are either negative or very small positive for all the solutions under investigation at all experimental temperatures. These results indicate the presence of very weak ion–ion interactions and these interactions further decrease with the rise of experimental temperatures and increase with an increase of catechol in the mixture.

The effects of ion–solvent interactions on the solution viscosity can be inferred from the B-coefficient [29, 30]. The viscosity B-coefficient is a valuable tool to provide information concerning the solvation of the solutes and their effects on the structure of the solvent. From table 6 it is evident that the values of the B-coefficient of phosphomolybdic acid in the studied solvent systems are positive, thereby suggesting the presence of strong ion – solvent interactions, and these types of interactions are strengthened with a rise in temperature and weakened with an increase of catechol in the mixture. These conclusions are in excellent agreement with those drawn from $V_\varnothing^\circ$ values discussed earlier.

Viscosity B-coefficient of transfer (ΔB) from water to different aqueous catechol solutions have been determined using the relation [22, 23]

Table 5. Limiting partial molar expansibilities for phosphomolybdic acid in different aqueous catechol mixtures at different temperatures

c_c, mol dm^3	$\varnothing_E^\circ$ m^3 mol^{-1} K^{-1}			$(\delta\varnothing_E^\circ/\delta T)_P$, dm^3 mol^{-1} K^{-2}
	298.15 K	308.15 K	318.15 K	
0.00	2.5100	10.2400	17.97	0.7730
0.05	0.4590	3.3190	6.1790	0.2860
0.1	5.3884	4.8531	4.3231	–0.0530
0.15	13.0040	6.3040	0.3960	–0.6700

$$\Delta B = B(\text{aqueous catechol solution}) - B(\text{water}). \quad (10)$$

The ΔB values as shown in Table 7 and depicted graphically in Fig. 2 (ΔB vs. molarity of catechol in solution) as a function of molarity of catechol in solution at the experimental temperature supports the result obtained from $\Delta V_\varnothing^\circ$ as discussed above.

The viscosity data have also been analyzed on the basis of transition state theory of relative viscosity of solutes as suggested by Feakings et al [31] using the following equation:

$$\Delta\mu_2^{0\neq} = \Delta\mu_1^{0\neq} + (1000B + \bar{V}_2^0 - \bar{V}_1^0)RT/\bar{V}_1^0, \quad (11)$$

where $\bar{V}_1^0$ and $\bar{V}_2^0$ are the partial molar volumes of the solvent and the solute respectively. The contribution per mole of the solute to the free energy of activation of viscous flow ($\Delta\mu_2^{0\neq}$) of the solutions was determined from the above relation and are listed in Table 8. The free energy of activation of viscous flow of the pure solvent ($\Delta\mu_1^{0\neq}$) is given by the relation:

$$\Delta\mu_1^{0\neq} = \Delta G_1^{0\neq} = RT\ln(\eta_0\bar{V}_1^0)/hN, \quad (12)$$

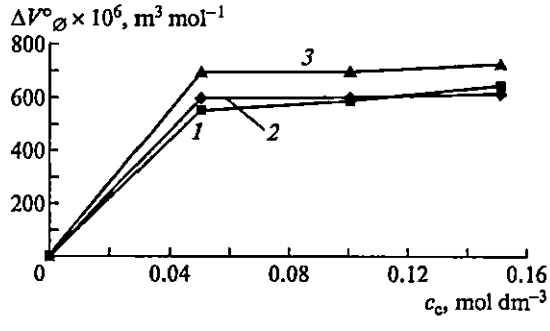

Fig. 1. Plots of partial molar volume ($\Delta V_\varnothing^\circ$) against molality for the transfer from water to different aqueous catechol solutions for phosphomolybdicacid at different temperatures: (*1*) 298.15, (*2*) 308.15, (*3*) 318.15K.

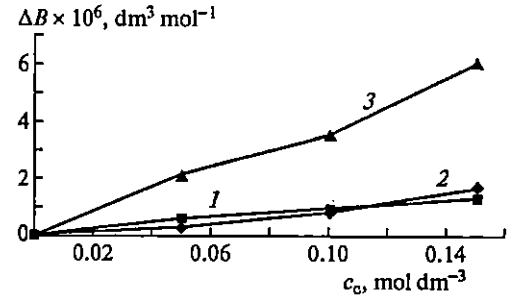

Fig. 2. Plots of partial molar volume (ΔB) against molality for the transfer from water to different aqueous catechol solutions for phosphomolybdicacid at different temperatures: (*1*) 298.15, (*2*) 308.15, (*3*) 318.15K.

Table 6. Values of A and B coefficients for phosphomolybdic acid in different aqueous catechol mixtures at different temperatures

c_c, mol dm^{-3}	A, dm$^{3/2}$ mol$^{-1/2}$			B, dm^3 mol^{-1}		
	298.15 K	308.15 K	318.15 K	298.15 K	308.15 K	318.15 K
0.00	−0.0363	−0.1251	−0.1438	2.2454	3.1624	8.0839
0.05	0.011	0.0010	−0.0025	1.663	2.8785	5.9650
0.1	0.0941	0.0307	0.0010	1.3220	2.3322	4.5261
0.15	0.1301	0.0355	0.0048	0.9717	1.4666	1.9682

where N is the Avogadro's number and the other symbols have their usual significance. The values of $\Delta\mu_2^{0\neq}$ and $\Delta\mu_1^{0\neq}$ are reported in Table 8. From Table 8 it is evident that $\Delta\mu_1^{0\neq}$ is practically constant at all the solvent composition and temperature, implying that

Table 7. Partial molar volumes $V^\circ_\varnothing$ (m^3 mol^{-1}) and viscosity B-coefficients ΔB (dm^3 mol^{-1}) of transfer from water to different aqueous catechol solutions for phosphomolybdic acid at different temperatures

c_c, mol dm^{-3}	$V^\circ_\varnothing \times 10^6$	$\Delta V^\circ_\varnothing \times 10^6$	$B \times 10^6$	$\Delta B \times 10^6$
		298.15 K		
0.00	1163.5	0.00	2.2454	0.00
0.05	607.33	556.17	1.663	0.5824
0.10	571.38	592.12	1.3220	0.9234
0.15	513.4	650.1	0.9717	1.2737
		308.15 K		
0.00	1227.3	0.00	3.1624	0.00
0.05	626.22	601.08	2.8785	0.2839
0.10	622.56	604.74	2.3322	0.8302
0.15	609.94	617.36	1.4666	1.6958
		318.15 K		
0.00	1368.4	0.00	8.0839	0.00
0.05	673.7	694.70	5.956	2.1279
0.10	668.44	699.96	4.5261	3.5578
0.15	639.48	728.92	1.9682	6.1157

$\Delta\mu_2^{0\neq}$ is mainly dependent on the viscosity B-coefficients and $(\bar{V}_2^0 - \bar{V}_1^0)$ terms. Also $\Delta\mu_2^{0\neq}$ values were found to be positive at all experimental temperatures and this suggests that the process of viscous flow becomes difficult as the temperature and molarity of catechol in solution increases. Hence the formation of transition becomes less favorable [31] . According to Feakins et al., $\Delta\mu_2^{0\neq} > \Delta\mu_1^{0\neq}$ for electrolytes having positive B-coefficients, this indicates a stronger ion–solvent interactions, thereby suggesting that the formation of transition state is accompanied by the rupture and distortion of the intermolecular forces in solvent structure [32] . The greater values of $\Delta\mu_2^{0\neq}$ supports the increased structure making tendency of the solute as discussed earlier. The entropy of activation for solutions has been calculated using the following relation [31]:

$$\Delta S_2^{0\neq} = -d(\Delta\mu_2^{0\neq})/dT, \qquad (13)$$

where $\Delta S_2^{0\neq}$ has been determined from the negative slope of the plots of $\Delta\mu_2^{0\neq}$ against T by using a least square treatment.

The activation enthalpy ($\Delta H_2^{0\neq}$) has been calculated using the relation [31]:

$$\Delta H_2^{0\neq} = \Delta\mu_2^{0\neq} + T\Delta S_2^{0\neq}. \qquad (14)$$

The values of $\Delta S_2^{0\neq}$ and $\Delta H_2^{0\neq}$ are listed in Table 8 and they are found to be negative for all the solutions and at all experimental temperatures suggesting that the transition state is associated with bond formation and increase in order. Although a detailed mechanism for this cannot be easily advanced, it may be suggested that the slip-plane is in the disordered state [31, 33].

Table 8. Values of $\bar{V}_1^0 - \bar{V}_2^0$ (m^3 mol^{-1}), $\Delta\mu_1^{0\neq}$, $\Delta\mu_2^{0\neq}$, $T\Delta S_2^{0\neq}$ and $\Delta H_2^{0\neq}$ (kJ mol^{-1}) for phosphomolybdic acid in different aqueous catechol mixtures at different temperatures

Parameter	298.15 K	308.15 K	318.15 K
	$c_c = 0$		
$(\bar{V}_1^0 - \bar{V}_2^0) \times 10^6$	1145.43	1209.17	1350.24
$\Delta\mu_1^{0\neq}$	60.82	62.86	64.90
$\Delta\mu_2^{0\neq}$	465.134	617.891	1373.86
$-T\Delta S_2^{0\neq}$	13546.71	14001.1	14455.5
$-\Delta H_2^{0\neq} \times 10^3$	13081.609	13383.21	13081.60
	$c_c = 0.05$ mol dm^{-3}		
$(\bar{V}_1^0 - \bar{V}_2^0) \times 10^6$	589.10	607.89	655.32
$\Delta\mu_1^{0\neq}$	60.84	62.89	64.93
$\Delta\mu_2^{0\neq}$	222.02	317.90	349.47
$-T\Delta S_2^{0\neq}$	1899.99	1963.72	2027.44
$-\Delta H_2^{0\neq} \times 10^3$	1677.97	1645.81	1677.97
	$c_c = 0.1$ mol dm^{-3}		
$(\bar{V}_1^0 - \bar{V}_2^0) \times 10^6$	553.12	604.20	650.00
$\Delta\mu_1^{0\neq}$	60.85	62.90	64.94
$\Delta\mu_2^{0\neq}$	187.13	228.51	257.89
$-T\Delta S_2^{0\neq}$	1054.85	1090.23	1125.61
$-\Delta H_2^{0\neq} \times 10^3$	867.72	861.72	867.72
	$c_c = 0.15$ mol dm^{-3}		
$(\bar{V}_1^0 - \bar{V}_2^0) \times 10^6$	495.10	591.54	621.00
$\Delta\mu_1^{0\neq}$	60.86	62.90	64.96
$\Delta\mu_2^{0\neq}$	88.55	147.27	177.11
$-T\Delta S_2^{0\neq}$	1320.21	1364.49	1408.77
$-\Delta H_2^{0\neq} \times 10^3$	1231.66	1217.22	1231.66

CONCLUSION

The values of apparent molar volume (V_ϕ°) and viscosity B-coefficients for phosphomolybdic acid indicate the presence of strong solute–solvent interactions and these interactions are further strengthened at higher temperature and higher molarity of catechol in the ternary solutions. Also phosphomolybdic acid acts as a water-structure promoter due to hydrophobic hydration in the presence of catechol and catechol has a dehydration effect on the hydrated phosphomolybdic acid.

ACKNOWLEDGMENTS

The authors are grateful to the Departmental Special Assistance Scheme under the University Grants Commission, New Delhi (No. 540 / 6 / DRS / 2002, SAP–1) for financial support.

REFERENCES

1. J. M. Mc Dowali, C. A. Vincent, J. Chem. Soc. Faraday Trans. I. **70**, 1862 (1974).
2. M. R. J. Deck, K. J. Bird, A. J. Parker. Aust. J. Chem. **28**, 955 (1975).
3. M. N. Roy, B. Sinha, R. Dey, A. Sinha. Int. J. Thermophysics. **26**, 1549 (2005).
4. R. H. Stokes, R. Mills, Int. Encyclopedia of Physical Chemistry and Chemical Physics (1965). P. 3.
5. P. S. Nikam, Hasan, Mehdi, J. Chem. Eng. Data. **33**, 165 (1988).
6. D. Nandi, M. N. Roy, D. K. Hazra, J. Indian. Chem. Soc. **70**, 305 (1993).
7. Holde Puchtler and H. Isler, Department of Anatomy, Mc Gill University, Montreal, Canada, 21st Jan (1958).
8. M. N. Roy, A. Sinha, B. Sinha, J. Solution. Chem. **34**, 1311 (2005).
9. M. N. Roy, B. Sinha, V. K. Dakua, J. Chem. Eng. Data **51**, 590 (2006).
10. M. N. Roy, A. Sinha, Fluid Phase Equilibria **243**, 133 (2006).
11. M. N. Roy, M. Das. Russian. J. Phys. Chem. **80**, S163 (2006).
12. D. O. Masson, Phil.Mag. **8**, 218 (1929).
13. E. Garland-Paneda, C. Yanes, J. J. Calventa, J. Chem. Soc. Faraday Trans. **94**, 573 (1994).
14. M. N. Roy, A. Jha, R. Dey, J. Chem. Eng. Data. **46**, 1247 (2001).
15. F. J. Millero, Structure and Transport Process in Water and Aqueous Solutions (R.A. Horne, New York) (1972).
16. M. L. Parmar, D. S. Banyal, Indian. J. Chem. **44A**, 1582 (2005).
17. L. G. Hepler, Can. J. Chem. **47**, 4617 (1969).
18. B. K. Sarkar, B. Sinha, M. N. Roy, Russian. J. Phys. Chem. (In press).
19. B. Sinha, B. K. Sarkar, M. N. Roy, J. Chem. Thermodynamics **40**, 394 (2008).
20. L. H. Blanco, E. F. Vargas, J. Solution. Chem. **35**, 21 (2006).

21. W. Y. Wen, in: R. A. Horne (Ed). Water and Aqueous Solution. Willey-Intersciences, New York p. 613 (1972).
22. K. Belibagli, E. Agranci. J. Solution. Chem. **19**, 867 (1990).
23. C. Zhao, P. Ma, J. Li, J. Chem. Thermodynamics. **37**, 37 (2005).
24. H. L. Friedman, C. V. Krishnan // F. Franks (Ed). Water, A Comprehensive Treatise, Vol. 3, Plenum Press, New York. Chapter 1 (1973).
25. R. K. Wadi, P. Ramasami. J. Chem. Soc. Faraday Trans. **93**, 243 (1997).
26. R. Bhat, J. C. Ahliwalia, J. Phys. Chem. **89**, 1099 (1985).
27. A. K. Mishra, J. C. Ahliwalia, J. Chem. Soc. Faraday Trans I. **77**, 1469 (1981).
28. G. Jones, M. Dole, J. Am. Chem. Soc. **51**, 2950 (1929).
29. F. J. Millero, Chem. Rev. **71**, 147 (1971).
30. F. J. Millero, A. Losurdo, C. Shin. J. Phys. Chem. **82**, (1978) 784.
31. D. Feakins, D. J. Freemantle, K. G. Lawrence, J. Chem. Soc. Faraday Trans. I. **70**, 795 (1974).
32. B. Samantaray, S. Mishra, U. N. Dash, J. Teach. Res. Chem. **11**, 87 (2005).
33. Mithlesh, M. Singh, J. Indian. Chem. Soc. **83**, 803 (2000).